

**A new class of intercellular signal controls toxin production  
and virulence of human bacterial pathogen *Streptococcus*  
*pyogenes***



**Dissertation zur Erlangung des Doktorgrades der Naturwissenschaften**

**(Dr. rer. nat.)**

**an der Fakultät für Biologie der  
Ludwig-Maximilians-Universität München**

Vorgelegt von

Nishanth Makthal

im Juli 2019

## **EIDESSTATTLICHE VERSICHERUNG:**

Ich versichere hiermit an Eides statt, dass die vorgelegte Dissertation von mir selbstständig und ohne unerlaubte Hilfe angefertigt ist.

München, den

Houston, USA. Date: 01.07.2019

---

Nishanth Makthal

## **ERKLÄRUNG**

Hiermit erkläre ich, dass die Dissertation nicht ganz oder in wesentlichen Teilen einer anderen Prüfungskommission vorgelegt worden ist. Ich habe nicht versucht, anderweitig eine Dissertation einzureichen oder mich einer Doktorprüfung zu unterziehen.

München, den

Houston, USA. Date: 01.07.2019

---

Nishanth Makthal

Erstgutachter: Prof. Dr. Kai Papenfort

Zweitgutachter: Prof. Dr. Marc Bramkamp

Tag der Abgabe: 17.07.2019

Tag der mündlichen Prüfung: 28.10.2019

This study was conducted in Prof. Dr. Muthiah Kumaraswami's lab, Houston Methodist Research Institute, Houston, Texas, USA.

**TABLE OF CONTENTS**

**DECLARATION OF CONTRIBUTION ..... 5**

**LIST OF PUBLICATIONS ..... 8**

**LIST OF ABBREVIATIONS ..... 11**

**ABSTRACT ..... 14**

**INTRODUCTION ..... 16**

1. Group A *Streptococcus* and its pathogenesis ..... 16

2. Virulence factors ..... 19

    2.1. Cell-associated virulence factors ..... 19

    2.2. Extracellular secreted virulence factors ..... 21

3. Major virulence factor – Streptococcal pyrogenic exotoxin B ..... 22

    3.1. Role of SpeB in GAS pathogenesis ..... 22

    3.2. Biogenesis of SpeB protease ..... 25

    3.3. Transcription regulation of *speB* ..... 27

4. Quorum-sensing in bacteria ..... 28

5. RopB ..... 29

    5.1. Peptide signals controlling the regulatory activity of RRNPP regulators ..... 31

**AIM AND SCOPE OF THE STUDY ..... 33**

**CHAPTER 1 ..... 35**

Leaderless secreted peptide signaling molecule alters global gene expression and increases virulence of a human bacterial pathogen

Published: September 18<sup>th</sup> 2017. PNAS 114:E8498-E8507

**CHAPTER 2 ..... 91**

Signaling by a Conserved Quorum Sensing Pathway Contributes to Growth *Ex Vivo* and Oropharyngeal Colonization of Human Pathogen Group A Streptococcus.

Published: March 12<sup>th</sup> 2018. Infect Immun 86:e00169-18.

**DISCUSSION ..... 110**

1. Mechanism of SIP export ..... 111
2. Import of extracellular SIP to the GAS cytoplasm ..... 113
3. Binding of SIP to RopB and its implications in *speB* expression ..... 114
4. Allosteric changes in RopB upon SIP binding ..... 116
5. Role of SIP in GAS pathogenesis ..... 118
6. General model of quorum sensing mediated regulation of SpeB ..... 120
7. Perspectives and future directions ..... 121

**REFERENCES ..... 122**

**ACKNOWLEDGEMENT ..... 132**

**Nishanth Makthal CV ..... 133**

## DECLARATION OF CONTRIBUTION

I hereby declare that this Ph.D. thesis entitled “A new class of intercellular signal controls toxin production and virulence of human pathogen *Streptococcus pyogenes*” was carried out by me for the degree of Doctor of Philosophy conducted from January 2016 to August 2019 under the guidance and supervision of Dr. Muthiah Kumaraswami, Houston Methodist Research Institute, Houston, USA and Dr. Kai Papenfort, Ludwig-Maximilians University of Munich, Munich, Germany. Results obtained from this study are published as two chapters. Chapter 1 was published in Proceedings of the National Academy of Sciences (PNAS). Chapter 2 was published in Infection and Immunity. Work published in both chapters are a result of collaboration with other scientists.

### Chapter 1:

Do H\*, **Makthal N\***, VanderWal AR, Rettel M, Savitski MM, Peschek N, Papenfort K, Olsen RJ, Musser JM, Kumaraswami M. Leaderless secreted peptide signaling molecule alters global gene expression and increases virulence of a human bacterial pathogen. Proceedings of the National Academy of Sciences 114:E8498-E8507.

\* Equal contribution

Hackwon Do, Muthiah Kumaraswami and I designed, performed, analyzed most of the experiments. I contributed in writing, proofreading and finalizing the manuscript. Following are my specific contributions

- Created one isogenic mutant strain for figures 1D, 1E, and 1F
- Prepared the RNA samples for figure 2A
- Created all the isogenic mutant strains for figures 2B and 2C

## DECLARATION OF CONTRIBUTION

- Performed the quantitative RT-PCR and milk plate assay for figures 2B and 2C respectively
- Performed the fluorescent polarization (FP) studies and generated the figures 4A, 4B, 4E and 4F
- Performed native gel electrophoresis for figures 4I and S8
- Prepared mutant strains for mice infection studies in figures 5 and 6A
- Performed quantitative RT-PCR and generated the figure 6A
- Performed RNA-sequencing, analyzed the results and generated the tables S1-4

Signature of first co-author

Signature of first co-author

Signature of Supervisor

---

Hackwon Do

---

Nishanth Makthal

---

Muthiah Kumaraswami

### Chapter 2:

**Makthal N, Do H, VanderWal AR, Olsen RJ, Musser JM, Kumaraswami M.** Signaling by a Conserved Quorum Sensing Pathway Contributes to Growth *Ex Vivo* and Oropharyngeal Colonization of Human Pathogen Group A Streptococcus. *Infect Immun* 86:e00169-18.

Muthiah Kumaraswami and I designed the study, prepared the figures and wrote the manuscript. I performed and analyzed most of the experiments except the following

- Hackwon Do and Arica VanderWal performed experiments corresponding to figure 7.
- Randall Olsen contributed to figure 4 by collecting the oropharyngeal swabs from mice.

## DECLARATION OF CONTRIBUTION

Signature of first author

Signature of Supervisor

---

Nishanth Makthal

---

Muthiah Kumaraswami

## LIST OF PUBLICATIONS

### Publication 1

Do H\*, **Makthal N\***, VanderWal AR, Rettel M, Savitski MM, Peschek N, Papenfort K, Olsen RJ, Musser JM, Kumaraswami M. Leaderless secreted peptide signaling molecule alters global gene expression and increases virulence of a human bacterial pathogen. *Proceedings of the National Academy of Sciences* 114:E8498-E8507.

\* Equal contribution

#### Abstract

Successful pathogens use complex signaling mechanisms to monitor their environment and reprogram global gene expression during specific stages of infection. Group A Streptococcus (GAS) is a major human pathogen that causes significant disease burden worldwide. A secreted cysteine protease known as streptococcal pyrogenic exotoxin B (SpeB) is a key virulence factor that is produced abundantly during infection and is critical for GAS pathogenesis. Although identified nearly a century ago, the molecular basis for growth phase control of speB gene expression remains unknown. We have discovered that GAS uses a previously unknown peptide-mediated intercellular signaling system to control SpeB production, alter global gene expression, and enhance virulence. GAS produces an eight amino acid leaderless peptide [SpeB-inducing peptide (SIP)] during high cell density and uses the secreted peptide for cell-to-cell signaling to induce population-wide speB expression. The SIP signaling pathway includes peptide secretion, reimportation into the cytosol, and interaction with the intracellular global gene regulator regulator of Protease B (RopB), resulting in SIP-dependent modulation of DNA binding and regulatory activity of RopB. Notably, SIP signaling causes differential expression of ~14% of GAS core

genes. Several genes that encode toxins and other virulence genes that enhance pathogen dissemination and infection are significantly up-regulated. Using three mouse infection models, we show that the SIP signaling pathway is active during infection and contributes significantly to GAS pathogenesis at multiple host anatomic sites. Together, our results delineate the molecular mechanisms involved in a previously undescribed virulence regulatory pathway of an important human pathogen and suggest new therapeutic strategies.

## Publication 2

**Makthal N, Do H, VanderWal AR, Olsen RJ, Musser JM, Kumaraswami M.** Signaling by a Conserved Quorum Sensing Pathway Contributes to Growth *Ex Vivo* and Oropharyngeal Colonization of Human Pathogen Group A Streptococcus. *Infection and Immunity* 86:e00169-18.

### Abstract

Bacterial virulence factor production is a highly coordinated process. The temporal pattern of bacterial gene expression varies in different host anatomic sites to overcome niche-specific challenges. The human pathogen group A streptococcus (GAS) produces a potent secreted protease, SpeB, that is crucial for pathogenesis. Recently, we discovered that a quorum sensing pathway comprised of a leaderless short peptide, SpeB-inducing peptide (SIP), and a cytosolic global regulator, RopB, controls *speB* expression in concert with bacterial population density. The SIP signaling pathway is active *in vivo* and contributes significantly to GAS invasive infections. In the current study, we investigated the role of the SIP signaling pathway in GAS-host interactions during oropharyngeal colonization. The SIP signaling pathway is functional during growth *ex vivo* in human saliva. SIP-mediated *speB* expression plays a crucial role in GAS colonization of the mouse oropharynx. GAS employs a distinct pattern of SpeB production during growth *ex vivo* in

saliva that includes a transient burst of *speB* expression during early stages of growth coupled with sustained levels of secreted SpeB protein. SpeB production aids GAS survival by degrading LL37, an abundant human antimicrobial peptide. We found that SIP signaling occurs during growth in human blood *ex vivo*. Moreover, the SIP signaling pathway is critical for GAS survival in blood. SIP-dependent *speB* regulation is functional in strains of diverse *emm* types, indicating that SIP signaling is a conserved virulence regulatory mechanism. Our discoveries have implications for future translational studies.

## LIST OF ABBREVIATIONS

%	Percent
°C	Celsius
$\alpha$	Alpha
$\beta$	Beta
$\Delta$	Delta
AIs	Autoinducers
AMPs	Antimicrobial peptides
APSGN	Acute post-streptococcal glomerulonephritis
ARF	Acute rheumatic fever
bp	Basepair
CDM	Chemically defined medium
CFUs	Colony forming units
CO <sub>2</sub>	Carbon dioxide
DMSO	Dimethyl sulfoxide
DNA	Deoxyribonucleic acid
dsDNA	Double-strand deoxyribonucleic acid
Eep	Enhanced expression pheromone
ELISA	Enzyme-linked immunosorbent assay
EMSA	Electrophoretic mobility shift assay
F	Free (probe)
FITC	Fluorescein isothiocyanate
FP	Fluorescence polarization
GAS	Group A <i>Streptococcus</i>
h	Hour
H <sub>2</sub> O	Water
HCl	Hydrochloric acid
HRP	Horseradish peroxidase
HTH	Helix-turn-helix

## LIST OF ABBREVIATIONS

i.m.	Intramuscular
i.p.	Intraperitoneal
Ig	Immunoglobulin
IL-1 $\beta$	Interleukin 1 $\beta$
IPTG	Isopropyl $\beta$ -D-1-thiogalactopyranoside
$K_d$	Dissociation constant
kDa	Kilodalton
LB	Lysogeny broth
LE	Late exponential
M	Marker
M	Molar
mAU	Milli absorbance unit
ME	Mid exponential
mg	Milligram
min	Minute
ml	Milliliter
mm	Millimeter
mM	Millimolar
mP	Millipolarization
n.d	Not detected
<i>n.s</i>	Not significant
NaCl	Sodium chloride
NaHCO <sub>3</sub>	Sodium bicarbonate
NETs	Neutrophil extracellular traps
nM	Nanomolar
nm	Nanometer
nt	Nucleotide
<i>orf</i>	Open reading frame
<i>P</i>	Promoter
p.i.	Post infection

## LIST OF ABBREVIATIONS

PAGE	Polyacrylamide gel electrophoresis
PBS	Phosphate buffered saline
pH	Potential hydrogen
qRT-PCR	Quantitative Reverse Transcription PCR
QS	Quorum sensing
RBS	Ribosomal-binding site
RFU	Relative fluorescence unit
RHD	Rheumatic heart disease
RNA	Ribonucleic acid
s.c.	Subcutaneous
SAgs	Superantigens
SCRA	Scrambled
SD	Standard deviation
SEC	Secretome
SEM	Standard error of the mean
Seq	Sequencing
sORFs	Small open reading frames
STAT	Stationary
THY	Todd-hewitt broth
TPR	Tetratricopeptide repeat
TSS	Transcription start site
WT	Wild-type
µm	Micrometer
µg	Microgram
µM	Micromolar

**ABSTRACT**

Quorum sensing (QS) is a process in which bacteria use diverse signaling molecules to monitor their population density and regulate population-wide expression of genes involved in several key bacterial processes such as virulence, biofilm formation, and antibiotic resistance. Gram-positive bacteria typically use oligopeptides as intercellular signaling molecules. The secreted oligopeptides modulate gene expression by either activating the sensor kinase of a two-component system on the bacterial surface or by interacting with cognate transcription regulator in the bacterial cytosol. The gram-positive bacteria Group A *Streptococcus* (GAS) is a major human pathogen responsible for over 700 million infections annually worldwide. GAS produces a wide spectrum of virulence factors that play crucial roles in disease pathogenesis. Among the many toxins produced by GAS, Streptococcal pyrogenic exotoxin B (SpeB) is one of the well-studied virulence factor. SpeB is a secreted cysteine protease that is produced abundantly during infection and is critical for GAS pathogenesis. Although SpeB is extensively studied for a century, the precise regulatory events that govern *speB* gene expression are not fully understood. In this study, we have discovered that GAS employs a previously unknown peptide-mediated quorum sensing pathway to control *speB* expression during high bacterial population density. GAS genome encodes a novel class of leaderless peptide signal, SpeB-Inducing Peptide (SIP). SIP lacks several characteristic features that are hallmarks of bacterial peptide signals. Contrary to all the characterized bacterial peptide signals, SIP is produced in its mature form and lacks amino acid sequences in the amino terminus required for secretion. Nevertheless, SIP functions as an effective intercellular signal. SIP is secreted and reinternalized into GAS cytosol where it interacts with its cognate regulator, Regulator of proteinase B (RopB). SIP binding to RopB induces allosteric changes in the regulator, which leads to high affinity RopB-DNA interactions, RopB

oligomerization and activation of *speB* gene expression. Importantly, we demonstrate that the SIP signaling pathway is active *in vivo* and contributes significantly to GAS virulence in multiple mouse models of GAS infection. We also show that the SIP signaling occurs during GAS growth *ex vivo* in human saliva and blood and SIP-mediated *speB* expression is crucial for GAS survival in both saliva and blood. Together, our discoveries in this study identify a novel bacterial signaling pathway and suggest new therapeutic strategies for future translation studies.

## INTRODUCTION

The discovery of antibiotics and the ability to treat bacterial infections have revolutionized human health care in many respects (5). Since the discovery of penicillin in 1928, several natural or synthetic antimicrobial agents have been developed (6). However, abuse and overuse of antibiotics in the subsequent decades have endangered the efficacy of antibiotics due to the rapid emergence of drug-resistant bacteria (7-9). New drugs are being developed by the pharmaceutical industry to overcome bacterial antimicrobial resistance. However, the pipeline began to dry out in the recent years, posing an imminent threat to human health care (6, 10). Thus, novel approaches are needed to identify and characterize new antimicrobials to prevent/treat drug-resistant bacterial infections. In this regard, a complete understanding of bacterial virulence mechanisms is crucial in our efforts to devise targeting strategies and develop future antimicrobials (5).

### 1.1 Group A *Streptococcus* and its pathogenesis

*Streptococcus pyogenes*, also known as Group A *Streptococcus* (GAS), is a gram-positive, non-spore forming, cocci bacterium (11). GAS is an exclusive human pathogen that causes a vast spectrum of pyogenic disease conditions in oropharyngeal (throat) and skin mucosal surfaces, resulting in pharyngitis (commonly known as “strep throat”) and impetigo respectively (Fig. 1) (2, 12-16). Pharyngitis is the most common GAS disease manifestation with over 600 million cases worldwide, affecting approximately 20 – 40% of children and 10 – 15% of adults every year (17, 18). GAS persists in human saliva by overcoming the host innate and acquired immune system. The survival of GAS in saliva is crucial for person-to-person disease transmission, presumably via saliva droplets (18-20). Impetigo is a highly contagious skin disease spread through direct skin

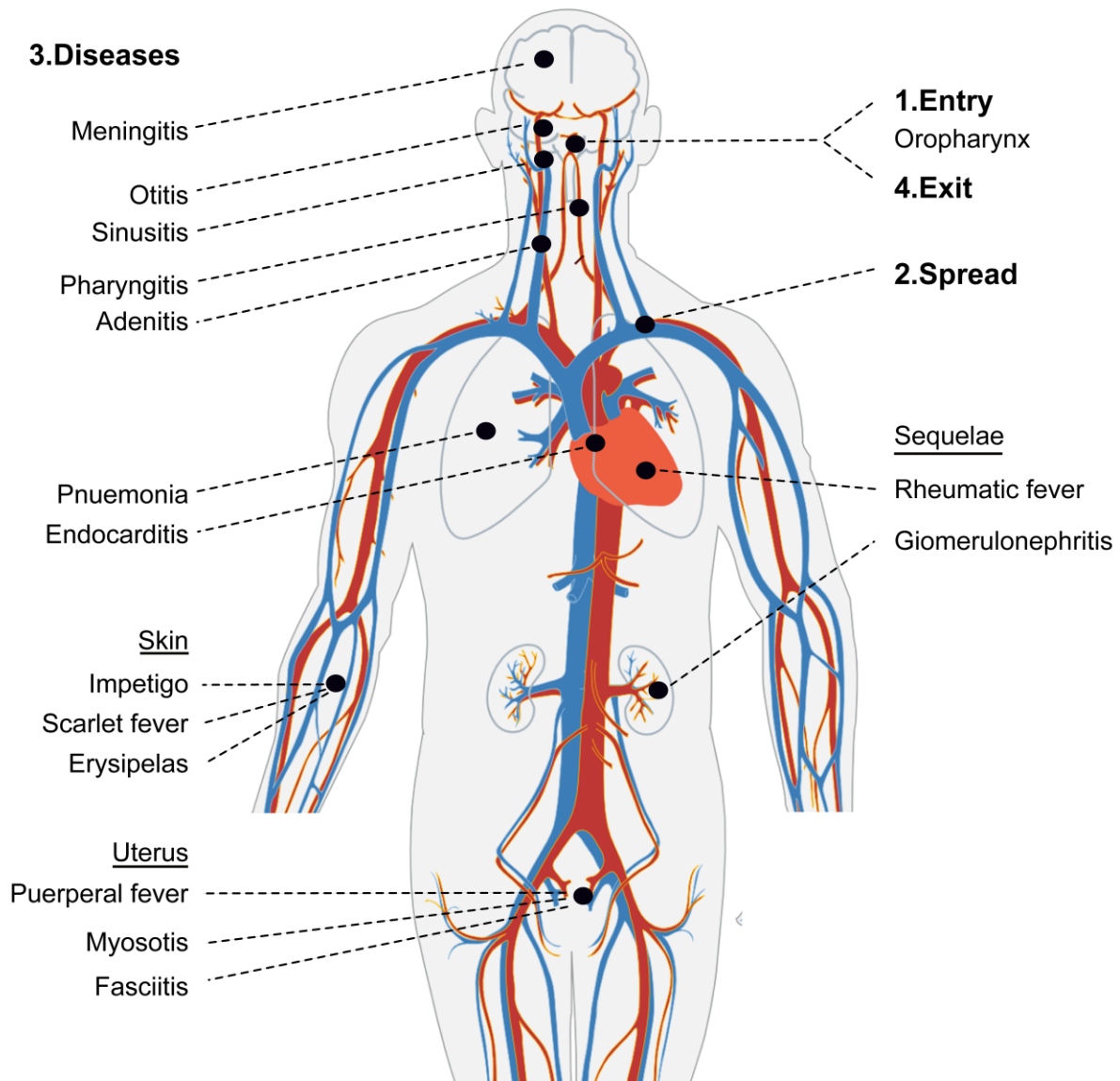


**Figure 1. Overview of diseases caused by GAS infections.** Common disease manifestations caused by GAS infections in human. Adapted from (1).

contact resulting in approximately 111 million global cases every year, mostly in children from developing countries (19, 21).

Recurring untreated pharyngitis can lead to post-infection auto immune disorders such as acute rheumatic fever (ARF), rheumatic heart disease (RHD), and acute post-streptococcal

glomerulonephritis (APSGN) (Fig. 1) (19, 22, 23). ARF and RHD constitute the major cause of morbidity and mortality caused by GAS infections. Globally, approximately 2.4 million children develop heart disease as a result of RHD every year (15, 24). Consequently, RHD is the most preventable pediatric heart disease in the world (25, 26). APSGN is an autoimmune disorder of kidneys, sequelae of GAS pharyngitis or impetigo. The most common clinical features include edema, hypertension, proteinuria, urinary sediment abnormalities (19, 27). Half a million cases are recorded every year worldwide that results in approximately 1% mortality (13).

In complicated cases, GAS invades epithelial barriers and penetrates into deeper tissues, which can lead to severe life-threatening invasive infections (11, 28). Bacteremia and cellulitis are the most common GAS invasive diseases. GAS infections can also lead to less common, but difficult to treat invasive diseases such as necrotizing fasciitis (also known as “flesh-eating disease”), and streptococcal toxic shock syndrome (STSS) (also known as “bacterial sepsis”) (15, 19, 29-31). Invasive infections are responsible for approximately 500,000 deaths every year worldwide (19, 32). Due to the global disease and economic burden caused by GAS infections, GAS is listed as one of the top ten infectious causes of mortality (19, 33).

Though mild GAS infections can be treated with penicillin and cephalosporin, recent studies have reported a 20 – 40% failure rate of penicillin in treating pharyngitis (34, 35). Moreover, GAS resistance to other antibiotics in developing countries is on the rise and is a worldwide concern (19). Contrary to mild infections, invasive infections are unresponsive to antibiotics treatment and often require surgical intervention for infection control. Similarly, RHD disease control requires expensive long-term antibiotics administration, and/or surgical debridement of infected valves (15, 19). Thus, a human GAS vaccine will be highly beneficial in GAS disease prevention. A great deal of work has been done in the last 70 years on M protein

(encoded by *emm* gene) as a potential candidate for the development of a vaccine. However, the existence of more than 200 *emm* type variations in GAS and the associated antigenic diversity pose a major roadblock for the development of single effective universal M protein based GAS vaccine (20). Furthermore, the antibodies developed against M protein cross-react with human heart tissue and trigger the development of ARF and RHD. Thus, the need for the identification of novel vaccine or antimicrobial targets to treat or prevent GAS diseases is urgent (36-38). As a result, continued investigations into basic virulence pathways is imperative to elucidate novel therapeutic and/or prophylactic strategies toward GAS infection control.

## **2. Virulence factors**

The ability of GAS to successfully colonize, evade the immune system and invade different host niches depends on the spatiotemporal production of wide array of virulence factors (Fig. 2) (37). GAS virulence factors are categorized into two groups depending on their location; cell surface-associated and secreted toxins (2, 16, 37).

### **2.1 Cell-associated virulence factors**

GAS genome encodes multiple adhesins such as collagen binding proteins, fibronectin (Fn) binding proteins (Sfb1, SfbII, SOF, PrtF2, FbpA, FbaB and Pfbp), lipoteichoic acids (LTA), and plasminogen binding proteins that play a crucial role in host cell attachment (Fig. 2) (37, 39, 40). Virulence factors such as the immunoglobulin binding proteins (M protein superfamily, SibA), C5a peptidase, hyaluronic acid capsule, lipoprotein (Lsp), streptococcal protective antigen (Spa), heme-binding protein, HtrA protease, streptococcal collagen-like surface proteins (Sc11 and Sc12),

CD15s-related antigen, plasminogen binding proteins and serum opacity factor cleave host immune factors and aid GAS in immune evasion (Fig. 2) (37). Amongst the many cell-associated virulence factors, M protein and hyaluronic acid capsule (produced by *hasABC* gene cluster) are the two best-studied factors (15, 37). M protein confers phagocytosis resistance by binding to host immune effectors such as complement-inhibitory proteins C4BP, factor H, and factor H-like protein (41-43). Similarly, hyaluronic acid capsule also provides antiphagocytic function by restricting the access of GAS surface to opsonins (44, 45).

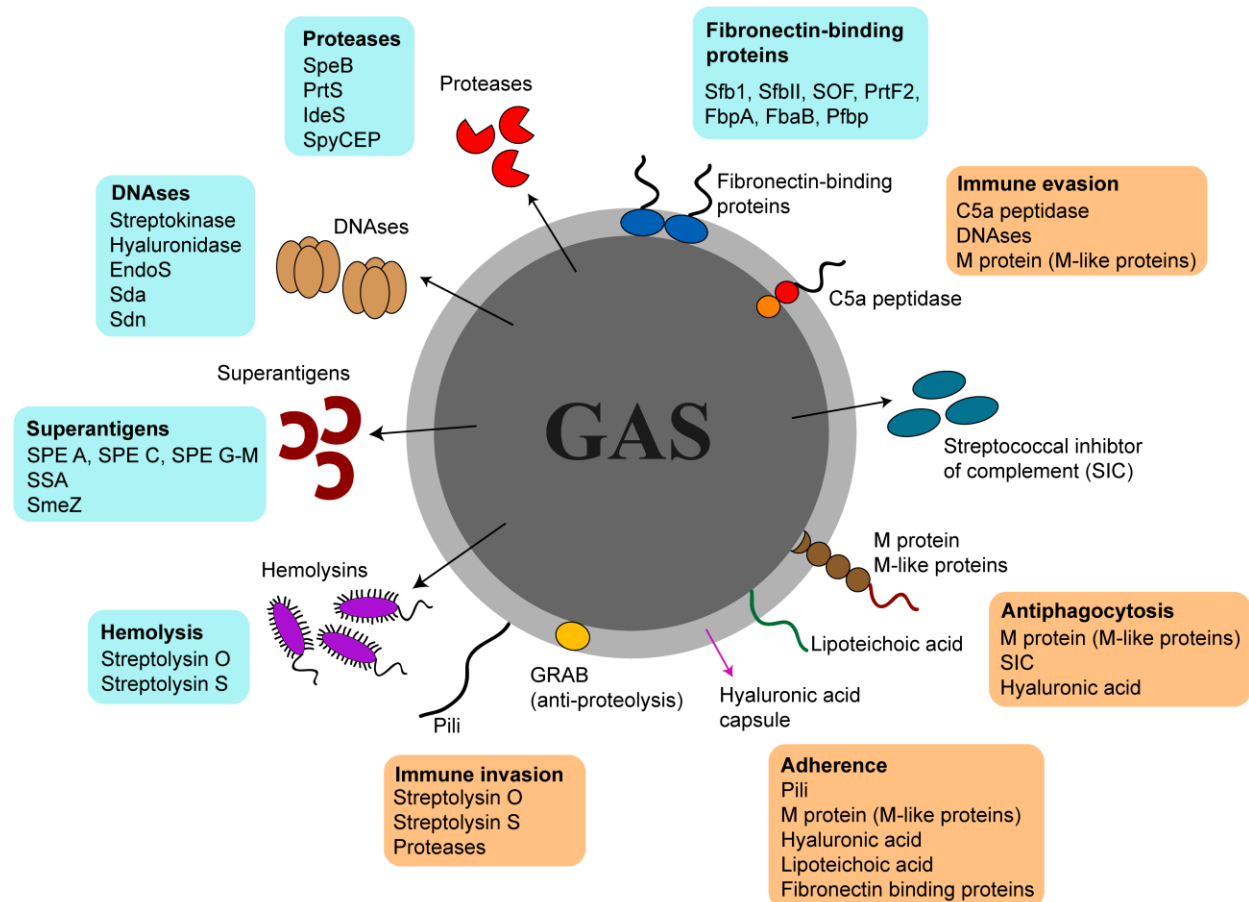


**Figure 2. Virulence factors encoded in GAS genome.** GAS produces several virulence factors that contributes to disease pathogenesis by facilitating host cell attachment, anti-phagocytosis, immune invasion, and immune evasion. Cell-associated factors are shown on the surface of GAS and secreted factors are indicated by black arrows. Blue boxes show the list of virulence factors. Orange boxes show the list of virulence factors participating in the indicated cellular process.

## 2.2 Extracellular secreted virulence factors

GAS produces several major secreted virulence factors such as hemolysins, DNAses, superantigens (SAGs), and proteases (Fig. 2) (46). Streptolysin O (SLO) is a major pore-forming hemolysin that disrupts the integrity of host cell membrane and induces apoptosis (47). Streptolysin S (SLS), a second hemolysin encoded by GAS, contributes to GAS virulence in several ways that include host cell cytotoxicity, activation of inflammatory responses, and antiphagocytosis (46, 48). The host innate immune system deploys neutrophil extracellular traps (NETs) to control bacterial growth. NETs contain bactericidal proteases on webs of DNA (49). To counter this, GAS produces several secreted DNAses, such as streptodornase (Sdn), and streptodornase- $\alpha$  (Sda). GAS-encoded DNAses degrade NETs by digesting DNA and aid immune evasion (46, 49). Streptococcal inhibitor of complement (SIC) contributes to GAS pathogenesis by degrading several host cells, including lymphocytes and erythrocytes (50). SIC can also disrupt the host signals involved in producing antimicrobial peptides (AMPs) and facilitate GAS survival in the host (51, 52). GAS superantigen proteins such as SPE A, SPE C, SPE G-M, streptococcal mitogenic exotoxin Z (SmeZ) and streptococcal superantigen A (SSA) belong to a family of highly mitogenic exotoxins (53, 54). SAGs share the ability to trigger overstimulation of T lymphocytes, which leads to the release of pro-inflammatory cytokines and development of STSS (53). GAS secretes many proteases such as SpeB, PrtS, IdeS, and SpyCEP that contribute significantly to GAS pathogenesis by facilitating host tissue degradation and disease dissemination (46). In addition, GAS produces secreted esterases such as SsE, CAMP factor, hyaluronidases such as HlyP, HlyA, and soluble M proteins that contributes significantly towards the success of GAS pathogenesis (46).

### 3. Major virulence factor - Streptococcal pyrogenic exotoxin B

Among the several virulence factors produced by GAS, SpeB is a major secreted toxin that plays a critical role in GAS disease pathogenesis (55). Streptococcal pyrogenic exotoxin B (SpeB), also known as streptopain, is one of the most extensively studied GAS virulence factors (2, 14). SpeB is the predominant extracellular virulence factor in GAS culture supernatant during growth *in vitro* (56). Although the established name for this enzyme is SpeB, SPE B is still occasionally used in the literature (2, 14). Two separate branches of investigation independently identified the same molecule but classified it differently (2). Nearly a century ago, a secreted protease activity was observed in streptococcal growth (57). Subsequent biochemical studies demonstrated that the protease activity in the secreted component of streptococcal growth was similar to cysteine protease papain and classified it as a cysteine protease (2, 14, 58). In a parallel line of investigation, exotoxins were identified in the streptococci culture filtrates obtained from patients with scarlet fever and were designated as superantigens SPE A, SPE B, and SPE C (53, 59). Significant technological advances in the molecular techniques later revealed that the observed superantigen activity of SPE B was likely the result of other streptococcal contaminants (60). In subsequent years, detailed genetic analysis revealed that SPE B and cysteine protease are the same protein encoded by the GAS genome. Importantly, it was concluded that SpeB is not a superantigen, it is rather a cysteine protease (61). Although SpeB is neither pyrogenic nor exotoxin, the designation is widely employed by researchers over the years and retained in the current literature.

#### 3.1 Role of SpeB in GAS pathogenesis

Several lines of study have provided evidence that SpeB is a critical player in GAS pathogenesis (62-66). The chromosomally encoded *speB* gene is highly conserved in virtually all disease-causing GAS isolates (67-69). Inactivation of SpeB attenuated GAS virulence in multiple mouse models and non-human primate model of GAS infection (70-75). SpeB is crucial for GAS survival and proliferation *ex vivo* in human saliva and blood (76-81), suggesting that the protease activity of SpeB is critical for GAS virulence. SpeB contributes to GAS pathogenesis in two major ways, immune evasion by degrading immune molecules and disease dissemination by proteolytic degradation of host tissue matrix proteins and GAS surface proteins (Fig. 3) (14).

The substrate profile of SpeB includes a myriad of host and bacterial proteins. Immunoglobulins (Ig), secreted by B cells of the host adaptive immune system plays a critical role in neutralizing pathogens. SpeB aids GAS immune evasion by degrading multiple classes of immunoglobulins including IgA, IgM, IgD, and IgE (82). SpeB-mediated cleavage of IgG results in decreased opsonophagocytosis (14, 83). In addition to Ig, SpeB also cleaves several host immune effectors such as complement component C3b (84), signals required for the activation of antimicrobial cytokines (14, 85), host interleukin I  $\beta$  (IL-1 $\beta$ ) (63), and kininogen (86), resulting in induction of inflammatory responses. SpeB can degrade the antimicrobial peptide (AMP) LL-37 directly (87) or indirectly by promoting the release of dermatan sulfate from decorin (88). The proteolytic activity of SpeB contributes indirectly to GAS immune evasion by releasing several GAS surface associated virulence factors (14, 89, 90). SpeB releases the mature form of M protein from GAS surface to confer resistance to phagocytosis (90, 91). SpeB-dependent cleavage of protein H aids GAS immune evasion by the binding of protein H fragment to host IgG and inhibition of host complement activation (92). C5a peptidase is an important virulence factor

anchored to GAS surface and C5a released by SpeB-mediated cleavage inhibits chemotactic recruitment of phagocytic cells to the site of infection (90, 93).

The proteolytic activity of SpeB contributes to GAS dissemination into deeper host tissues by enzymatic degradation of host tissue (72, 74, 75, 94-96). SpeB cleaves major host tissue matrix proteins fibronectin and degrades vitronectin and contributes to tissue destruction (97). The

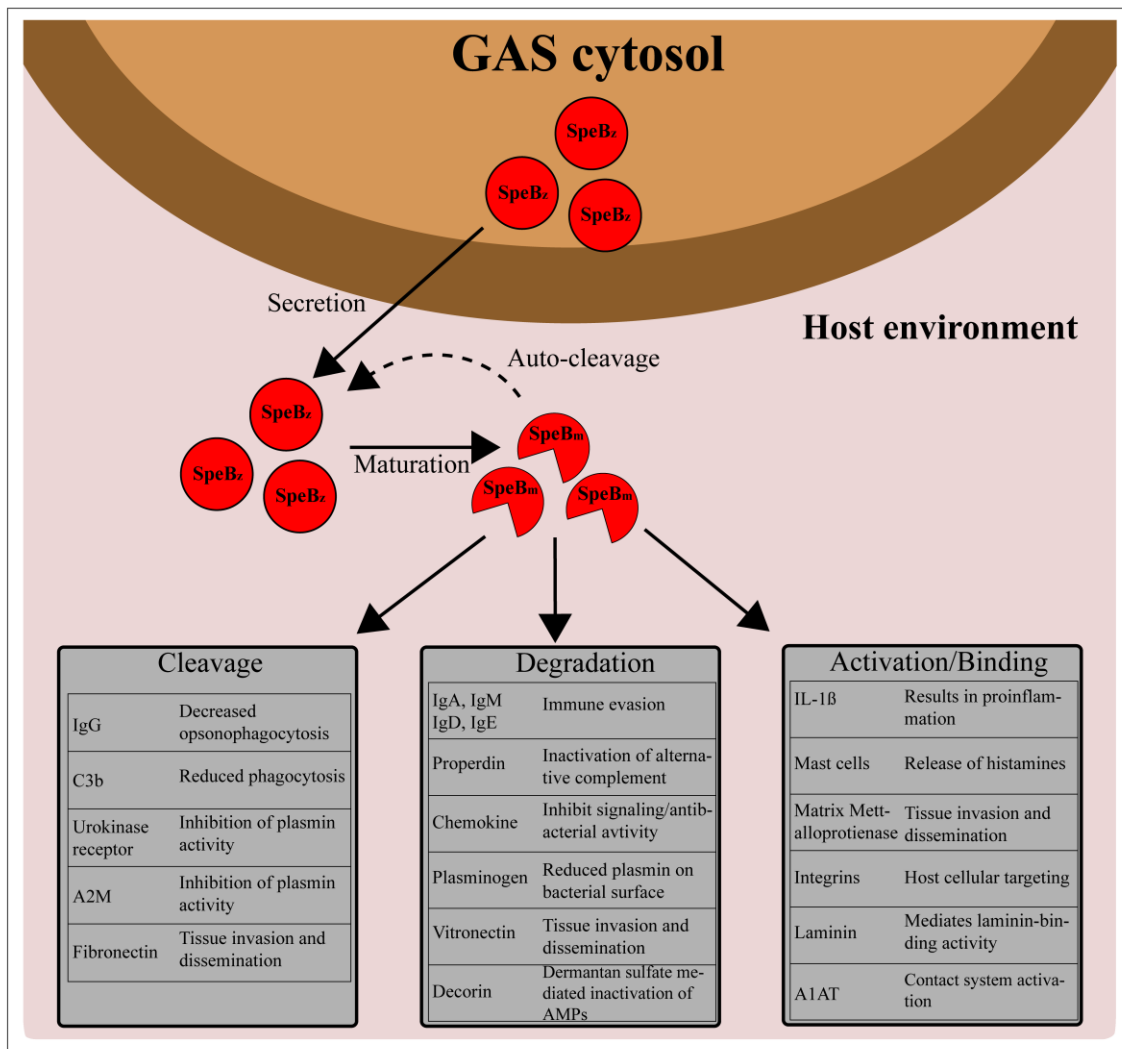


**Figure 3. SpeB biogenesis and its contribution to GAS pathogenesis.** SpeB is produced and secreted in an inactive zymogen precursor form (SpeB<sub>Z</sub>). Auto-cleavage of SpeB<sub>Z</sub> results in the release of mature active cysteine protease (SpeB<sub>M</sub>). The title of individual gray boxes represents the SpeB<sub>M</sub> activity on host factors. Left column in each gray box indicates the identity of SpeB<sub>M</sub> substrate, whereas the right column represents the consequences of SpeB<sub>M</sub> activity on those factors. Adapted from (2)

protease activity of SpeB has been implicated in the induction of caspase-dependent apoptosis in host epithelial cells (98).

GAS produces SpeB during human infection (99, 100). Infected humans produce anti-SpeB antibodies (101, 102) and low antibody titers correlate with severe invasive disease (102, 103), suggesting that SpeB participates in GAS pathogenesis during natural infection. Consistent with this, immunization of mice with SpeB reduced mortality caused by experimental GAS infections (104-107). Similarly, mice treated with a small molecule protease inhibitor conferred protection against GAS invasive diseases (62), suggesting that SpeB is an ideal therapeutic or prophylactic target to treat GAS infections. Collectively, these observations indicate that SpeB is a major GAS virulence factor that contribute to GAS pathogenesis in the host.

### 3.2 Biogenesis of SpeB protease

The full-length SpeB is a 398 amino acid long protein with a molecular mass of 43 kilo daltons (kDa) (Fig. 4). The first 27 amino acids in the amino terminus of SpeB harbor the secretion signal sequence that facilitates its transport out of the cytosol. SpeB is initially made in an inactive form, known as zymogen (SpeB<sub>Z</sub>) (amino acids 28 – 398) (Fig. 3 and 4). The pro-domain (amino acids 28 – 145) is inserted into the active site of SpeB in the zymogen form and keeps the protease

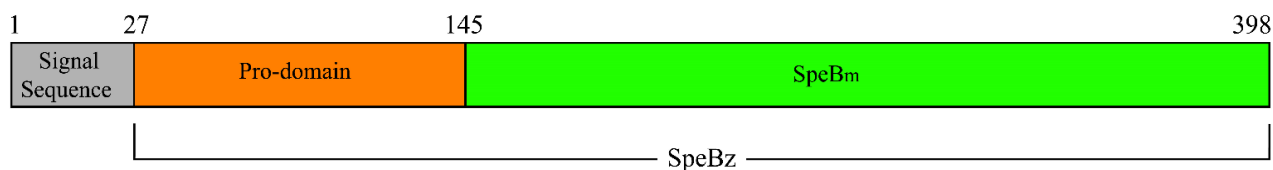


**Figure 4. Schematic diagram showing the domain architecture of SpeB.** The individual domains and motifs in the full-length SpeB are marked and labeled as follows: grey box represents the secretion signal sequence; orange box indicates the pro-domain; and green box represent the mature cysteine protease (SpeB<sub>M</sub>). The structural elements color coded in orange and green boxes represent the inactive pre-cursor SpeB zymogen form. The numbers above indicate the amino acids that constitute each highlighted SpeB domain. Adapted from (2).

enzymatically inactive in GAS cytosol. Upon secretion to the extracellular environment, SpeB<sub>Z</sub> undergoes several autocatalytic steps, which results in the cleavage of pro-domain and release of the mature active cysteine protease (amino acids 146 – 398, SpeB<sub>M</sub>) (Fig. 3 and 4) (2). Genetic and structural studies identified the active site of the protease that is comprised of amino acids cysteine 192, histidine 340 and tryptophan 357. The catalytic site of SpeB<sub>M</sub> is essential for SpeB maturation and its proteolytic activity (2, 108, 109). In accordance with the role of SpeB as a major GAS virulence factor, the biogenesis of SpeB is a multistage process that is controlled by several GAS factors at transcriptional, post-transcriptional and translational levels (Fig. 5) (2, 68).

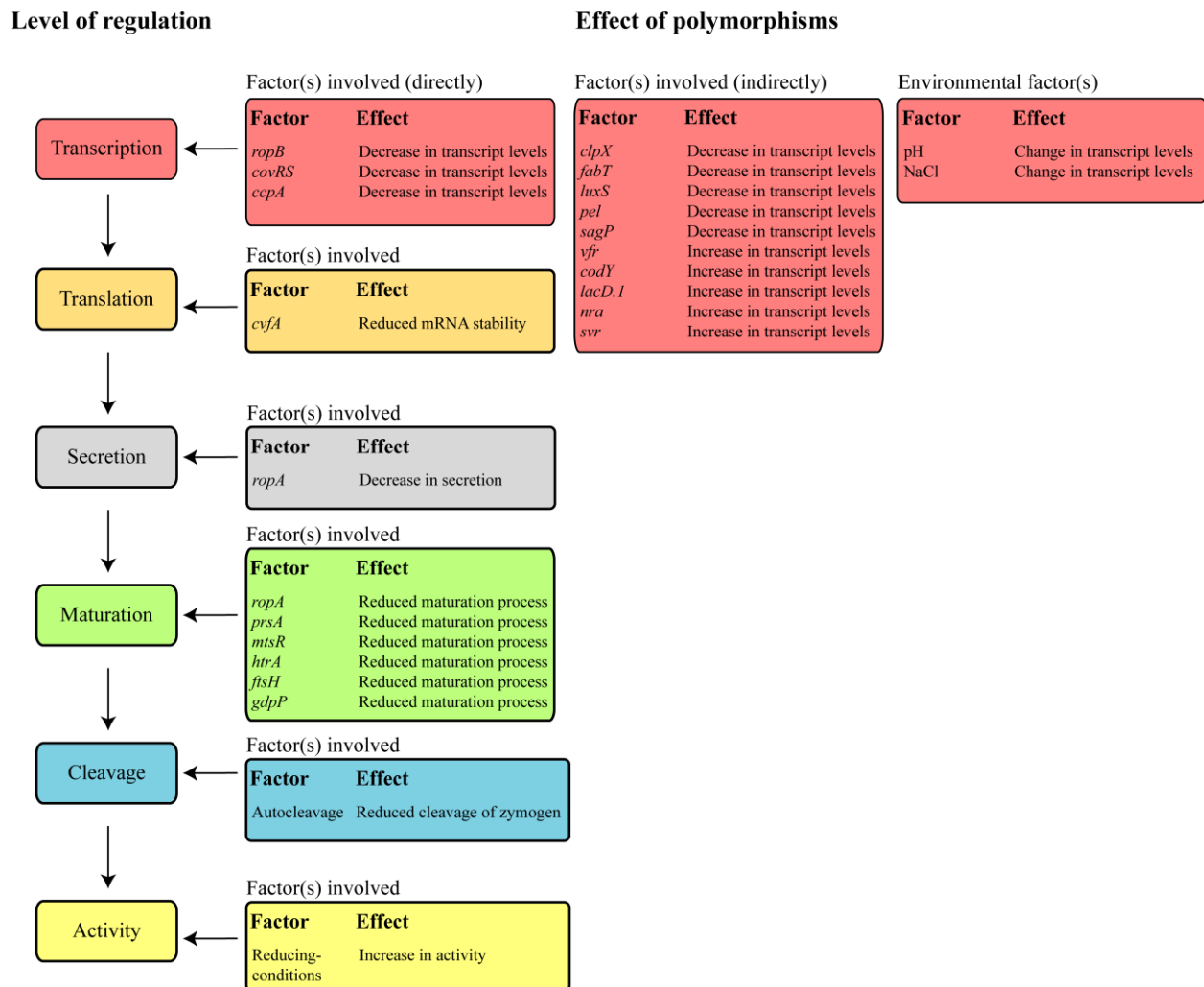


**Figure 5. Schematic diagram showing the factors involved in the regulation of SpeB.** Boxes to the left represent the level of SpeB regulation. Corresponding color-coded boxes to the right show the factors involved and their known effect on the respective level of regulation.

### 3.3 Transcription regulation of *speB*

GAS-encoded factors as well as environmental factors such as pH and NaCl were implicated in the regulation of *speB* expression (Fig. 5) (2, 89, 110-112). Although the environmental signals contribute to transcription regulation of *speB*, the molecular mechanisms of how pH and salt mediate transcription regulation of *speB* are yet to be elucidated. It is possible that specific pH and salt requirements for *speB* expression may mimic host niche environments GAS encounters during infection (110). Expression of *speB* is under the control of 13 different GAS-encoded transcription factors (Fig. 5) (2). The GAS global transcription regulator, the **Regulator of proteinase B** (RopB), is located in the genetic vicinity of *speB* gene and is essential for *speB* expression (2, 71, 113, 114). The *ropB* and *speB* genes are divergently transcribed and separated by a 940 nt intergenic region (Fig. 6) (71, 114). Expression of *speB* is driven from two individual transcription start sites (TSS), *P* and *P1*, located 842 nt and 697 nt upstream of the *speB* gene (115, 116). A third TSS, *P2* located at 137 nt upstream of *speB* gene was previously identified, however, it was recently re-annotated as a RNase Y processing site of *speB* mRNA (Fig. 6) (114, 116). In addition to the complex transcription process (Fig. 5), the intergenic region also harbors several important regulatory factors and small open reading frames (*orf*) whose functions are yet to be elucidated (Fig. 6) (2, 114-116).

SpeB production is growth phase-dependent and *speB* expression predominantly occurs during stationary phase of GAS growth or high GAS population density (110, 117). Similar to *speB*, maximum expression of *ropB* also occurs during late exponential phase (114). Transcription of *speB* is under the direct control of RopB. The *speB* promoter has binding sites for RopB and the occupancy of RopB at *speB* promoter is critical for the upregulation of *speB* expression (2, 114). Although RopB is essential for the activation of *speB* transcription, ectopic expression of *ropB*

from a constitutive promoter during early exponential phase of growth or low population density was not sufficient to activate *speB* expression (2, 114). These observations suggest that additional high population density-specific regulatory factors are required to activate RopB-dependent *speB* expression. Consistent with this, the addition of cell-free culture supernatant obtained from high GAS population density to cells grown to low bacterial population density induced *speB* expression, suggesting the presence of unidentified high population density-specific secreted activation factor(s) (71).

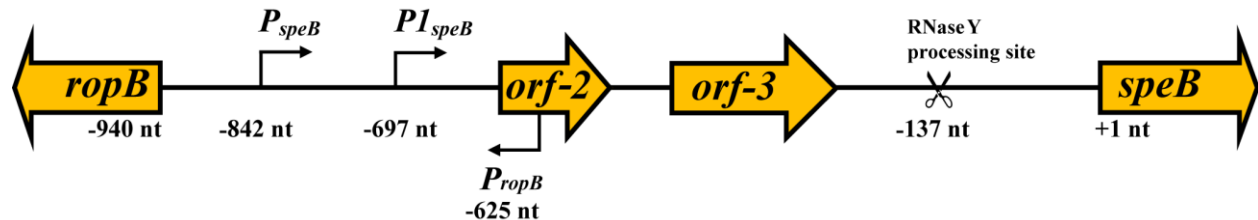


**Figure 6. Schematic diagram showing the genetic organization of *ropB* and *speB* genes.** Promoter region of *speB* ( $P_{speB}$ ) and *ropB* ( $P_{ropB}$ ) are marked by bent arrows above and below the line, respectively. The coding regions of *ropB*, *speB* and predicted open reading frames, *orf-2* and *orf-3*, are shown as block arrows. The start codon of *SpeB* coding region is marked as +1 and the number below the line indicate the location of identified genetic elements relative to *speB* start codon.

#### 4. Quorum-sensing in bacteria

Bacteria communicate with each other by a process called quorum sensing (118, 119). It involves the production and secretion of small molecules known as autoinducers (AIs), and sensing of the AIs by cognate receptors in the neighboring cells (118-120). At low bacterial population density, the concentration of AIs is below the threshold concentration required to elicit responses in the neighboring cells. However, at high bacterial population density, AIs reach critical threshold concentration and evoke transcriptional responses in a population-wide fashion (118, 120-122).

The AIs at high concentrations are recognized by their cognate sensory receptors and control the expression of genes involved in several bacterial traits, including virulence (120, 121, 123). Gram-negative bacteria uses small chemical molecules as intercellular signals (121), whereas Gram-positive bacteria uses either linear or modified oligopeptides to communicate with each other (120). The secreted extracellular peptides are sensed by either a membrane-bound sensor kinase of two-component signaling system or by intracellular transcription regulators (124). The intracellular quorum-sensing transcription regulators belong to the RRNPP family of regulators (4, 125-128). RRNPP family regulators comprises of the **R**ap phosphatases from *Bacillus subtilis*, **R**gg from *Streptococcus* species, **N**prR from *B. cereus* group, **P**lcR from *B. cereus* group, and **P**rgX from *Enterococcus faecalis* (4, 71, 125, 126, 129).

## 5. RopB

RopB belongs to Rgg subfamily of RRNPP super family of transcription regulators. RopB influences the transcription of approximately 25% of the GAS genome during stationary phase of growth (71). Consistent with its role in SpeB regulation, genetic inactivation of *ropB* results in the attenuation of GAS virulence in animal models of GAS infection (4, 70, 130).

RopB shares significant structural homology with the RRNPP family regulators (Fig. 7) (4, 71). All the characterized RRNPP family regulators use high bacterial population density-specific linear oligopeptides as cognate signals and mediate target gene regulation (131, 132). The RRNPP regulators control several bacterial traits such as biofilm formation, virulence, sporulation, necrotrophic lifestyle, and antibiotic resistance (4, 133-135). Structurally, RRNPP family regulators are characterized by a two-domain architecture: an amino-terminal DNA binding domain, and a C-terminal peptide binding and oligomerization domain. The amino-terminal and

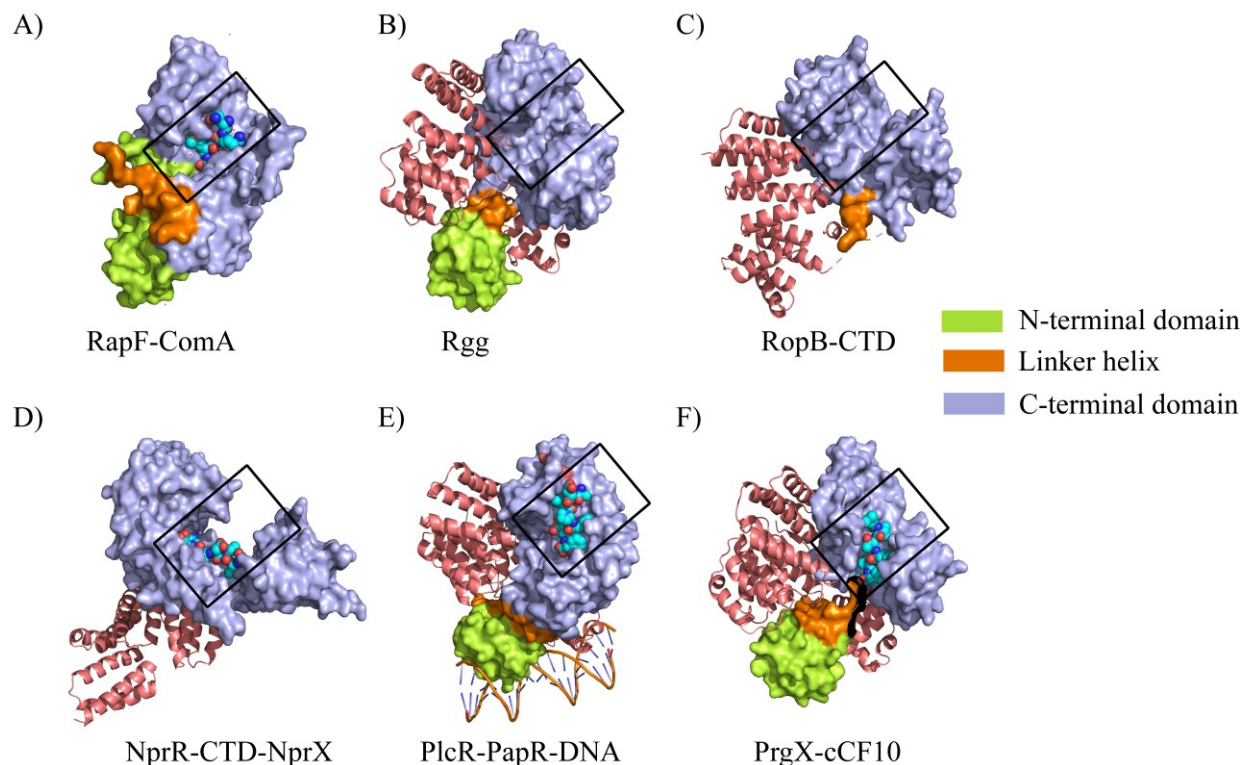


**Figure 7. Domain architecture of the RRNPP-family regulators.** Overall architecture of the crystal structure of RapF bound to its cognate peptide signal ComA (pdb code: 3ULQ) (A), Rgg (pdb code: 4YV6) (B), RopB-CTD (pdb code: 5DL2) (C), NprR-CTD bound to its cognate peptide signal NprX (pdb code: 4GPK) (D), PlcR bound to its cognate peptide signal PapR and DNA (pdb code: 3U3W) (E), PrgX bound to its cognate peptide signal cCF10 (pdb code: 2AXZ) (F) are shown. Residues colored in green represent the N-terminal domain, blue represent the C-terminal domain and the linker helix connecting both the domains are shown in orange. In panels B-F, ribbons colored in pink represent the second subunit of the dimer molecules. Black rectangle boxes show the concave peptide binding pockets. The cognate peptide signals of the respective regulator is shown as spheres located inside the box. Note: Surface residues on top of the peptide binding pocket are removed for panels A, D, E and F. Figure generated using Pymol (3). Adapted from (4).

C-terminal domains are connected by a linker helix (Fig. 7) (125, 129, 132, 136, 137). With the exception of Rap phosphatases, all RRNPP regulators contain a helix-turn-helix (HTH) DNA binding motif in the amino-terminal domain that binds DNA. Contrary to this, the amino-terminal domain of Rap proteins contains a 3-helix bundle that directly interacts with a target transcription regulator and modulates gene expression by blocking the interactions between regulator-DNA (4, 138-142). The C-terminal domain of the RRNPP family regulators are characterized by the

presence of tandem repeats of tetratricopeptide repeat (TPR)-motifs. Each TPR motif is comprised of a pair of antiparallel helices, and TPR domains typically contain 5 TPR motifs (4). TPR domain of the RRNPP family regulators forms a right handed super helical structure which results in a convex exterior and a peptide or protein binding concave interior surface (Fig. 7) (4, 143). Typically, TPR motifs identified in eukaryotic and prokaryotic proteins are involved in protein-protein or protein-peptide interactions (144, 145). Consistent with its structural homology, the C-terminal domain of RopB also contain a TPR domain comprised of 5 TPR motifs (71). Given that RopB shares high degree of structural homology with RRNPP family regulators (4) and its role in population density-specific regulation of *speB*, it is likely that RopB uses GAS population density-specific peptide signals to control *speB* expression.

### **5.1 Peptide signals controlling the regulatory activity of RRNPP regulators**

The cognate mature peptide signals of the RRNPP regulators are linear, hydrophobic and short 5-8 amino acids long oligopeptides (4, 125). The peptide signals are synthesized as inactive pre-peptides in the bacterial cytosol (4, 146). The pre-peptides of cognate RRNPP regulators are encoded by small open reading frame (sORF) genes. The pre-peptides of Rap, NprR and PlcR are typically 40 – 50 amino acids in length, whereas the pre-peptides of Rgg regulators are 15 to 35 amino acids long (125, 147). The peptide signals of the RRNPP family share several amino acid sequence traits: i) the peptides are made in their longer, pre-cursor form, ii) contain a recognizable amino-terminal secretion signal sequence required for the peptide secretion, iii) contain amino acid sequences that function as processing sites for intramembrane and/or secreted proteases, iv) during secretion, the pre-peptides undergo intramembrane and extracellular proteolytic processing that result in the release of mature active peptide signals (4, 118, 120, 146). The mature peptide signals

are imported back to the bacterial cytosol by the highly conserved oligopeptide transporter, Opp permeases (4, 125). The cytosolic cognate receptors sense the reinternalized peptides and the peptide-bound receptors mediate gene regulation (4, 125). Typically, the sORF encoding the cognate peptide signals of RRNPP family regulators are located in the immediate genetic vicinity of their respective regulators (Fig 8) (4, 125). However, our initial nucleotide sequence analysis of the genetic vicinity of *ropB* gene failed to identify a peptide signal-like sORF. As a result, RopB was considered as an orphan regulator.

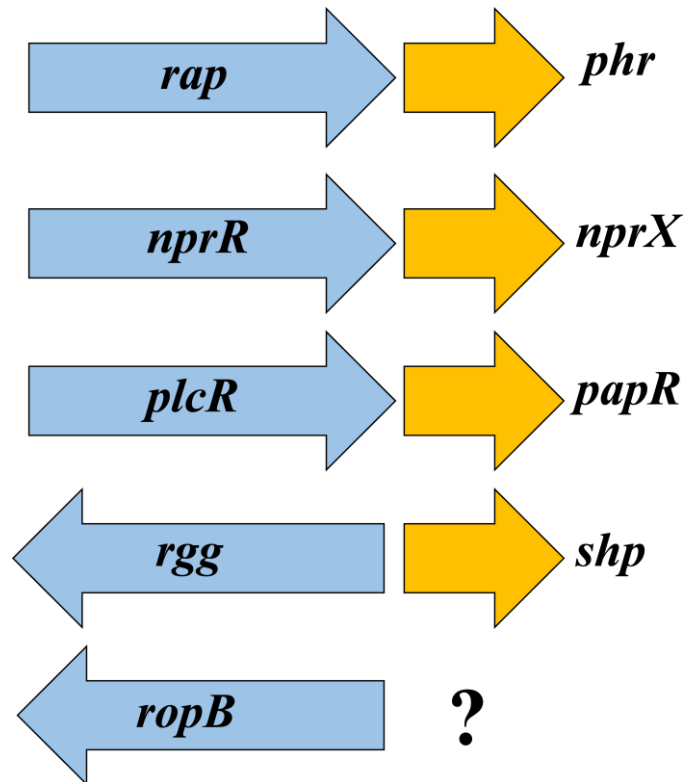


**Figure 8. Genetic location of RRNPP family regulators and their cognate peptide signals.** Blue arrows indicate the gene encoding the regulator and yellow arrows indicate the gene encoding the cognate peptide signal of the respective regulator. Transcription direction is indicated by the direction of the arrow.

## AIM AND SCOPE OF THE STUDY

Despite the significant advances in the understanding of structure and function of SpeB protease and its contribution to GAS pathogenesis, the precise molecular mechanisms governing *speB* gene regulation remain poorly understood (2). Given that the gene regulatory activity of RopB requires stationary growth phase-specific regulatory factor(s) and RopB shares structural homology with peptide-sensing RRNPP family of quorum-sensing regulators, we hypothesized that the factor responsible for stationary phase or high GAS population density-specific activation of *speB* expression is a peptide signal. Thus, the major goal of this study was to identify the peptide signal and characterize signaling mechanism during GAS growth *in vitro* and during infection.

To that end, the work presented in chapter 1 identifies and characterizes a novel peptide signal in the genetic vicinity of *ropB* that controls *speB* expression. However, the identified peptide signal is a leaderless peptide as it lacks several amino acid characteristics of characterized peptide signals. This lack of conformity hampered our initial efforts in the identification of peptide signal. Despite the lack of several traits of bacterial peptide signals, the cognate peptide signal for RopB is secreted, reimported into GAS cytosol, sensed by RopB, and control RopB-dependent *speB* gene expression. We further show the global impact of the peptide signal on the GAS transcriptome using RNA-sequencing studies. Finally, we show that the peptide signal pathway is active during infection and crucial for GAS virulence in multiple mouse models of infection.

In chapter 2, using *ex vivo* gene expression, mouse infection, and immunological studies, we show that the peptide signal pathway is active and control *speB* expression during GAS growth *ex vivo* in human saliva and blood. Importantly, we show that the peptide signaling pathway

contributes significantly to GAS survival *ex vivo* in human saliva and blood, and is critical for mouse oropharyngeal GAS colonization.

## CHAPTER 1

### **Leaderless secreted peptide signaling molecule alters global gene expression and increases virulence of a human bacterial pathogen**

Do H\*, **Makthal N\***, VanderWal AR, Rettel M, Savitski MM, Peschek N, Papenfort K, Olsen RJ, Musser JM, Kumaraswami M.

\*Equal contribution

Published: September 18<sup>th</sup> 2017. PNAS 114:E8498-E8507



# Leaderless secreted peptide signaling molecule alters global gene expression and increases virulence of a human bacterial pathogen

Hackwon Do<sup>a,b,1</sup>, Nishanth Makthal<sup>a,b,1</sup>, Arica R. VanderWal<sup>a,b</sup>, Mandy Rettel<sup>c</sup>, Mikhail M. Savitski<sup>c</sup>, Nikolai Peschek<sup>d</sup>, Kai Papenfort<sup>d</sup>, Randall J. Olsen<sup>a,b,e</sup>, James M. Musser<sup>a,b,e</sup>, and Muthiah Kumaraswami<sup>a,b,2</sup>

<sup>a</sup>Center for Molecular and Translational Human Infectious Diseases Research, Houston Methodist Research Institute, Houston Methodist Hospital, Houston, TX 77030; <sup>b</sup>Department of Pathology and Genomic Medicine, Houston Methodist Hospital, Houston, TX 77030; <sup>c</sup>Genome Biology Unit, European Molecular Biology Laboratory, 69117 Heidelberg, Germany; <sup>d</sup>Munich Center for Integrated Protein Science, Department of Microbiology, Ludwig Maximilians University of Munich, 82152 Martinsried, Germany; and <sup>e</sup>Department of Pathology and Laboratory Medicine, Weill Medical College of Cornell University, New York, NY 10021

Edited by Richard P. Novick, New York University School of Medicine, New York, NY, and approved August 2, 2017 (received for review April 18, 2017)

**Successful pathogens use complex signaling mechanisms to monitor their environment and reprogram global gene expression during specific stages of infection. Group A *Streptococcus* (GAS) is a major human pathogen that causes significant disease burden worldwide. A secreted cysteine protease known as streptococcal pyrogenic exotoxin B (SpeB) is a key virulence factor that is produced abundantly during infection and is critical for GAS pathogenesis. Although identified nearly a century ago, the molecular basis for growth phase control of *speB* gene expression remains unknown. We have discovered that GAS uses a previously unknown peptide-mediated intercellular signaling system to control SpeB production, alter global gene expression, and enhance virulence. GAS produces an eight-amino acid leaderless peptide [SpeB-inducing peptide (SIP)] during high cell density and uses the secreted peptide for cell-to-cell signaling to induce population-wide *speB* expression. The SIP signaling pathway includes peptide secretion, reimportation into the cytosol, and interaction with the intracellular global gene regulator Regulator of Protease B (RopB), resulting in SIP-dependent modulation of DNA binding and regulatory activity of RopB. Notably, SIP signaling causes differential expression of ~14% of GAS core genes. Several genes that encode toxins and other virulence genes that enhance pathogen dissemination and infection are significantly up-regulated. Using three mouse infection models, we show that the SIP signaling pathway is active during infection and contributes significantly to GAS pathogenesis at multiple host anatomic sites. Together, our results delineate the molecular mechanisms involved in a previously undescribed virulence regulatory pathway of an important human pathogen and suggest new therapeutic strategies.**

*Streptococcus pyogenes* | SpeB | virulence regulation | quorum sensing | leaderless peptide

**S**patiotemporal regulation of virulence factor production is a fundamental trait required to be a successful pathogen. Bacterial pathogens sense their environment at infection sites and respond by modulating expression of genes involved in pathogen–host interactions (1–6). In addition to host-derived signals, bacteria monitor their population density using secreted small molecules and modulate gene expression during high cell density by a process called quorum sensing (2, 7, 8). Quorum sensing includes production and secretion of signaling molecules, signal detection, and altered gene regulation (7–9). Typically, gram-positive bacteria use either linear or modified oligopeptides as quorum-sensing molecules to monitor their population density (7–9). Quorum sensing controls several bacterial properties, including virulence (7, 8). However, a direct link between quorum signaling and bacterial virulence is limited to the *agr* signaling pathway in *Staphylococcus aureus* and other related gram-positive pathogens (10).

Group A *Streptococcus* (GAS) is an exclusive human pathogen that causes a spectrum of diseases, including mild pharyngitis

(“strep throat”) and life-threatening necrotizing fasciitis (“flesh-eating disease”) (11, 12). GAS produces many bacterial surface-bound or secreted virulence factors, including superantigens, cytolytic toxins, and proteases (11, 12). Streptococcal pyrogenic exotoxin B (SpeB) is a potent secreted cysteine protease that functions as a major GAS virulence factor (13–20). SpeB is produced abundantly in infected humans and during experimental animal infection (13–19). The protease degrades various host proteins to contribute to tissue damage and cleaves bacterial cell-surface proteins to promote disease dissemination (14–19, 21, 22). Consistent with its documented significance in infection, interference strategies targeting SpeB or its proteolytic activity confer protection against GAS infection (23–26).

SpeB production *in vitro* is greatly up-regulated late in growth at high bacterial cell density (18, 27). Since the discovery of SpeB nearly a century ago, regulation of its biogenesis has been the focus of extensive investigation (18, 21, 22, 27–38). Several regulatory circuits converge on transcriptional and posttranscriptional control of SpeB production (18, 21, 22, 27–36). However, the exact molecular mechanism underlying cell density-dependent up-regulation of SpeB has remained elusive. The Regulator of Protease B (RopB), a global gene regulator, directly controls *speB* expression

## Significance

Regulation of virulence factor production is critical for bacterial pathogenesis. The human pathogen group A *Streptococcus* (GAS) produces a potent secreted protease, streptococcal pyrogenic exotoxin B (SpeB), that is crucial for pathogenesis. Although it is known that GAS produces SpeB at high population density, the molecular mechanism whereby GAS coordinates temporal SpeB production is unknown. Here, we identify a GAS-encoded short leaderless intercellular peptide signal [SpeB-inducing peptide (SIP)], and define the mechanism by which SIP induces population-wide SpeB production and contributes to GAS virulence. Furthermore, discovery of SIP provides a framework for the identification of SIP-like leaderless peptide signals in other microorganisms. Thus, our data reveal a paradigm of bacterial signaling and identify previously unknown molecules that may serve as therapeutic targets.

Author contributions: H.D., N.M., M.M.S., K.P., R.J.O., and M.K. designed research; H.D., N.M., A.R.V., M.R., M.M.S., N.P., K.P., R.J.O., and M.K. performed research; H.D., N.M., A.R.V., M.R., M.M.S., N.P., K.P., R.J.O., J.M.M., and M.K. analyzed data; and H.D., N.M., M.M.S., K.P., J.M.M., and M.K. wrote the paper.

The authors declare no conflict of interest.

This article is a PNAS Direct Submission.

<sup>1</sup>H.D. and N.M. contributed equally to this work.

<sup>2</sup>To whom correspondence should be addressed. Email: mkumaraswami@houstonmethodist.org.

This article contains supporting information online at [www.pnas.org/lookup/suppl/doi:10.1073/pnas.1705972114/-DCSupplemental](http://www.pnas.org/lookup/suppl/doi:10.1073/pnas.1705972114/-DCSupplemental).

during the stationary growth phase (18, 22, 27, 35). Although RopB is indispensable for growth phase-dependent transcription of *speB*, RopB alone is not sufficient to activate *speB* expression; additional unknown cell density-specific regulatory factors are required (27, 35). Consistent with this, recent findings suggest that transcriptional regulation of *speB* is controlled by a RopB-dependent quorum-sensing signaling pathway (18, 35). Several lines of evidence support this model, which includes cell density-dependent regulation of *speB*, structural homology of RopB with the Rgg-Rap-NprR-PlcR-PrgX (RRNPP) family of quorum-sensing transcription regulators, and antagonistic effects of cell density-specific secreted proteinaceous factors on *speB* expression (18, 35, 39). However, due to the lack of precise delineation of all necessary genetic and biochemical regulatory signals, quorum-sensing regulation of *speB* expression remains only a formal possibility.

We here report that GAS uses a short peptide-mediated intercellular communication mechanism to modulate virulence gene expression in a cell density-dependent fashion. The short peptide lacks a secretion signal sequence. Our results support a model in which the leaderless peptide is produced by GAS at high cell density, secreted extracellularly, imported into the cytosol, and subsequently interacts with RopB. Peptide binding to RopB promotes high-affinity RopB-DNA interactions and RopB polymerization, resulting in activation of RopB-dependent *speB* expression. Importantly, we show that this peptide signaling pathway is active during infection and contributes significantly to GAS virulence in multiple mouse models of infection.

## Results

**The *ropB-speB* Intergenic Region Encodes a Factor That Up-Regulates *speB* Expression.** The structural homologs of RopB have their cognate regulatory peptides encoded in their immediate genomic vicinity (SI Appendix, Fig. S1A). Thus, we analyzed the 940-bp *ropB-speB* intergenic region for ability to alter *speB* expression (Fig. 1A). To identify the region that may encode an activation factor, we constructed three *trans*-complementation plasmids that contain different fragments of the intergenic region (Fig. 1B and C). Typically, gene expression is higher from a multicopy plasmid than the chromosome (SI Appendix, Fig. S1B). Thus, we hypothesized that higher expression levels of a gene encoding the putative activation factor will decouple growth phase-dependent *speB* expression. To test this hypothesis, we introduced each of the three plasmids into wild-type (WT) GAS and characterized the resulting strains for early onset of *speB* expression by qRT-PCR. Relative to the WT strain, each of the three intergenic fragments caused an 8- to 14-fold increase in *speB* transcript level in the late exponential phase of growth. These results suggest that the activation factor for *speB* expression is likely encoded within the shortest of the three fragments, that is, the 257-bp fragment located between -775 and -519 bp upstream of the *SpeB* translation start site (Fig. 1A and B).

Analysis of the 940-bp intergenic region identified three hypothetical ORFs (*orf*), termed *orf-1*, *orf-2*, and *orf-3* (Fig. 1A). Given that the intergenic region contains *cis*-acting regulatory elements required for *speB* expression (27), genetic alterations within the promoter in the form of nucleotide deletions or insertions might disrupt the regulatory elements and spacing between the regulatory elements in the promoter. Thus, to preserve the overall architecture of the promoter, we constructed isogenic mutant strains that replace the start codon (ATG) of each *orf* with a stop codon (TAG) in the chromosome. None of the resulting three mutant strains grew differently than the WT strain (SI Appendix, Fig. S1C). Translational disruption of *orf-1* (i.e., *orf-1*\* mutant) abolished *speB* expression, *SpeB* protein levels, and *SpeB* protease activity (Fig. 1D-F and SI Appendix, Fig. S2). The transcript level of *speB* made by the *orf-1*\* mutant strain was comparable to that of the  $\Delta$ *ropB* mutant, suggesting that *orf-1* is a crucial factor in *speB* transcriptional regulation

(Fig. 1D-F). In contrast, the *orf-2*\* and *orf-3*\* mutant strains had WT-like *speB* transcript levels, suggesting that the putative polypeptides encoded by *orf-2* and *orf-3* are dispensable for *speB* expression (Fig. 1D-F). Provision of *orf-1* alone in *trans* (*pDC-orf-1*) was sufficient to rescue the defective phenotype of the *orf-1*\* mutant. Phenotype restoration in the *orf-1*\* mutant by the *trans*-complementation plasmid was reversed by translational disruption of *orf-1* in *trans* (*pDC-orf-1*\*) (Fig. 1D and F and SI Appendix, Figs. S2 and S3). To exclude the possibility that defective *speB* expression in the *orf-1*\* mutant is due to altered *ropB* expression, we measured the transcript levels of *ropB* in the WT, *orf-1*\* mutant, and *trans*-complemented strains. The transcript levels of *ropB* during different phases of growth in the *orf-1*\* mutant were comparable to those of WT and *trans*-complemented strains, suggesting that the nonsense substitution in the start codon of *orf-1* does not affect the expression of divergently transcribed *ropB* (SI Appendix, Fig. S4). Together, these results suggest that the observed phenotype of the *orf-1*\* mutant strain is caused by genetic inactivation of *orf-1*, not by promoter alterations (Fig. 1D-F and SI Appendix, Figs. S3 and S4). Importantly, *trans*-complementation plasmid *pDC-orf-1* failed to restore *speB* expression in the  $\Delta$ *ropB* mutant strain (Fig. 1D), indicating that the regulatory activity of the *orf-1* gene product requires RopB. Collectively, these data indicate that *orf-1* encodes the activation factor for RopB-dependent *speB* expression. For the purpose of clarity, due to its ability to induce *speB* expression, we will refer to the putative eight-amino acid polypeptide corresponding to the *orf-1* gene product as *SpeB*-inducing peptide (SIP).

## A GAS-Encoded Short Peptide Signal Activates RopB-Dependent *speB* Expression.

To determine if *orf-1* is transcribed, we performed Northern blot analysis using a probe complementary to *orf-1*. Consistent with the polycistronic nature of *speB* transcripts (34, 40), several bands ranging in size between 300 and 1,500 bases corresponding to the *orf-1* transcript were detected (Fig. 2A). Importantly, the *orf-1* transcript was detected only in WT GAS grown to the stationary phase, indicating that *orf-1* is expressed at high cell density (Fig. 2A). To investigate if the predicted short peptide encoded by *orf-1* acts as an intercellular signal and activates *speB* expression, we conducted two synthetic peptide addition experiments. First, synthetic peptides containing different fragments of SIP were tested for their ability to restore *speB* expression to an *orf-1*\* mutant (Fig. 2B). When the *orf-1*\* mutant strain was grown to stationary phase and supplemented with synthetic peptides of varying length, only the full-length SIP (SIP-1) caused robust induction of *speB* expression (>630 fold) and restored WT-like *speB* transcript levels, secreted *SpeB* levels, and *SpeB* protease activity (Fig. 2B-D). Synthetic peptide SIP-5 containing the N-terminal seven amino acids had weaker activity (>30 fold), whereas all other tested synthetic peptides failed to activate *speB* transcription (Fig. 2B-D). Second, we also tested the ability of SIP to cause early induction of *speB* expression by WT GAS. Consistent with our observations derived from the *orf-1*\* mutant strain, peptide SIP-1 decoupled growth phase dependency of *speB* expression and induced early onset of *speB* expression by the WT strain (>130 fold) in the late exponential growth phase (Fig. 2E).

To determine if the observed *speB* induction is specific for the primary amino acid sequence of SIP, we conducted analogous experiments with a scrambled (SCRA) peptide of identical length and amino acid composition of SIP (Fig. 2B). Importantly, SCRA peptide did not activate *speB* expression in either the *orf-1*\* mutant or WT strain. These results are consistent with the interpretation that induction is specific for SIP (Fig. 2B-E). As expected, addition of SIP-1 to the isogenic  $\Delta$ *ropB* mutant strain did not induce *speB* transcript production (Fig. 2B), even when SIP was added at 300-fold excess (Fig. 2B). Together, these data indicate that amino acid sequences corresponding to SIP-1 are

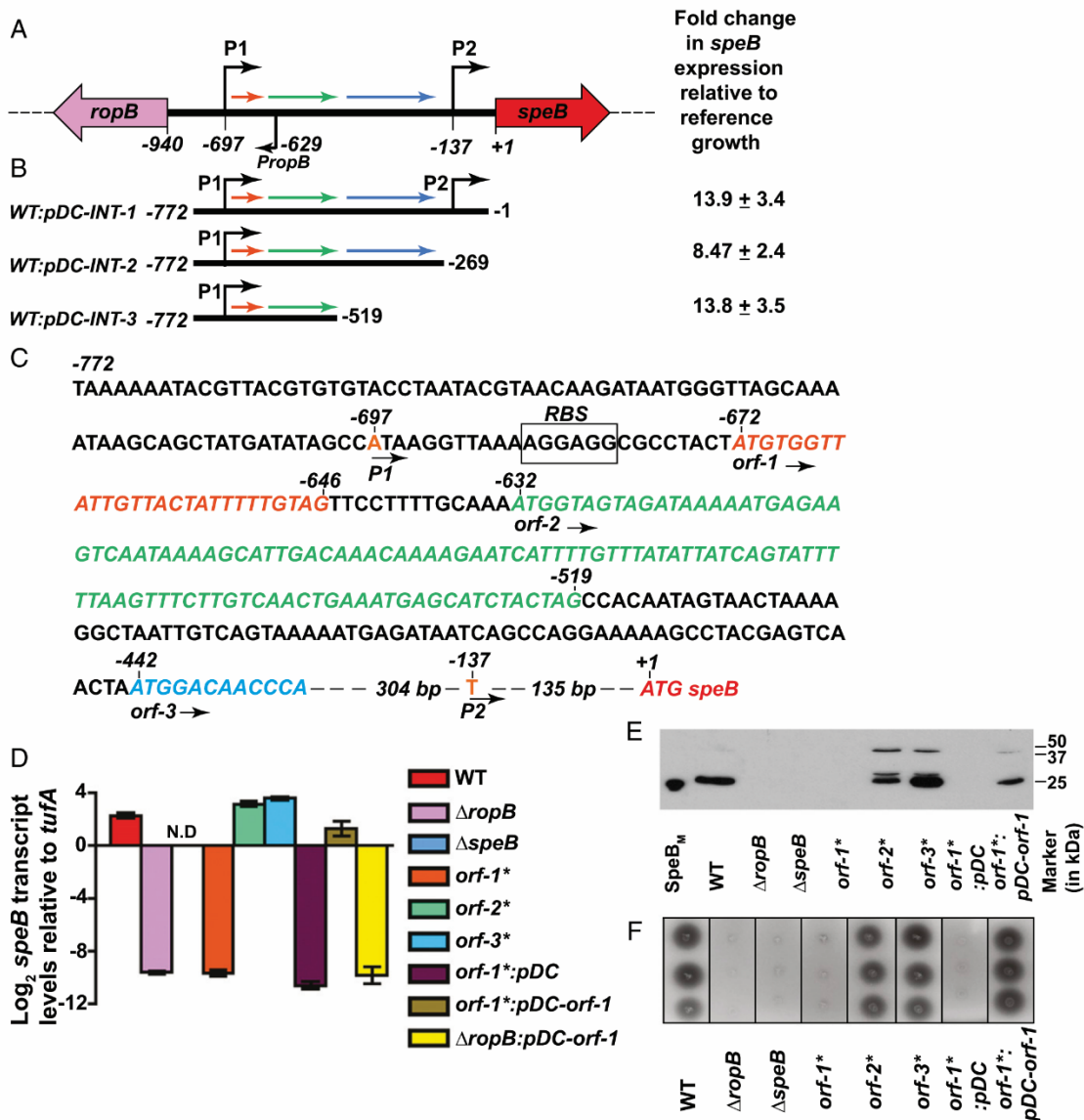


**Fig. 1.** The *ropB-speB* intergenic region has the genetic element encoding the activation peptide signal for RopB-dependent *speB* expression. (A) Organization of the *ropB* and *speB* gene region in GAS. The *ropB* and *speB* genes are divergently transcribed. The angled arrows above the line indicate two transcription start sites for *speB*, designated P1 and P2. The angled arrow below the line indicates the transcription start site for *ropB* (*PropB*). The intergenic region with three predicted ORFs, designated *orf-1* (orange), *orf-2* (green), and *orf-3* (blue), is shown as horizontal arrows. (B) Characterization of the sequences in the *ropB-speB* intergenic region for their role in *speB* expression. High-copy-number plasmids containing different fragments of the intergenic region were introduced individually into WT GAS, and the resulting strains were characterized for premature induction of *speB* expression. Cells were grown to the late exponential growth phase ( $A_{600} \sim 1.0$ ), and *speB* transcript levels were assessed by qRT-PCR. Numbers at either end of the constructs indicate the nucleotide positions relative to the first nucleotide of the *speB* start codon. Fold changes in *speB* transcript levels in the *trans*-complemented strains relative to reference GAS growth are shown. WT GAS (WT: empty vector) grown to late exponential growth was used as the reference. (C) Nucleotide sequence characteristics of the *ropB-speB* intergenic region. The numbers above the nucleotides indicate positions relative to the first nucleotide of the *speB* start codon. Nucleotides corresponding to transcription start sites P1 and P2 are highlighted in orange. Nucleotide sequences of *orf-1*, *orf-2*, *orf-3*, and *speB* are italicized and colored in red. An inferred ribosomal-binding site (RBS) located upstream of *orf-1* is boxed and labeled. (D) Analysis of *speB* transcript levels in the indicated strains as determined by qRT-PCR. N.D., not detected. (E) Western immunoblot analysis of secreted SpeB in filtered growth media from indicated strains. Growth media samples were probed with anti-SpeB polyclonal rabbit antibody and chemiluminescence. The masses of molecular weight markers in kilodaltons (kDa) are shown. The mature form of purified recombinant SpeB (SpeB<sub>M</sub>; 25 kDa) was used as a marker. (F) Milk plate clearing assay to assess SpeB protease activity in indicated strains. Protease activity was determined by the presence of a clear zone around the bacterial growth.

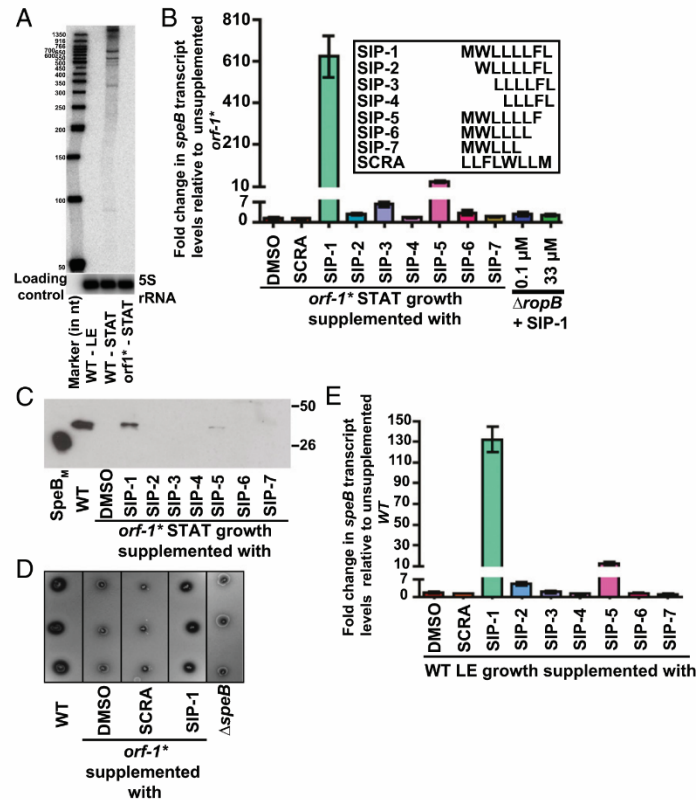


**Fig. 2.** Synthetic peptides containing the amino acid sequences of SIP activate *speB* expression. (A) The *orf1* gene, encoding SIP, is expressed during the stationary phase of GAS growth. Total RNA extracted from WT GAS grown to either the late exponential (LE;  $A_{600} \sim 1.0$ ) or stationary (STAT) phase of growth and *orf1\** mutant grown to the STAT phase of growth were analyzed by Northern blot. (B, Inset) Amino acid sequences of the synthetic peptides (SIP-1–SIP-7) used in the experiment. (B) SCRA peptide of an identical length and amino acid composition as SIP-1 but differing in the order of sequence was used as a negative control. The *orf1\** mutant strain was grown in chemically defined medium (CDM) to the early STAT phase ( $A_{600} \sim 1.7$ ) and supplemented with either 100 nM indicated synthetic peptide or the carrier for the synthetic peptides (DMSO). After 60 min of incubation, transcript levels of *speB* were assessed by qRT-PCR. The *orf1\** mutant strain supplemented with DMSO was used as a reference, and fold changes in *speB* transcript levels relative to the reference are shown. (C) Western immunoblot analysis of secreted SpeB in filtered growth media from the indicated samples. Cell growth and synthetic peptide supplementation were performed as described in A. Growth media collected were probed with anti-SpeB polyclonal rabbit antibody and detected by chemiluminescence. The masses of molecular weight markers in kilodaltons (kDa) are marked. (D) Milk plate clearing assay to assess the ability of various SIPs to induce SpeB protease activity in the *orf1\** mutant. (E) Addition of SIP-1 and SIP-5 decouples the growth phase dependency of *speB* expression in WT GAS. The WT GAS was grown in CDM to the mid-exponential growth phase ( $A_{600} \sim 0.6$ ), and cells were incubated with 100 nM of each synthetic peptide for 60 min. Transcript levels of *speB* were assessed by qRT-PCR, and the fold change in *speB* expression relative to DMSO-supplemented growth is shown.

the high cell density-specific activation peptide signal for RopB-dependent *speB* expression.

**Molecular Mechanism of GAS Intercellular Signaling.** Most of the characterized peptide signals in gram-positive bacteria are generated by proteolytic processing of a precursor propeptide form into mature active peptide by membrane-bound enhanced expression of pheromone (Eep) protease (41–44). However, SIP is unique in that it is made as a mature leaderless peptide (Fig. 3A). The extracellular mature peptides are subsequently reinternalized into the bacterial cytosol by oligopeptide permeases (Opp) (41, 45, 46). Consistent with this process, inactivation of *opp* or dipeptide permease (*dpp*) in GAS caused down-regulation of *speB* expression (47, 48). To test the hypothesis that SIP biosynthesis involves similar molecular mechanisms, we constructed isogenic single-mutant strains of *eep* ( $\Delta eep$ ), *opp* ( $\Delta oppDF$ ), or *dpp*

( $\Delta dppA$ ) and the double mutant,  $\Delta oppDF/\Delta dppA$ . When tested for *speB* expression, all four mutant strains had WT-like *speB* transcript levels and protease activity (Fig. 3B and C), indicating that the *eep*, *opp*, and *dpp* genes are not involved in SIP signaling.

To address the lack of influence of Opp and Dpp permeases on SIP signaling, we considered two possibilities: (i) SIP is not secreted, and thus does not require active import by peptide permeases, or (ii) SIP is secreted and internalized by a yet-to-be-identified mechanism. The results from secretome swap assays and synthetic peptide addition experiments suggest that SIP is secreted and internalized into the cytosol (35) (Fig. 2). To test the hypothesis that the regulatory factor in the secretome is encoded by the *sip* gene, we performed secretome swap assays using conditioned medium obtained from the WT or *orf1\** mutant strain. Consistent with our hypothesis, compared with the WT secretome, inactivation of SIP in the *orf1\** mutant resulted



into the bacterial cytoplasm using synthetic SIP peptide containing fluorescein modification at its amino terminus (FITC-SIP-1) (Fig. 3E). Peptide addition experiments with FITC-SIP-1 demonstrated that the modified FITC-SIP-1 is functional and retained the ability to induce *speB* expression in the *orf-1*\* mutant strain similar to unmodified SIP-1 (SI Appendix, Fig. S5). To determine if FITC-SIP-1 is reimported into the bacterial cytoplasm, we incubated the *orf-1*\* mutant with FITC-SIP-1 and assessed the cytosolic presence of FITC-SIP-1 by measuring the relative fluorescence in the clarified cell lysates. An FITC-SIP-1 concentration-dependent increase in fluorescence was observed in the cell lysates from FITC-SIP-1-treated samples compared with SIP-1-treated or untreated GAS (Fig. 3E). Next, we investigated the cytosolic presence of FITC-SIP-1 in the *orf-1*\* mutant strain by confocal microscopy. The fluorescence signal was present in the cytoplasm of GAS cells incubated with FITC-SIP-1, whereas no fluorescent signal was detected in the un-supplemented or unmodified SIP-1-supplemented GAS growth (Fig. 3F). These results are consistent with the interpretation that exogenously added FITC-SIP-1 is transported into the bacterial cytoplasm. To test the presence of additional import mechanisms, we constructed a triple-mutant strain ( $\Delta oppDF/\Delta dppA/orf-1^*$ ) in which the *orf-1*\* mutation was introduced into the isogenic double-mutant strain,  $\Delta oppDF/\Delta dppA$ . Expression of *speB* in this triple-mutant strain is dependent entirely on exogenously provided synthetic SIP peptide. Thus, we measured *speB* transcript levels in the triple-mutant strain grown in the presence or absence of exogenously added SIP. As observed in the *orf-1*\* mutant strain, addition of SIP restored WT levels of *speB* expression and SpeB protease activity in the triple mutant (Fig. 3B and C). Together, these data indicate that secreted SIP is reimported into the bacterial cytosol, and that GAS uses specialized export and import mechanisms for SIP signaling that are distinct from other characterized bacterial peptide signaling pathways.

To obtain information about the molecular mechanism of gene regulation by SIP, we used a fluorescence polarization (FP) assay to test the hypothesis that SIP directly interacts with RopB. RopB bound directly to SIP with a  $K_d$  of  $\sim 2.6$  nM, indicating a very high-affinity interaction between the two partners (Fig. 4A). This strong interaction was disrupted only by the addition of unlabeled SIP, indicating that the RopB-SIP interaction is sequence specific (Fig. 4B). To understand the downstream mechanistic consequences of RopB-SIP interaction, we first assessed the effect of SIP binding on RopB-DNA interactions using an oligoduplex containing the putative RopB-binding site located upstream of the P1 promoter (27) (Fig. 4C and D). Although apo-RopB had the ability to mediate sequence-specific DNA interactions ( $K_d$  of  $\sim 352$  nM) (Fig. 4E), SIP binding caused a ninefold increase in the affinity of the SIP-bound form of RopB for DNA ( $K_d$  of  $\sim 38$  nM) (Fig. 4F). These results suggest that SIP binding promotes high-affinity RopB-DNA interactions.

To further study RopB-DNA interactions, we analyzed the DNA-binding properties of RopB by electrophoretic mobility shift assay (EMSA). RopB bound to promoter sequences containing RopB-binding sites that are located upstream of the P1 promoter, whereas it failed to bind sequences upstream of the P2 promoter that lack the RopB-binding site, indicating that these interactions are sequence specific (SI Appendix, Fig. S6). However, no SIP-induced differences in RopB-DNA interactions were observed, as both apo- and SIP-bound RopB had similar DNA-binding properties (SI Appendix, Fig. S6). Given that apo-RopB binds DNA with relatively high affinity (Fig. 3E), it is likely that the sensitivity of EMSA is not sufficient to distinguish the differences in DNA-binding affinities of apo- and SIP-bound RopB. We also observed that RopB at higher concentrations formed multiple supershifted RopB-DNA complexes, suggesting that RopB multimerizes on the promoter sequences (SI Appendix, Fig. S6B and C). Finally, to rule out the possibility that the defective *speB* expression in the *orf-1*\* mutant is not due to impaired RopB binding to *speB* promoter

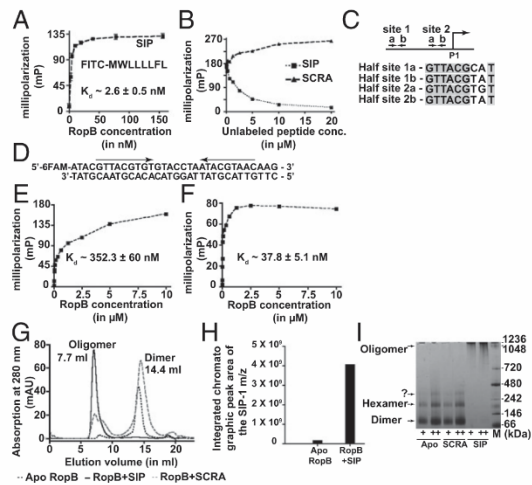


**Fig. 4.** SIP directly interacts with RopB and controls gene regulation by inducing allosteric changes in RopB. (A) Analysis of the binding between purified RopB and fluoresceinated SIP by an FP assay. (B) Ability of SIP or SCRA peptide to compete with the FITC-labeled SIP-RopB complex for binding. A preformed RopB (350 nM)-labeled SIP (10 nM) complex was titrated with the indicated unlabeled peptides. (C) Schematics of the location of RopB-binding sites within the P1 promoter. The transcription start site of the P1 promoter is shown as bent arrows, whereas the two RopB-binding sites with the inverted repeats are marked as arrows. Alignment of the nine-base-long nucleotide sequences of the RopB-binding half-sites from site 1 and site 2 are aligned from a 5'–3' direction, and the identical bases among the half-sites are shaded in gray. (D) Nucleotide sequence of the RopB-binding site used in the binding studies is shown. The pseudoinverted repeat within the RopB-binding site is marked by arrows. Analysis of the binding between the FITC-labeled oligoduplex containing the putative RopB-binding site and apo-RopB (E) or SIP-bound RopB (F) by FP assay is shown. (G) Size exclusion chromatography analysis of purified RopB with or without the presence of either synthetic SIP or SCRA peptide. Molecular masses were calculated based on the calibration curve using molecular weight standards. (H) Mass spectrometry analyses of the apo- or SIP-bound RopB complex purified as described in E for the presence of SIP. (I) Increasing concentrations of the apo- or peptide-bound form of RopB (+, 1.5  $\mu$ g; ++, 3  $\mu$ g) were analyzed by Blu-native PAGE. The oligomeric forms of RopB, assessed based on the molecular weight marker [M; in kilodaltons (kDa)], are labeled.

sequences, we carried out EMSA studies using *speB* promoter sequences from the WT or *orf-1*\* mutant strain. We observed no significant differences in RopB interactions with the WT and *orf-1*\* promoters (SI Appendix, Fig. S7). These data add further support to our conclusion that translation disruption of *orf-1* is the underlying cause for the defective *speB* expression in the *orf-1*\* mutant strain.

Purified apo-RopB typically eluted as a homodimer during size exclusion chromatography (Fig. 4G). However, we observed that the addition of SIP caused a shift from RopB dimer to a higher order oligomer much larger than a dodecamer (Fig. 4G). Mass spectrometry analysis of the oligomer fractionated by size exclusion chromatography confirmed that the oligomeric RopB contains bound SIP, indicating that SIP binding induces RopB oligomerization (Fig. 4G and H). These results were further confirmed by Blu-native PAGE analysis of RopB in the presence or absence of SIP. Although apo-RopB had the tendency to oligomerize, the higher order oligomeric form of RopB was stabilized only by SIP binding (Fig. 4I and SI Appendix, Fig. S8). To probe the structural components of RopB involved in SIP-dependent oligomerization, we conducted similar experiments using the C-terminal domain (residues 56–280) of RopB (RopB-

CTD) (35). Interestingly, SIP failed to induce RopB-CTD oligomerization (SI Appendix, Fig. S9), suggesting that an intact DNA-binding domain (residues 1–55) is required for SIP-dependent RopB oligomerization. To investigate if RopB binds DNA in both dimeric and oligomeric forms, we conducted EMSA with purified RopB dimer coincubated with SIP and DNA, or preformed RopB-SIP oligomer fractionated by size exclusion chromatography (Fig. 4G). Consistent with previous results, RopB dimer formed higher order RopB-SIP-DNA complex, whereas preformed RopB-SIP oligomer failed to bind DNA (SI Appendix, Fig. S10). These results indicate that the preformed RopB-SIP oligomer is not compatible for DNA binding and that SIP-induced high-affinity RopB-DNA interactions precede RopB multimerization. Together, the data suggest that SIP directly interacts with RopB and modulates gene regulation by inducing a two-pronged allostery in RopB, namely, high-affinity RopB-DNA interactions and RopB polymerization.

**Global Gene Regulatory Influence of SIP Signaling Pathway.** To test the hypothesis that SIP controls a global quorum-sensing regulon, we constructed an isogenic  $\Delta orf-1$  mutant strain with an in-frame deletion of the entire SIP coding region. Deletion of *orf-1* abolished *speB* expression, and addition of synthetic SIP peptide restored WT-like *speB* transcription and SpeB protease activity in the  $\Delta orf-1$  mutant, indicating the nonpolar nature of the  $\Delta orf-1$  mutant (SI Appendix, Fig. S11). We next used RNA-sequencing (RNA-seq) analysis to compare the global transcript profiles of the WT and  $\Delta orf-1$  mutant strains grown to stationary phase. Compared with the WT strain, 271 genes (14% of the GAS core chromosome,  $P < 0.05$ , and twofold differences) were differentially regulated in the  $\Delta orf-1$  mutant strain, of which 228 genes were up-regulated and 43 genes were down-regulated (SI Appendix, Tables S1 and S2). As expected, the level of *speB* transcript was drastically down-regulated in the  $\Delta orf-1$  mutant strain (>2,000-fold reduction) relative to the WT strain (SI Appendix, Fig. S12). Additional genes that were significantly down-regulated in the  $\Delta orf-1$  mutant include genes that encode known virulence factors, such as SagP, NdoS, Sdn, and HlyIII (SI Appendix, Table S1). Conversely, the up-regulated genes in the  $\Delta orf-1$  mutant strain belong to the following categories: (i) de novo protein synthesis (*rps*, *rpl*, and *rpm* operons that encode ribosomal subunits), (ii) DNA synthesis (*pyr*, *pur*, *guaAB*, *nrd*, *carAB*, and *rexAB* operons), (iii) cell wall synthesis and cell division (*murB*, *murN*, *pgdA*, *smc*, and *divIVA*), (iv) group A carbohydrate antigen synthesis (*rgpBCDEFG* operon), (v) transporters involved in nutrient acquisition (*dpp*, *opp*, and *pot* operons), (vi) proteases (*pcp*, *pepB*, *pepN*, *pepO*, *pepXP*, *cppA*, and *clpX*), and (vii) cell surface protein (*grab*) (SI Appendix, Table S2).

To further understand the effect of SIP on global gene regulation, we also performed RNA-seq analysis of WT and *orf-1*\* mutant strains grown to stationary phase. Compared with the WT strain, 72 genes (4% of the GAS core chromosome,  $P < 0.05$ , and twofold differences) were differentially expressed in the *orf-1*\* mutant strain, of which 31 genes were up-regulated and 41 genes were down-regulated (SI Appendix, Tables S3 and S4). As observed in the  $\Delta orf-1$  mutant strain, the level of *speB*, *spi*, and *orf-3* (*SpyM3\_1743*) transcripts was drastically down-regulated in the *orf-1*\* mutant strain (>1,300-fold reduction) relative to the WT strain (SI Appendix, Fig. S12). However, the SIP regulon identified in the *orf-1*\* mutant strain is relatively smaller compared with that of the  $\Delta orf-1$  mutant strain. To understand the differences in the global gene regulatory influence of SIP between *orf-1*\* and  $\Delta orf-1$  mutant strains, we compared the RNA-seq reads from the *orf-1*\* and  $\Delta orf-1$  mutant strains within the *ropB-speB* gene loci (SI Appendix, Fig. S12). Interestingly, the level of *ropB* transcript was significantly up-regulated in the  $\Delta orf-1$  mutant strain relative to the WT strain (greater than threefold increase) (SI Appendix, Fig. S12 and

Table S2), whereas no significant difference in the *ropB* transcript level was observed in the *orf-1*\* mutant strain. Thus, it is possible that transcription activation of *speB*, *spi*, and *orf-3* (*SpyM3\_1743*) by RopB is SIP-dependent; however, RopB has additional SIP-independent regulatory roles that may contribute to the larger regulon observed in the  $\Delta orf-1$  mutant strain. Together, the global transcriptome data demonstrate that the SIP signaling pathway directly or indirectly up-regulates the expression of several secreted virulence factors, including SpeB.

**RopB-SIP Signaling Pathway Is Required for WT GAS Virulence.** To test the hypothesis that the RopB-SIP signaling pathway participates in GAS pathogenesis, we compared the virulence of the

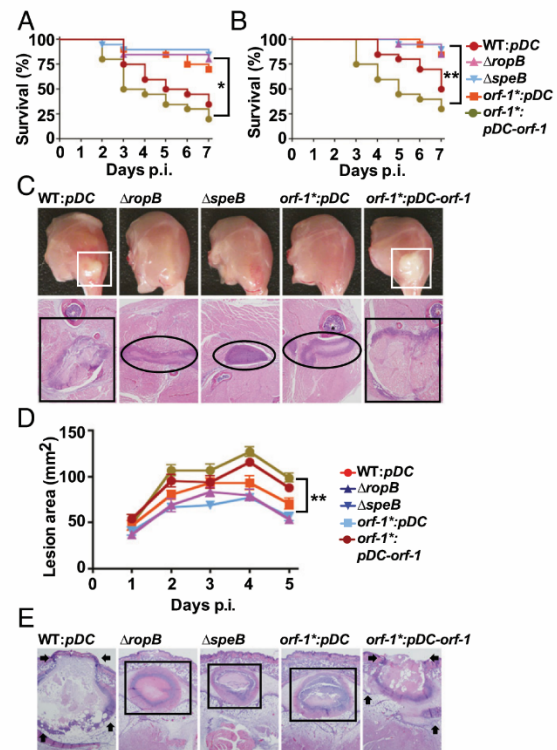


**Fig. 5.** SIP-mediated regulation of virulence genes is critical for GAS pathogenesis in mouse models of infection. (A) Twenty outbred CD-1 mice were inoculated i.p. with each indicated strain. Kaplan-Meier survival curves with  $P$  values derived by the log-rank test are shown. p.i., postinfection. (B) Twenty outbred CD-1 mice per strain were injected i.m. with each indicated strain. Kaplan-Meier survival curves with  $P$  values derived by the log-rank-test are shown. (C) Gross (Top) and microscopic (Bottom) analyses of hind-limb lesions from mice infected with each indicated strain. (Top) Larger lesions with extensive tissue damage in SpeB-expressing strains are boxed (white boxes). (Bottom) Areas of disseminated lesions in the infected tissues are boxed (black box), whereas confined, less destructive lesions are circled. (D) Fifteen immunocompetent hairless mice were infected s.c. with each indicated strain, and the lesion area produced by each strain was determined. The lesion area was measured and graphed (mean  $\pm$  SEM). The  $P$  value was derived by two-way ANOVA. (E) Histopathologic analysis of lesions from mice infected s.c. with each indicated strain. Areas of disseminated lesions and ulcerations on the skin surfaces caused by SpeB-producing strains are marked by arrows, whereas confined, less destructive lesions caused by SpeB-deficient strains are boxed. [Scale bars: C and E, 2.2 mm  $\times$  1.7 mm (y axis  $\times$  x axis) at 4 $\times$  magnification.]

WT and *orf-1*\* mutant strains in a mouse model of bacteremia (17, 49, 50). Consistent with its key role in SpeB production, the virulence of the *orf-1*\* mutant strain was significantly attenuated relative to the WT strain and comparable to that of the  $\Delta$ *ropB* and  $\Delta$ *speB* mutant strains that lack SpeB production (Fig. 5A). Next, we tested if SIP signaling is also critical for GAS virulence in invasive disease using a mouse model of necrotizing myositis (17, 49, 50). The *orf-1*\* mutant strain was significantly less virulent than the WT and *trans*-complemented strains (Fig. 5B). Inasmuch as SpeB contributes to host tissue damage and disease dissemination (14–18, 22, 51), we also investigated lesion character by visual and microscopic examination. Consistent with the virulence phenotype, the *orf-1*\*,  $\Delta$ *ropB*, and  $\Delta$ *speB* mutant strains caused smaller muscle lesions with less severe tissue destruction relative to WT and *trans*-complemented strains (Fig. 5C). Finally, we tested if the RopB-SIP signaling pathway contributes to GAS virulence in a mouse model of skin and soft tissue infection (17, 49, 50). Compared with WT and *trans*-complemented strains, the *orf-1*\*,  $\Delta$ *ropB*, and  $\Delta$ *speB* mutant strains caused significantly smaller and more confined lesions (Fig. 5D) with less tissue damage and ulceration (Fig. 5E). Together, these virulence data demonstrate that the RopB-SIP signaling pathway significantly contributes to GAS pathogenesis at multiple anatomic sites.

**RopB-SIP Signaling Pathway Is Active During Mouse Infection.** We next investigated if the RopB-SIP-mediated quorum-sensing pathway controls *speB* expression in vivo during the course of infection. Mice were inoculated s.c. with each of the indicated strains, and *speB* transcript levels in the infected lesions were measured by qRT-PCR. Compared with the WT strain grown to the late exponential phase in laboratory medium, the WT strain isolated from infected lesions had a 3,000-fold higher level of *speB* transcript (Fig. 6A). Consistent with the in vitro observations, lesions from mice infected with  $\Delta$ *ropB* and *orf-1*\* mutants had drastically decreased *speB* expression in vivo and *speB* transcript levels were comparable to those of the WT strain in the late exponential growth phase (Fig. 6A). Importantly, *trans*-complementation of the *orf-1*\* mutant strain with *pDC-orf-1* fully restored WT-like *speB* transcript levels, indicating that SIP-mediated *speB* regulation occurs in vivo (Fig. 6A). Finally, we assessed the ability of synthetic peptide SIP to activate *speB* expression in vivo and promote bacterial virulence using the s.c. mouse model of infection. Coinjection with SIP restored a WT-like virulence phenotype to the *orf-1*\* mutant strain, resulting in larger ulcerated lesions relative to *orf-1*\* mutant coinjected with the SCRA peptide (Fig. 6B–D). These data indicate that synthetic peptides containing the SIP amino acid sequences have biological activity in vivo, and are sufficient to restore GAS pathogenesis in the *orf-1*\* mutant strain. Collectively, our data demonstrate that SIP signaling is active during host infection and, moreover, show that SIP-mediated up-regulation of virulence gene expression contributes significantly to GAS virulence.

### Discussion

In the aggregate, we here show that GAS uses complex intercellular communication machinery to monitor its population density and determine whether to initiate a virulent lifestyle that involves host tissue damage and disease dissemination. The results presented herein show that an intercellular peptide signal, SIP, and the intracellular global gene regulator RopB form a signal/receptor pair that contributes significantly to GAS pathogenesis by modulating virulence gene expression. Importantly, the nucleotide sequence encoding the inferred eight amino acids of SIP is absolutely conserved, and the promoter sequences upstream of the SIP-coding region are highly conserved among 11 different GAS serotypes (SI Appendix, Fig. S13). Thus, the

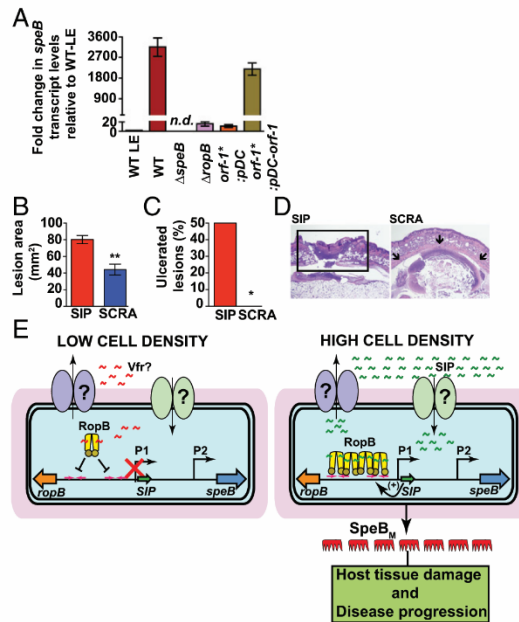


**Fig. 6.** SIP signaling controls *speB* expression during infection. (A) Analysis of the *speB* transcript level in the s.c. lesions from mice infected with the indicated strains. Samples were collected 24 h postinfection (P.I.) from the lesions of four mice per strain and analyzed in triplicate. Data were graphed as mean SD, with *P* values derived from a two-sample *t* test. Ten immunocompetent hairless mice per group were infected s.c. with the *orf-1*\* mutant coinjected with either 10  $\mu$ g of synthetic SIP or SCRA peptide. LE, late exponential GAS growth in laboratory medium. The lesion area (B) and ulceration (C) caused by each peptide at 24 h P.I. were determined. The lesion area was measured and graphed (mean  $\pm$  SEM). The *P* value was derived by the Mann-Whitney test. \**P* < 0.05; \*\**P* < 0.001. (D) Histopathologic analysis of lesions from mice coinjected s.c. with SIP or SCRA peptide. SIP-induced ulcerated lesions that extend beyond the field of view are boxed. Coinjection with SCRA peptide caused small abscesses that are confined to the inoculation site (indicated by arrows). [Scale bars: 3.3 mm  $\times$  4.4 mm (y axis  $\times$  x axis) at 2 $\times$  magnification.] (E) Proposed model for the mechanism of intercellular communication and GAS virulence regulation. (Left) At low cell density, the secretion signal sequence of Vfr binds to RopB and negatively influences RopB-dependent transcription activation from the P1 promoter, possibly by disrupting RopB-DNA interactions. (Right) At high cell density, SIP is produced, secreted, and reimported into the cytosol. The high-affinity RopB-DNA interactions and RopB polymerization aided by SIP binding lead to up-regulation of *sip* expression, which results in robust induction of SIP production by a positive-feedback mechanism. In addition to up-regulation of virulence genes, the SIP signaling circuit down-regulates the expression of categories of genes involved in GAS growth and host cell attachment. Finally, the SIP-dependent up-regulation of *speB* leads to abundant secretion of mature SpeB (Spe<sub>M</sub>), which facilitates host tissue damage and disease dissemination by cleavage of various host and GAS proteins.

SIP signaling pathway likely represents a virulence regulatory mechanism conserved among many GAS M-protein serotypes.

All previously characterized bacterial peptide signals are produced as propeptides that have a cleavable amino-terminal secretion signal sequence and protease cleavage sites, resulting in a mature peptide (8) (Fig. 3A). The secretion signal sequence targets the propeptide to the secretion machinery at the cell membrane, where the propeptide undergoes proteolytic cleavage. The released mature peptide is exported, and subsequently reimported into the cytosol by Opp permeases (39). In contrast, SIP lacks the distinctive sequence motifs of bacterial peptide

signals. GAS produces SIP in a mature form that is devoid of a secretion signal sequence and protease cleavage site (Fig. 3A). Nevertheless, SIP is secreted and reimported by an Opp permease-independent import mechanism. These differences indicate that SIP biosynthesis is an important exception to the established paradigm of bacterial peptide signaling. Thus, SIP belongs to a previously undescribed new class of leaderless bacterial peptide signals. Such lack of conformity likely hobbled previous extensive efforts to identify SIP (18, 21, 22, 27, 30–33, 35, 36). Given that RRNPP family proteins are widespread among low guanine + cytosine gram-positive bacteria and bacteriophages (42, 52), and the cognate peptide signals for the vast majority of these regulators have not yet been identified, we speculate that leaderless peptides analogous to SIP will participate in other microbial signaling pathways. Thus, our delineation of SIP signaling may accelerate discovery of similar peptide signals in other microorganisms.

Typically, the internalized cognate peptides bind to the respective regulators and trigger regulator-specific conformational changes that modulate gene regulation (39). The characterized activation peptide-induced allostery among RRNPP family regulators includes disruption of tetramerization in PrgX from *Enterococcus faecalis*, induction of tetramerization in NprR from *Bacillus cereus*, and unmasking of the N-terminal DNA-binding domain that aids promoter binding by PlcR from *B. cereus* (39, 53–55). Our results indicate that SIP controls RopB regulatory activity by facilitating high-affinity RopB–DNA interactions and RopB polymerization (Fig. 4). The sequences upstream of the P1 promoter have two putative RopB-binding sites, site 1 and site 2, and these two sites are separated by a 121-bp-long spacer region. The two sites are highly similar (Fig. 4C), and RopB binds to each site with comparable affinity. Thus, it is plausible that SIP promotes RopB interactions with the two high-affinity operator sequences. Using these interactions as nucleation events, RopB polymerizes on the spacer between the two sites, resulting in RopB-dependent transcription activation from the P1 promoter. However, additional investigations will be required to test the proposed model and elucidate the mechanism by which RopB polymerization contributes to its regulatory activity.

Based on earlier work (18) and results presented here, we propose the following model (Fig. 6E). During low cell density, the inhibition peptide signal derived from the secretion signal sequence of Vfr interacts with RopB and negatively influences *speB* expression, possibly by inhibiting RopB–DNA interactions (Fig. 6E). Conversely, during high cell density, expression of *vfr* is down-regulated, which results in low-level SIP production. The initial SIP production acts as a positive feedback loop, resulting in robust induction of SIP. The SIP-bound RopB binds to operator sequences, polymerizes on the promoter, and mediates transcription activation of target genes.

To summarize, the data we present here provide detailed molecular and mechanistic understanding of a key virulence regulatory pathway of an abundant human pathogen responsible for greater than 700 million human infections annually worldwide (56, 57). Moreover, the work identified previously unknown molecular targets that may be exploited to develop new therapeutics.

## Materials and Methods

**Bacterial Strains, Plasmids, and Experimental Procedures.** The bacterial strains and plasmids used in this study are listed in *SI Appendix, Table S5*. Probes and primers used in this study are listed in *SI Appendix, Table S6*. The composition of the chemically defined medium (58) is provided in *SI Appendix, Table S7*. Details of the isogenic mutant strain construction, *trans*-complementation plasmids, and plasmids for overexpression are included in *SI Appendix, Supplemental Materials and Methods*. Details of protein overexpression and purification are provided in *SI Appendix, Supplemental Materials and Methods*. Preparation of synthetic peptides used for SIP addition experiments, FP assays, EMSA, and animal infection studies is described in *SI Appendix, Supplemental Materials and Methods*. Details of *speB* transcript level analysis by qRT-PCR, secreted SpeB protein levels by Western immunoblotting, and SpeB protease activity by milk plate clearing assay are provided in *SI Appendix, Supplemental Materials and Methods*. Secretome swap assays were performed as described previously (8), and the details are given in *SI Appendix, Supplemental Materials and Methods*. Details of confocal microscopy studies and fluorescence measurements to monitor the uptake of fluorescein-labeled SIP are included in *SI Appendix, Supplemental Materials and Methods*.

**Northern Blot and RNA-Seq Analysis.** Northern blot analysis was performed as previously described (59). Membranes were hybridized in ULTRAhyb Ultra-sensitive Hybridization Buffer (Thermo Fisher) at 42 °C with <sup>32</sup>P-end-labeled DNA oligonucleotides. Signals were visualized with a Typhoon phosphor-imager (GE Healthcare), and band intensities were quantified using GelQuant software (BiochemLabSolutions). RNA-seq experiments were performed as described previously (60). Experimental details are given in *SI Appendix, Supplemental Materials and Methods*.

**RopB–DNA Interaction Studies.** Interactions between RopB and SIP and dsDNA were studied by FP assay and EMSA. Details of binding isotherm measurement conditions and protocols are given in *SI Appendix, Supplemental Materials and Methods*.

**Analysis of RopB Oligomerization State.** Size exclusion chromatography and blue-native polyacrylamide gel electrophoresis were used to determine the oligomerization state of recombinant RopB in the presence and absence of synthetic peptides. Experiment details are provided in *SI Appendix, Supplemental Materials and Methods*. Details of sample preparation and mass spectrometry analysis of the different oligomeric forms of RopB fractionated by size exclusion chromatography are described in *SI Appendix, Supplemental Materials and Methods*.

**Animal Virulence Studies.** Mouse experiments were performed according to protocols approved by the Houston Methodist Research Institute Institutional Animal Care and Use Committee. The studies were carried out in accordance with the recommendations in the *Guide for the Care and Use of Laboratory Animals* (61). Virulence of the isogenic mutant GAS strains was assessed using three mouse models of infection, namely, i.p., i.m., and s.c. inoculation (17, 18, 62) (approved nos. AUP-0716-0038, AUP-0615-0041, and AUP-0416-0019). Details of mouse infection studies and data analyses are given in *SI Appendix, Supplemental Materials and Methods*.

**ACKNOWLEDGMENTS.** We thank Frank DeLeo for critical reading of the manuscript, and an anonymous reviewer for scholarly suggestions to improve the manuscript. This work was supported by NIH Grant 1R01AI109096-01A1 (to M.K.), by the Deutsche Forschungsgemeinschaft (Exc114-2) (to K.P.), and by funds from the Fondren Foundation (to J.M.M.).

- Parker CT, Sperandio V (2009) Cell-to-cell signalling during pathogenesis. *Cell Microbiol* 11:363–369.
- Hughes DT, Sperandio V (2008) Inter-kingdom signalling: Communication between bacteria and their hosts. *Nat Rev Microbiol* 6:111–120.
- Sanson M, et al. (2015) Phosphorylation events in the multiple gene regulator of group A *Streptococcus* significantly influence global gene expression and virulence. *Infect Immun* 83:2382–2395.
- Dubbs JM, Mongkolsuk S (2012) Peroxide-sensing transcriptional regulators in bacteria. *J Bacteriol* 194:5495–5503.
- Hood MI, Skaar EP (2012) Nutritional immunity: Transition metals at the pathogen-host interface. *Nat Rev Microbiol* 10:525–537.
- Somerville GA, Proctor RA (2009) At the crossroads of bacterial metabolism and virulence factor synthesis in staphylococci. *Microbiol Mol Biol Rev* 73:233–248.
- Rutherford ST, Bassler BL (2012) Bacterial quorum sensing: Its role in virulence and possibilities for its control. *Cold Spring Harb Perspect Med* 2:a012427.
- Dunny GM, Leonard BA (1997) Cell-cell communication in gram-positive bacteria. *Annu Rev Microbiol* 51:527–564.
- Papenfort K, Bassler BL (2016) Quorum sensing signal-response systems in gram-negative bacteria. *Nat Rev Microbiol* 14:576–588.
- Thoendel M, Kavanaugh JS, Flack CE, Horswill AR (2011) Peptide signaling in the staphylococci. *Chem Rev* 111:117–151.
- Olsen RJ, Shelburne SA, Musser JM (2009) Molecular mechanisms underlying group A streptococcal pathogenesis. *Cell Microbiol* 11:1–12.
- Cunningham MW (2000) Pathogenesis of group A streptococcal infections. *Clin Microbiol Rev* 13:470–511.
- Carroll RK, Musser JM (2011) From transcription to activation: How group A *Streptococcus*, the flesh-eating pathogen, regulates SpeB cysteine protease production. *Mol Microbiol* 81:588–601.
- Lukomski S, et al. (1997) Inactivation of *Streptococcus pyogenes* extracellular cysteine protease significantly decreases mouse lethality of serotype M3 and M49 strains. *J Clin Invest* 99:2574–2580.

15. Lukomski S, et al. (1999) Extracellular cysteine protease produced by *Streptococcus pyogenes* participates in the pathogenesis of invasive skin infection and dissemination in mice. *Infect Immun* 67:1779–1788.
16. Lukomski S, et al. (1998) Genetic inactivation of an extracellular cysteine protease (SpeB) expressed by *Streptococcus pyogenes* decreases resistance to phagocytosis and dissemination to organs. *Infect Immun* 66:771–776.
17. Olsen RJ, et al. (2010) Decreased necrotizing fasciitis capacity caused by a single nucleotide mutation that alters a multiple gene virulence axis. *Proc Natl Acad Sci USA* 107:888–893.
18. Shelburne SA, 3rd, et al. (2011) An amino-terminal signal peptide of Vfr protein negatively influences RopB-dependent SpeB expression and attenuates virulence in *Streptococcus pyogenes*. *Mol Microbiol* 82:1481–1495.
19. Svensson MD, et al. (2000) Role for a secreted cysteine proteinase in the establishment of host tissue tropism by group A streptococci. *Mol Microbiol* 38:242–253.
20. Olsen RJ, et al. (2015) The majority of 9,729 group A *Streptococcus* strains causing disease secrete SpeB cysteine protease: Pathogenesis implications. *Infect Immun* 83:4750–4758.
21. Loughman JA, Caparon M (2006) Regulation of SpeB in *Streptococcus pyogenes* by pH and NaCl: A model for in vivo gene expression. *J Bacteriol* 188:399–408.
22. Lyon WR, Gibson CM, Caparon MG (1998) A role for trigger factor and an rgg-like regulator in the transcription, secretion and processing of the cysteine proteinase of *Streptococcus pyogenes*. *EMBO J* 17:6263–6275.
23. Ulrich RG (2008) Vaccine based on a ubiquitous cysteinyl protease and streptococcal pyrogenic exotoxin A protects against *Streptococcus pyogenes* sepsis and toxic shock. *J Immune Based Ther Vaccines* 6:8.
24. Wang AY, González-Páez GE, Wolan DW (2015) Identification and co-complex structure of a new *S. pyogenes* SpeB small molecule inhibitor. *Biochemistry* 54:4365–4373.
25. Kapur V, et al. (1994) Vaccination with streptococcal extracellular cysteine protease (interleukin-1) convertase) protects mice against challenge with heterologous group A streptococci. *Microb Pathog* 16:443–450.
26. Björck L, et al. (1989) Bacterial growth blocked by a synthetic peptide based on the structure of a human proteinase inhibitor. *Nature* 337:385–386.
27. Neely MN, Lyon WR, Runft DL, Caparon M (2003) Role of RopB in growth phase expression of the SpeB cysteine protease of *Streptococcus pyogenes*. *J Bacteriol* 185:5166–5174.
28. Graham MR, et al. (2002) Virulence control in group A *Streptococcus* by a two-component gene regulatory system: Global expression profiling and in vivo infection modeling. *Proc Natl Acad Sci USA* 99:13855–13860.
29. Miller AA, Engleberg NC, DiRita VJ (2001) Repression of virulence genes by phosphorylation-dependent oligomerization of CsrR at target promoters in *S. pyogenes*. *Mol Microbiol* 40:976–990.
30. Kietzman CC, Caparon MG (2010) CcpA and LacD.1 affect temporal regulation of *Streptococcus pyogenes* virulence genes. *Infect Immun* 78:241–252.
31. Shelburne SA, et al. (2010) A combination of independent transcriptional regulators shapes bacterial virulence gene expression during infection. *PLoS Pathog* 6:e1000817.
32. Podbielski A, Woischnik M, Pohl B, Schmidt KH (1996) What is the size of the group A streptococcal vir regulon? The Mga regulator affects expression of secreted and surface virulence factors. *Med Microbiol Immunol (Berl)* 185:171–181.
33. Ribardo DA, McIver KS (2006) Defining the Mga regulon: Comparative transcriptome analysis reveals both direct and indirect regulation by Mga in the group A *Streptococcus*. *Mol Microbiol* 62:491–508.
34. Ma Y, et al. (2006) Identification and characterization of bicistronic *speB* and *prsA* gene expression in the group A *Streptococcus*. *J Bacteriol* 188:7626–7634.
35. Makthal N, et al. (2016) Structural and functional analysis of RopB: A major virulence regulator in *Streptococcus pyogenes*. *Mol Microbiol* 99:1119–1133.
36. Podbielski A, Woischnik M, Kreikemeyer B, Bettenbrock K, Buttaro BAL (1999) Cysteine protease SpeB expression in group A streptococci is influenced by the nutritional environment but SpeB does not contribute to obtaining essential nutrients. *Med Microbiol Immunol (Berl)* 188:99–109.
37. Elliott SD (1945) A proteolytic enzyme produced by group A streptococci with special reference to its effect on the type-specific M antigen. *J Exp Med* 81:573–592.
38. Tongs MS (1919) Ectoenzymes of streptococci. *JAMA* 73:1277–1279.
39. Do H, Kumaraswami M (2016) Structural mechanisms of peptide recognition and allosteric modulation of gene regulation by the RRNPP family of quorum-sensing regulators. *J Mol Biol* 428:2793–2804.
40. Chen Z, Itzek A, Malke H, Ferretti JJ, Kreth J (2012) Dynamics of *speB* mRNA transcripts in *Streptococcus pyogenes*. *J Bacteriol* 194:1417–1426.
41. Chang JC, LaSarre B, Jimenez JC, Aggarwal C, Federle MJ (2011) Two group A streptococcal peptide pheromones act through opposing Rgg regulators to control biofilm development. *PLoS Pathog* 7:e1002190.
42. Fleuchot B, et al. (2011) Rgg proteins associated with internalized small hydrophobic peptides: A new quorum-sensing mechanism in streptococci. *Mol Microbiol* 80:1102–1119.
43. An FY, Clewell DB (2002) Identification of the cAD1 sex pheromone precursor in *Enterococcus faecalis*. *J Bacteriol* 184:1880–1887.
44. Chandler JR, Dunny GM (2008) Characterization of the sequence specificity determinants required for processing and control of sex pheromone by the intramembrane protease Eep and the plasmid-encoded protein PrgY. *J Bacteriol* 190:1172–1183.
45. Gominet M, Slamti L, Gilois N, Rose M, Lereclus D (2001) Oligopeptide permease is required for expression of the *Bacillus thuringiensis* *plcR* regulon and for virulence. *Mol Microbiol* 40:963–975.
46. Leonard BA, Podbielski A, Hedberg PJ, Dunny GM (1996) *Enterococcus faecalis* pheromone binding protein, PrgZ, recruits a chromosomal oligopeptide permease system to import sex pheromone cCF10 for induction of conjugation. *Proc Natl Acad Sci USA* 93:260–264.
47. Podbielski A, et al. (1996) Molecular characterization of group A streptococcal (GAS) oligopeptide permease (*opp*) and its effect on cysteine protease production. *Mol Microbiol* 21:1087–1099.
48. Podbielski A, Leonard BA (1998) The group A streptococcal dipeptide permease (*Dpp*) is involved in the uptake of essential amino acids and affects the expression of cysteine protease. *Mol Microbiol* 28:1323–1334.
49. Olsen RJ, Musser JM (2010) Molecular pathogenesis of necrotizing fasciitis. *Annu Rev Pathol* 5:1–31.
50. Watson ME, Jr, Neely MN, Caparon MG (2016) Animal models of *Streptococcus pyogenes* infection. *Streptococcus pyogenes: Basic Biology to Clinical Manifestations*, eds Ferretti J, Stevens D, Fischetti V (University of Oklahoma Health Sciences Center, Oklahoma City), pp 629–660.
51. Kapur V, et al. (1993) A conserved *Streptococcus pyogenes* extracellular cysteine protease cleaves human fibronectin and degrades vitronectin. *Microb Pathog* 15:327–346.
52. Erez Z, et al. (2017) Communication between viruses guides lysis-lysogeny decisions. *Nature* 541:488–493.
53. Grenha R, et al. (2013) Structural basis for the activation mechanism of the PlcR virulence regulator by the quorum-sensing signal peptide PapR. *Proc Natl Acad Sci USA* 110:1047–1052.
54. Zouhir S, et al. (2013) Peptide-binding dependent conformational changes regulate the transcriptional activity of the quorum-sensor NprR. *Nucleic Acids Res* 41:7920–7933.
55. Shi K, et al. (2005) Structure of peptide sex pheromone receptor PrgX and PrgX/pheromone complexes and regulation of conjugation in *Enterococcus faecalis*. *Proc Natl Acad Sci USA* 102:18596–18601.
56. Sanyahumbi AS, Colquhoun S, Wyber R, Carapetis JR (2016) Global disease burden of group A *Streptococcus*. *Streptococcus pyogenes: Basic Biology to Clinical Manifestations*, eds Ferretti J, Stevens D, Fischetti V (University of Oklahoma Health Sciences Center, Oklahoma City), pp 661–704.
57. Ralph AP, Carapetis JR (2012) Group A streptococcal diseases and their global burden. *Host-Pathogen Interactions in Streptococcal Diseases*, ed Chhatwal SG (Springer, Heidelberg), pp 1–27.
58. van de Rijn I, Kessler RE (1980) Growth characteristics of group A streptococci in a new chemically defined medium. *Infect Immun* 27:444–448.
59. Fröhlich KS, Haneke K, Papenfort K, Vogel J (2016) The target spectrum of SdsR small RNA in *Salmonella*. *Nucleic Acids Res* 44:10406–10422.
60. Sanson M, et al. (2015) Adhesin competence repressor (AdcR) from *Streptococcus pyogenes* controls adaptive responses to zinc limitation and contributes to virulence. *Nucleic Acids Res* 43:418–432.
61. National Research Council (2011) *Guide for the Care and Use of Laboratory Animals* (National Academies Press, Washington, DC), 8th Ed.
62. VanderWal AR, et al. (2017) Iron efflux by PmtA is critical for oxidative stress resistance and contributes significantly to group A *Streptococcus* virulence. *Infect Immun* 85:e00091–17.

## Supporting Information

### Contents:

SI Appendix Figures

SI Appendix Table S1: Genes that are downregulated in  $\Delta SIP$  mutant

SI Appendix Table S2: Genes that are upregulated in  $\Delta SIP$  mutant

SI Appendix Table S3: Genes that are downregulated in *orf-1\** mutant

SI Appendix Table S4: Genes that are upregulated in *orf-1\** mutant

SI Appendix Table S5: Bacterial strains and plasmids used in this study

SI Appendix Table S6: Primers and probes used in this study

SI Appendix Table S7: Preparation of Chemically-Defined Medium

SI Appendix Supplemental Materials and Methods

SI Appendix References

Figure S1

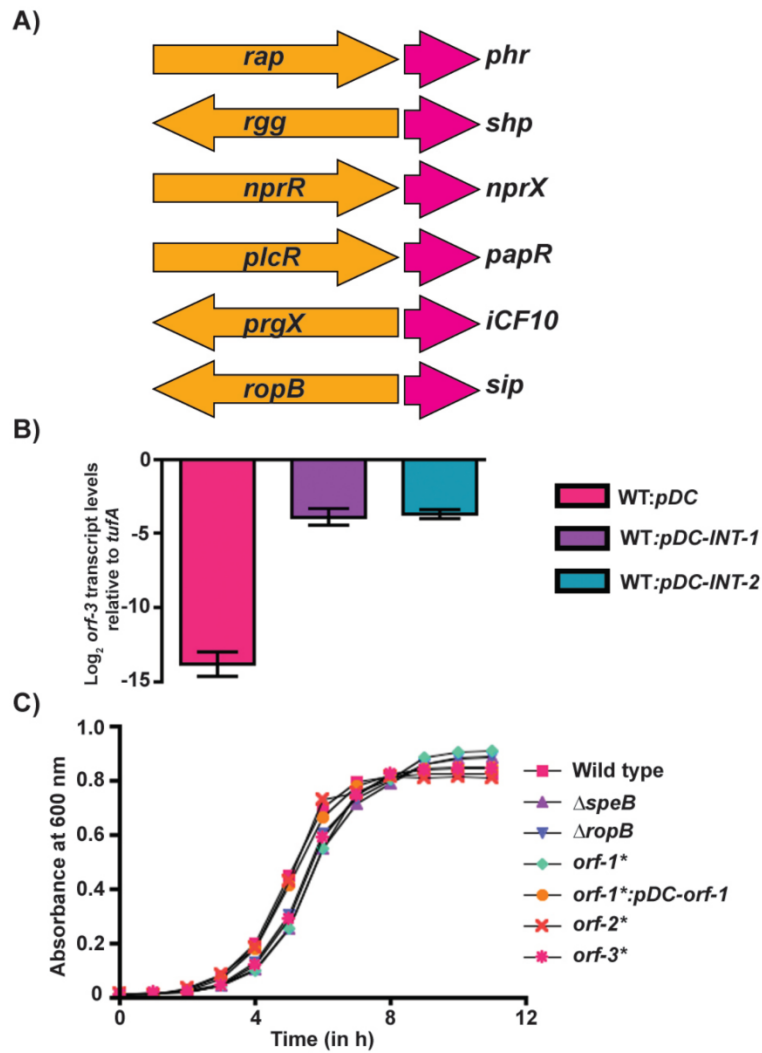


Figure S1. (A) The genetic organization of the coding regions of different members of RRNPP family regulators and their characterized cognate peptides are shown. (B) Complementation of WT GAS by *trans*-complementation plasmid containing different fragments of the *ropB*-*speB* intergenic region. Transcript levels of *orf-3* in the indicated strains as measured by qRT-

PCR. Samples were collected at late exponential ( $A_{600} = 1.0$ ) phase of growth for transcript level analysis. Triplicate biological replicates were grown on two different occasions and analyzed in duplicate. Data graphed are mean  $\pm$  standard deviation. (C) Growth kinetics of the indicated strains in THY broth. Three biological replicates were grown and the graph represents mean  $\pm$  standard deviation.

Figure S2

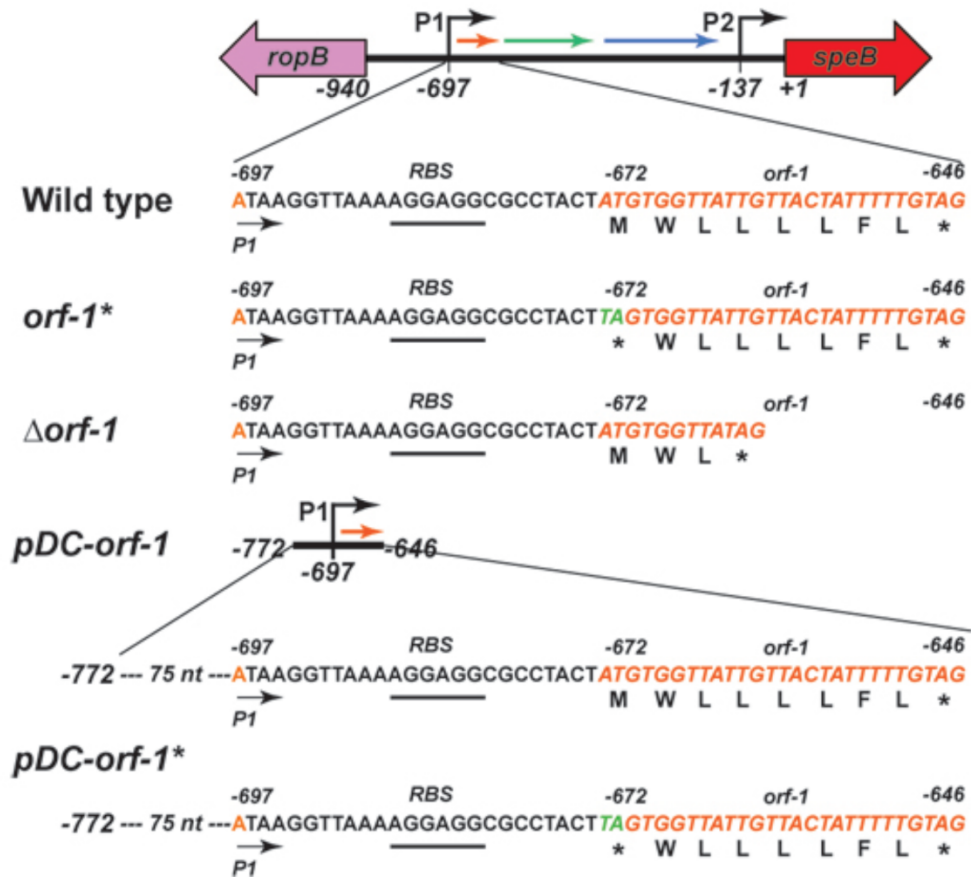


Figure S2. Schematics showing the organization of genetic elements in different GAS strains and *trans*-complementation plasmids used in this study. The *ropB* and *speB* genes are divergently transcribed. The angled arrows above the line indicate two transcription start sites for *speB*, designated P1 and P2. The intergenic region with three predicted open reading frames, designated *orf-1* (orange), *orf-2* (green), and *orf-3* (blue), are shown as horizontal arrows. Numbers indicate the nucleotide positions relative to the first nucleotide of *speB* start codon. Nucleotides corresponding to transcription start sites, P1 and P2, are highlighted in

orange. Inferred ribosomal binding site (RBS) located upstream of *orf-1* is underlined and labeled. Nucleotide sequences of *orf-1* are italicized and colored in orange. Amino acid sequence corresponding to each codon of *orf-1* is given below. \* indicates stop codon. Substitution of *orf-1* start codon with stop codon in *orf-1\** and *trans*-complementation plasmid, *pDC-orf-1\**, is highlighted in green.

Figure S3

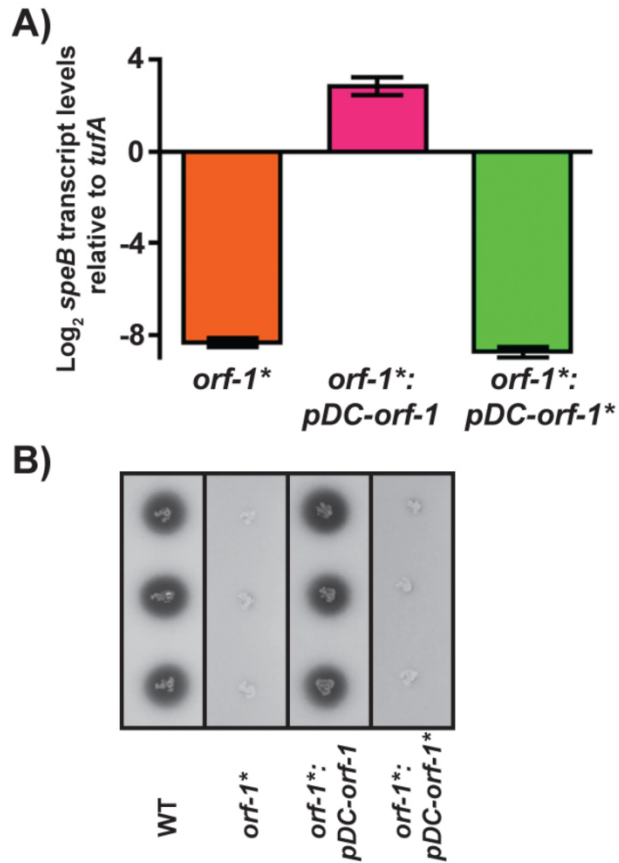


Figure S3. Translation disruption of *orf-1* in the *trans*-complementation plasmid, *pDC-orf-1* (*pDC-orf-1*\*), failed to rescue the defective *speB* expression in isogenic *orf-1*\* mutant. (A) Transcript levels of *speB* in the indicated strains as measured by qRT-PCR. Samples were collected at stationary ( $A_{600} > 1.8$ ) phase of growth for transcript level analysis. Triplicate biological replicates were grown on two different occasions and analyzed in duplicate. Data graphed are mean  $\pm$  standard deviation. (B) Milk plate assay to assess the protease activity of SpeB in the indicated strains.

Figure S4

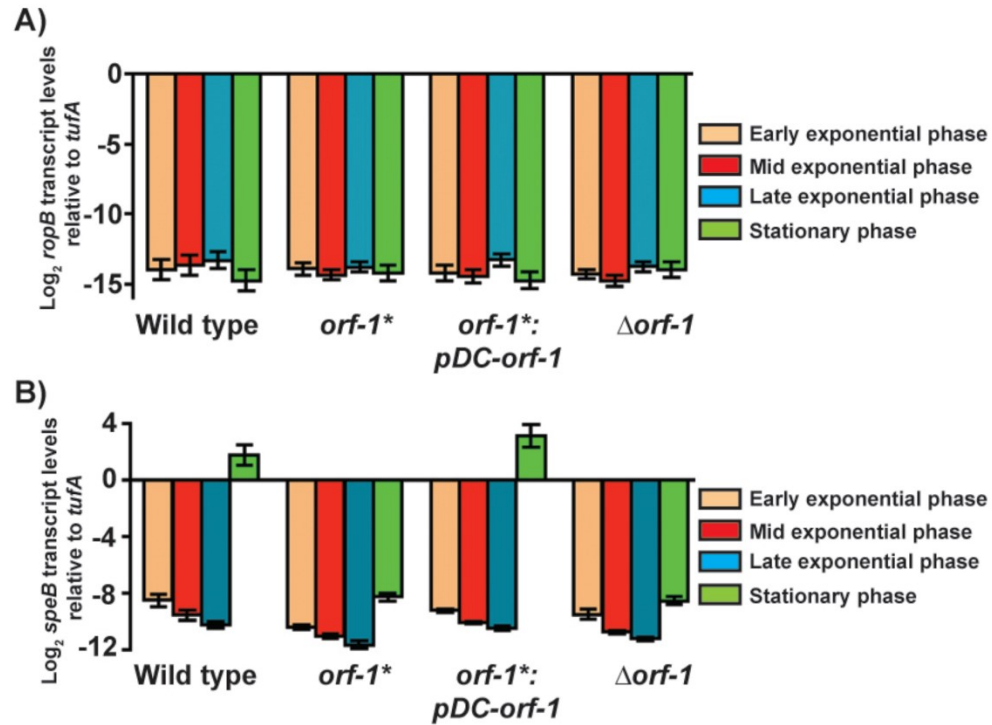


Figure S4. Genetic inactivation of *orf-1* does not alter *ropB* expression profile. Transcript levels of *ropB* (A) and *speB* (B) in the indicated strains measured by qRT-PCR. Samples were collected at early exponential ( $A_{600} - 0.25$ ), mid-exponential ( $A_{600} - 0.5$ ), late exponential ( $A_{600} - 1.0$ ), and stationary phase ( $A_{600} - >1.8$ ). Triplicate biological replicates were grown on two different occasions and analyzed in duplicate. Data graphed are mean  $\pm$  standard deviation.

Figure S5

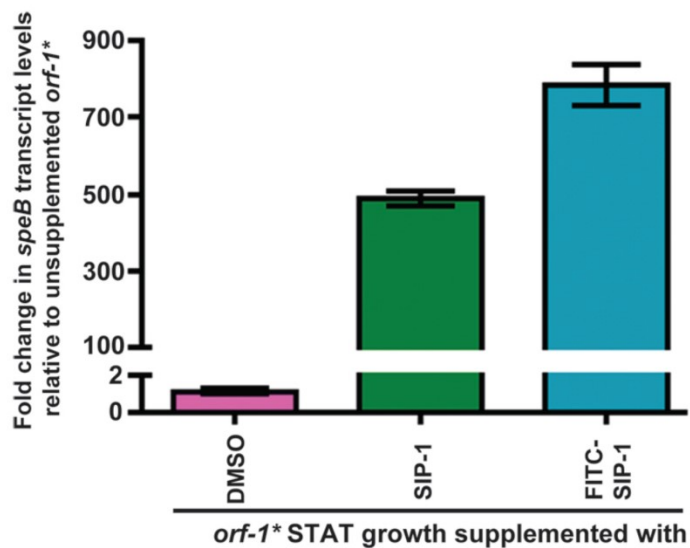


Figure S5. Fluorescein modification of SIP-1 (FITC-SIP-1) at its amino-terminus does not affect its ability to induce *speB* expression. The *orf-1\** mutant was grown in chemically defined medium (CDM) to early stationary phase (STAT,  $A_{600} \sim 1.7$ ) and supplemented either with 100 nM of indicated synthetic peptide or DMSO. After 60 min incubation, transcript levels of *speB* were assessed by qRT-PCR. The *orf-1\** mutant supplemented with DMSO was used as a reference and fold changes in *speB* transcript levels relative to the reference are shown.

Figure S6

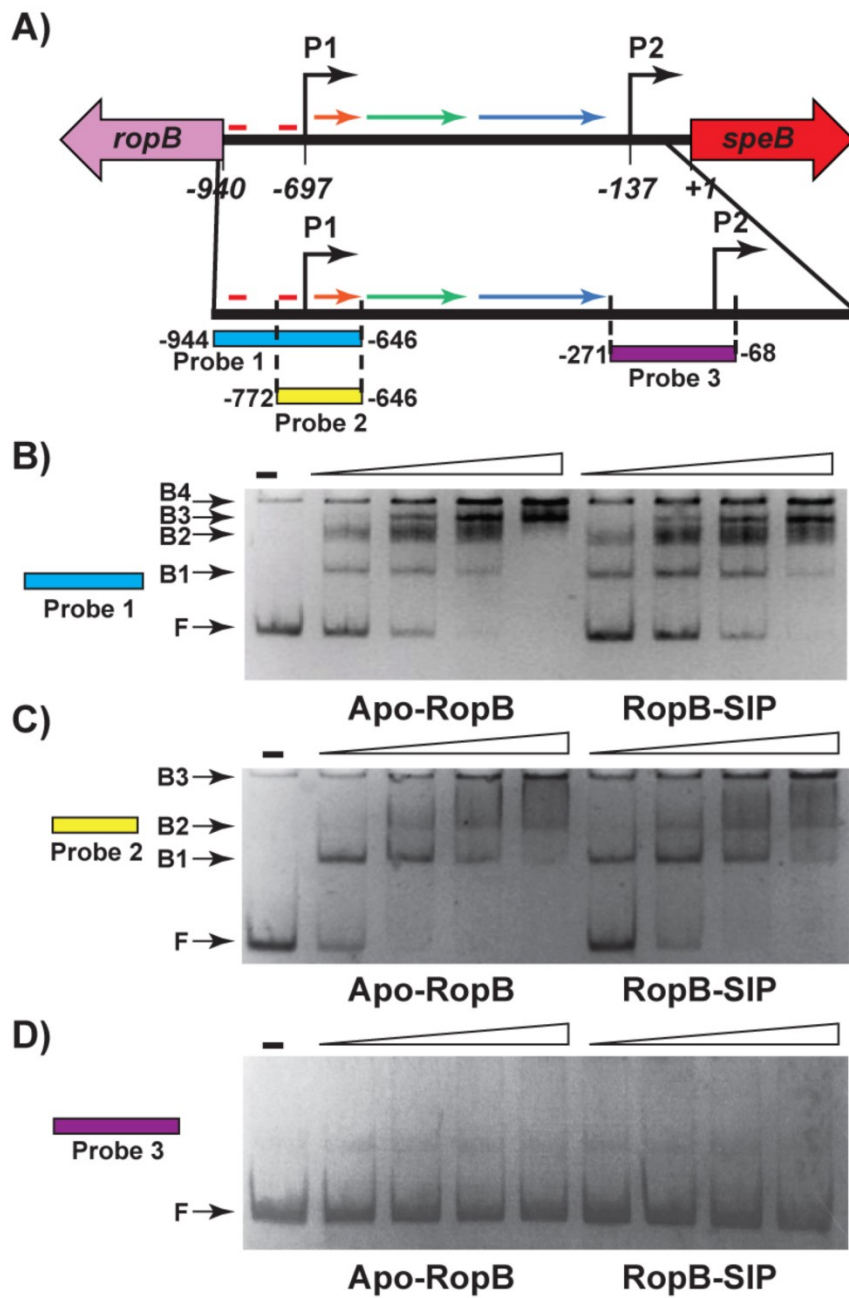


Figure S6. Analysis of RopB binding sites within the *ropB-speB* intergenic region. (A) The *ropB* and *speB* genes are divergently transcribed. The angled arrows above the line indicate two transcription start sites for *speB*, designated P1 and P2. The intergenic region with three predicted open reading frames, designated *orf-1* (orange), *orf-2* (green), and *orf-3* (blue), are shown as horizontal arrows. The putative RopB-binding sites located upstream of P1 is shown as horizontal arrows. The putative RopB-binding sites located upstream of P1 is shown as red rectangles. Numbers indicate the nucleotide positions relative to the first nucleotide of *speB* start codon. Promoter fragments (probes 1-3) tested for RopB binding in the electrophoretic mobility shift assay (EMSA) are shown as bars and the numbers at either sides of each probe indicate the positions of 5' and 3' ends of the fragment relative to the first nucleotide of the *speB* start codon. (B-D) Increasing concentrations of purified apo-RopB or SIP-bound RopB (70, 140, 210, and 280 nM of RopB dimer) were incubated with the indicated probe and reaction mixtures were resolved on a 10% native-PAGE. SIP was added in the reaction mixture at a final concentration of 4  $\mu$ M to generate SIP-bound RopB. The positions of free (F) and different RopB oligomer-bound (B1-B3) probes are indicated.

Figure S7

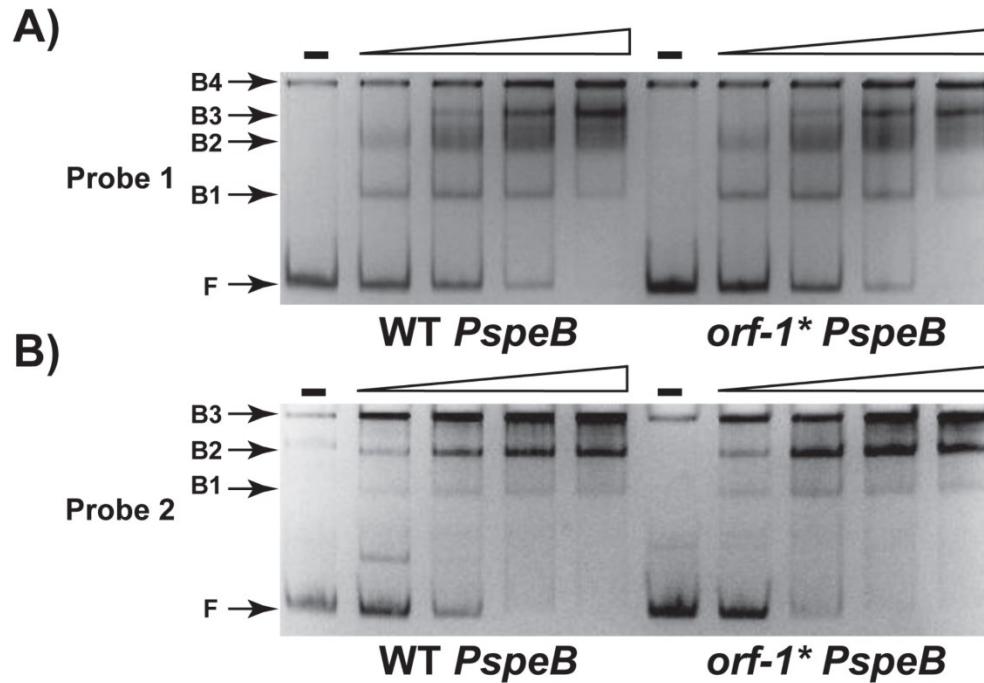


Figure S7. Genetic alterations in *orf-1\** mutant does not affect the interactions between RopB and *speB* promoter (*PspeB*). Promoter sequences corresponding to probe 1 or probe 2 fragments were amplified from wild type (WT) and *orf-1\** mutant strains. Interactions between the indicated promoter sequences and RopB-SIP-1 were assessed by EMSA. Increasing concentrations of purified apo-RopB dimer incubated with 4  $\mu$ M SIP (70, 140, 210, and 280 nM of RopB dimer) were incubated with each indicated probe and reaction mixtures were resolved on a 10% native-PAGE. Probes 1 and 2 were prepared as described in Fig. S5, panel A. The positions of free (F) and different RopB oligomer-bound (B1-B4) probes are indicated.

Figure S8

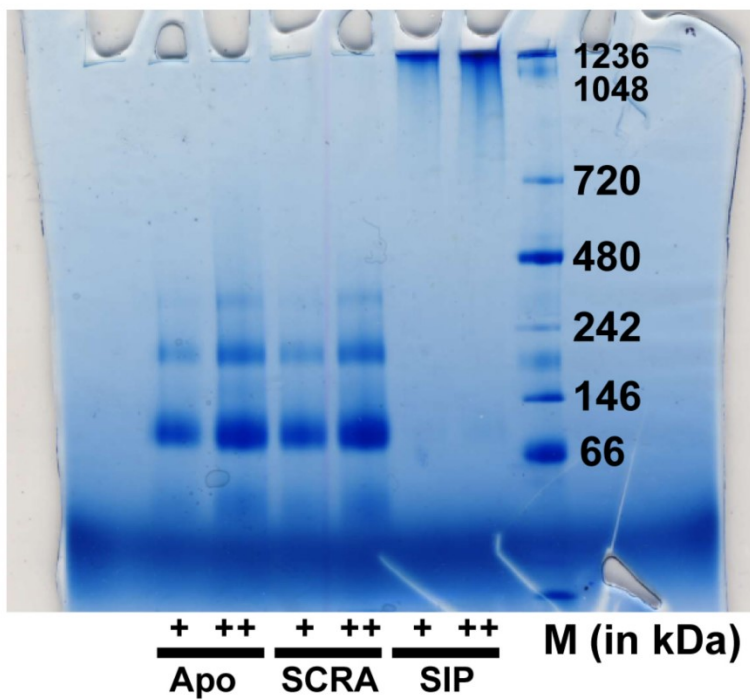


Figure S8. Blu-native PAGE analysis of the apo- or peptide-bound forms of RopB. An uncropped image of the Blu-native gel presented in panel 4/ is shown. Increasing concentrations of the apo- or peptide-bound forms of RopB (+ - 1.5  $\mu$ g: ++ - 3  $\mu$ g) were analyzed by Blu-native PAGE. The masses of the molecular weight marker (M, in kilodaltons) are labeled.

Figure S9

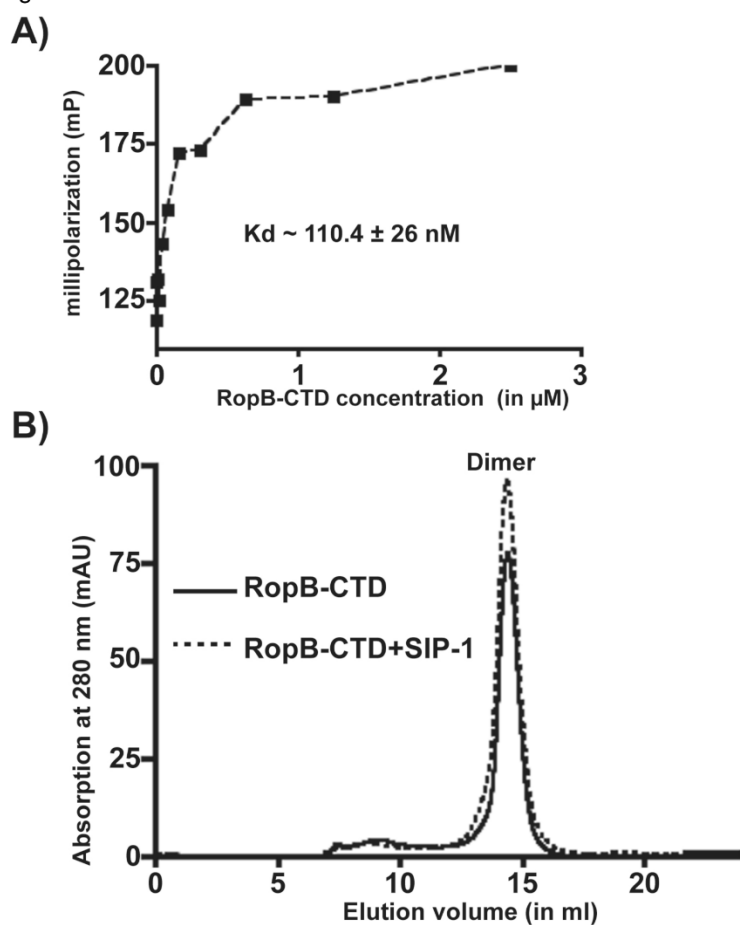


Figure S9. SIP binding does not induce the higher oligomer formation of RopB-CTD. (A) Analysis of the binding between purified RopB-CTD and fluoresceinated SIP-1 by fluorescent polarization (FP) assay. (B) Size exclusion chromatography analysis of purified RopB-CTD with or without the presence of either synthetic SIP-1 or SCRA peptides. Molecular masses were calculated based on the calibration curve using molecular weight standards.

Figure S10

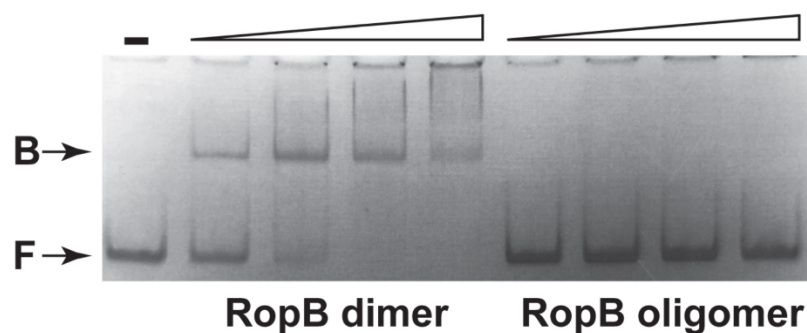


Figure S10. Pre-formed RopB-SIP oligomer does not bind *speB* promoter. Interactions between promoter sequence of *speB* and different oligomeric forms of RopB were assessed by EMSA. Increasing concentrations of purified apo-RopB dimer incubated with SIP (RopB dimer) or pre-formed RopB-SIP oligomer (RopB oligomer) fractionated by size exclusion chromatography (70, 140, 210, and 280 nM of RopB dimer) were incubated with probe 2 and reaction mixtures were resolved on a 10% native-PAGE. Probe 2 was prepared as described in Fig. S5, panel A. The positions of free (F) and different RopB oligomer-bound (B1 and B2) probes are indicated.

Figure S11

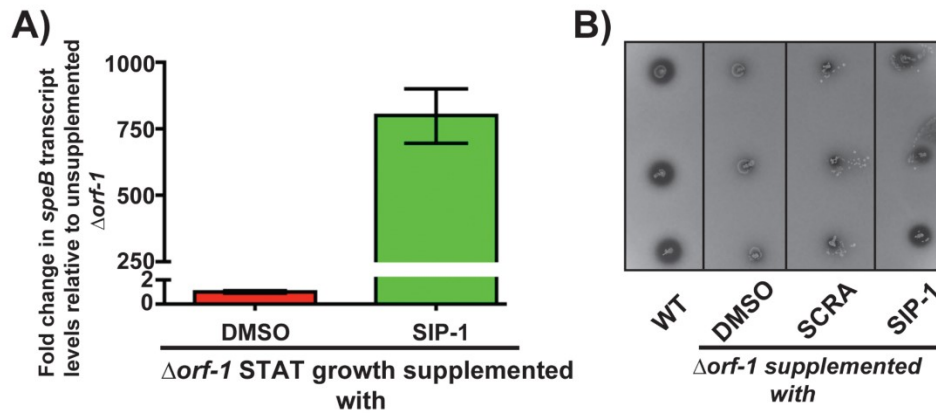


Figure S11. (A) The  $\Delta orf-1$  mutant was grown in chemically defined medium (CDM) to early stationary phase (STAT,  $A_{600} \sim 1.7$ ) and supplemented either with 100 nM of indicated synthetic peptide or DMSO. After 60 min incubation, transcript levels of *speB* were assessed by qRT-PCR.  $\Delta orf-1$  mutant supplemented with DMSO was used as a reference and fold changes in *speB* transcript levels relative to the reference are shown. (B) Milk plate assay to assess the ability of SIP to induce SpeB protease activity in  $\Delta orf-1$  mutant.

Figure S12

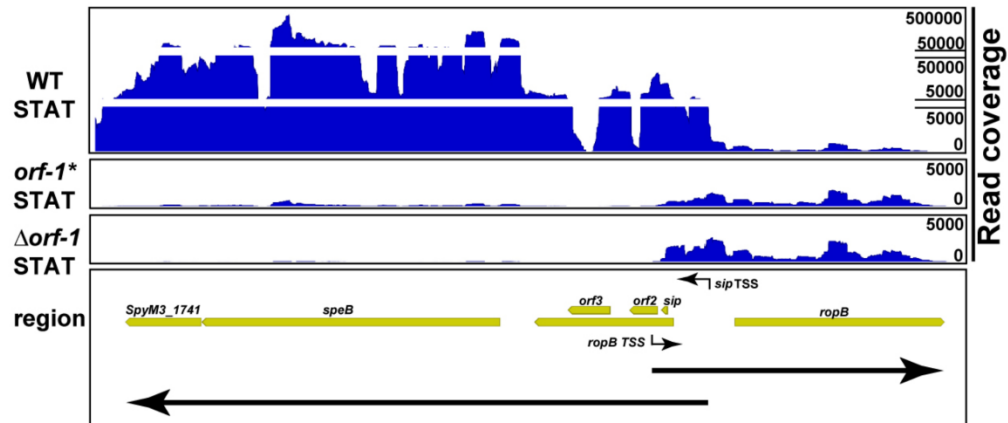


Figure S12. Visualization of RNA sequencing reads for *ropB-speB* genomic locus in the indicated strains. The bottom panel shows the location of annotated and identified genes within the *ropB-speB* genomic locus. Individual genes are shown as bars and labeled above the bar. Transcription start sites (TSS) for *ropB* and *sip* genes are marked as bent arrows below and above the bars, respectively. The direction of gene expression is shown as arrows in the bottom.

Figure S13

```

M1      ATGTCAAGCCTTCCTAGTTGATGTCAAAAAACGTTACGCATGTACCTAATACGTAACAA
M3      ATGTCAAGCCTTCCTAGTTGATGTCAAAAAACGTTACGCATGTACCTAATACGTAACAA
M4      ATGTCAAGCCTTCCTAGTTGATGTCAAAAAACGTTACGCATGTACCTAATACGTAACAA
M5      ATGTCAAGCCTTCCTAGTTGATGTCAAAAAACGTTACGCACGTACCTAATACGTAACAA
M6      ATGTCAAGCCTTCCTAGTTGATGTCAAAAAACGTTATGCATGTACCTAATACGTAACAA
M12     ATGTCAAGCCTTCCTAGTTGATGTCAAAAAACGTTACGCATGTACCTAATACGTAACAA
M18     ATGTCAAGCCTTCCTAGTTGATGTCAAAAAACGTTACGCATGTACCTAATACGTAACAA
M28     ATGTCAAGCCTTCCTAGTTGATGTCAAAAAACGTTACGCATGTACCTAATACGTAACAA
M49     ATGTCAAGCCTTCCTAGTTGATGTCAAAAAACGTTACGCATGTACCTAATACGTAACAA
M53     ATGTCAAGCCTTCCTAGTTGATGTCAAAAAACGTTACGCATGTACCTAATACGTAACAA
M59     ATGTCAAGCCTTCCTAGTTGATGTCAAAAAACGTTACGCATGTACCTAATACGTAACAA
***** **

M1      GTTGAATGTTTCGGATGATAGTCGGTTATGATAGGTGCATAAGGTCAATAGCCAGATGCG
M3      GTTGAATGTTTCGGATGATAGTCGGTTATGATAGGTGCATAAGGTCAATAGCCAGATGCG
M4      GTTGAATGTTTCGGATGATAGTCGGTTATGATAGGTGCATAAGGTCAATAGCCAGATGCG
M5      GTTGAATGTTTCGGATGATAGTTGGTTATGATAGGTGCATAAGGTCAATAGCCAGATGCG
M6      GTTGAATGTTTCGGATGATAGTCGGTTATGATAGGTGCATAAGGTCAATAGCCAGATGCG
M12     GTTGAATGTTTCGGATGATAGTCGGTTATGATAGGTGCATAAGGTCAATAGCCAGATGCG
M18     GTTGAATGTTTCGGATGATAGTCGGTTATGATAGGTGCATAAGGTCAATAGCCAGATGCG
M28     GTTGAATGTTTCGGATGATAGTCGGTTATGATAGGTGCATAAGGTCAATAGCCAGATGCG
M49     GTTGAATGTTTCGGATGATAGTCGGTTATGATAGGTGCATAAGGTCAATAGCCAGATGCG
M53     GTTGAATGTTTCGGATGATAGTTGGTTATGATAGGTGCATAAGGTCAATAGCCAGATGCG
M59     GTTGAATGTTTCGGATGATAGTCGGTTATGATAGGTGCATAAGGTCAATAGCCAGATGCG
***** *

M1      ATAGTTTTATCAACTGTCATATGTTAAACCTTTCTAATCTAATAGATGTTAAAAATACGT
M3      ATAGTTTTATCAACTGTCATATGTTAAACCTTTCTAATCTAATAGATGTTAAAAATACGT
M4      ATAGTTTTATCAACTGTCATATGTTAAACCTTTCTAATCTAATAGATGTTAAAAATACGT
M5      ATAGTTTTATCAACTGTCATATGTTAAACCTTTCTAATCTAATAGATGTTAAAAATACGT
M6      ATAGTTTTATCAACTGTCATATGTTAAACCTTTCTAATCTAATAGATGTTAAAAATACGT
M12     ATAGTTTTATCAACTGTCATATGTTAAACCTTTCTAATCTAATAGATGTTAAAAATACGT
M18     ATAGTTTTATCAACTGTCATATGTTAAACCTTTCTAATCTA-TAGATGTTAAAAATACGT
M28     ATAGTTTTATCAACTGTCATATGTTAAACCTTTCTAATCTAATAGATGTTAAAAATACGT
M49     ATAGTTTTATCAACTGTCATATGTTAAACCTTTCTAATCTAATAGATGTTAAAAATACGT
M53     ATAGTTTTATCAACTGTCATATGTTAAACCTTTCTAATCTAATAGATGTTAAAAATACGT
M59     ATAGTTTTATCAACTGTCATATGTTAAACCTTTCTAATCTAATAGATGTTAAAAATACGT
*****

M1      TACGTGTGTACCTAATACGTAACAAAATAATGGGTTAGCAAAAATAAGCAGCTATGATATA
M3      TACGTGTGTACCTAATACGTAACAAAATAATGGGTTAGCAAAAATAAGCAGCTATGATATA
M4      TACGTGTGTACCTAATACGTAACAAAATAATGGGTTAGCAAAAATAAGCAGCTATGATATA
M5      TACGTGTGTACCTAATACGTAACAAAATAATGGGTTAGCAAAAATAAGCAGCTATGATATA
M6      TACGTGTGTACCTAATACGTAACAAAATAATGGGTTAGCAAAAATAAGCAGCTATGATATA
M12     TACGTGTGTACCTAATACGTAACAAAATAATGGGTTAGCAAAAATAAGCAGCTATGATATA
M18     TACGTGTGTACCTAATACGTAACAAAATAATGGGTTAGCAAAAATAAGCAGCTATGATATA
M28     TACGTGTGTACCTAATACGTAACAAAATAATGGGTTAGCAAAAATAAGCAGCTATGATATA
M49     TACGTGTGTACCTAATACGTAACAAAATAATGGGTTAGCAAAAATAAGCAGCTATGATATA
M53     TACGTGTGTACCTAATACGTAACAAAATAATGGGTTAGCAAAAATAAGCAGCTATGATATA

```

```

M59  TACGTGTGTACCTAATACGTAACAAATAATGGGTTAGCAAAATAAGCAGCTATGATATA
      *****
M1    GCCATAAGGTTAAAAGGAGGCGCCTACTATGTGGTTATTGTTACTATTTTTGTAG
M3    GCCATAAGGTTAAAAGGAGGCGCCTACTATGTGGTTATTGTTACTATTTTTGTAG
M4    GCCATAAGGTTAAAAGGAGGCGCCTACTATGTGGTTATTGTTACTATTTTTGTAG
M5    GCCATAAGGTTAAAAGGAGGCGCCTACTATGTGGTTATTGTTACTATTTTTGTAG
M6    GCCATAAGGTTAAAAGGAGGCGCCTACTATGTGGTTATTGTTACTATTTTTGTAG
M12   GCCATAAGGTTAAAAGGAGGCGCCTACTATGTGGTTATTGTTACTATTTTTGTAG
M18   GCCATAAGGTTAAAAGGAGGCGCCTACTATGTGGTTATTGTTACTATTTTTGTAG
M28   GCCATAAGGTTAAAAGGAGGCGCCTACTATGTGGTTATTGTTACTATTTTTGTAG
M49   GCCATAAGGTTAAAAGGAGGCGCCTACTATGTGGTTATTGTTACTATTTTTGTAG
M53   GCCATAAGGTTAAAAGGAGGCGCCTACTATGTGGTTATTGTTACTATTTTTGTAG
M59   GCCATAAGGTTAAAAGGAGGCGCCTACTATGTGGTTATTGTTACTATTTTTGTAG
      *****

```

Figure S13. Nucleotide sequences containing the P1 promoter sequences and *SIP*-coding region are highly conserved among GAS serotypes. Alignment of the nucleotide sequences of *SIP*-coding region, and the upstream P1 promoter sequences located between *SIP*- and *ropB*-coding regions from different M serotypes of GAS is shown. Identical positions among the serotypes are marked with asterisks (\*). The operator sequences, site1 and site2, containing RopB binding sites are underlined and shaded in grey. The transcription start site of P1 promoter is highlighted in blue and the putative ribosomal binding site for *SIP* translation is underlined. The *SIP*-coding region is indicated in bold and highlighted in grey.

Table S1. Genes that are downregulated in  $\Delta SIP$  mutant

Locus tag	Spy Number <sup>a</sup>	Fold-change <sup>b</sup>	Annotation <sup>c</sup>
<b>Virulence factors</b>			
<i>speB</i>	SpyM3_1742	2420	Pyrogenic exotoxin B
<i>spi</i>	SpyM3_1741	2291	Intracellular SpeB inhibitor
<i>sdn</i>	SpyM3_1409	3.1	Streptodornase (sdn) – phage associated
<i>ndoS</i>	SpyM3_1568	2.2	Secreted endoglycosidase
<i>hlyIII</i>	SpyM3_0815	2.1	Putative hemolysin
<i>sagP</i>	SpyM3_1196	6.4	Anti-tumor glycoprotein
<b>Stress responses</b>			
<i>dnaK</i>	SpyM3_1531	2.4	Molecular chaperone DnaK
<i>groEL</i>	SpyM3_1765	2.0	Molecular chaperone GroEL
<i>groES</i>	SpyM3_1766	2.3	Molecular chaperone GroES
<i>grpE</i>	SpyM3_1532	3.2	Heat shock protein GrpE
<i>clpL</i>	SpyM3_0607	2.5	ATP-dependent Clp protease
<i>clpP</i>	SpyM3_0287	2.0	ATP-dependent Clp protease subunit
<i>hrcA</i>	SpyM3_1533	4.2	Heat-inducible transcription repressor
<i>arcB</i>	SpyM3_1194	5.4	Ornithine carbomoyl transferase
<i>arcC</i>	SpyM3_1191	2.1	Carbamate kinase
<b>Others</b>			
<i>copA</i>	SpyM3_1491	3.1	Copper transporting ATPase
<i>copy</i>	SpyM3_1492	3.9	Copper responsive regulator
<i>copZ</i>	SpyM3_1490	2.1	Copper chaperone
<i>serS</i>	SpyM3_1516	3.2	Seryl-tRNA synthase
<i>scrA</i>	SpyM3_1569	2.3	Sucrose-specific PTS transporter subunit IIABC
<i>xerS</i>	SpyM3_0839	2.3	Site-specific tyrosine recombinase
<b>Hypothetical proteins</b>			
<i>M3_0377</i>	SpyM3_0377	2.3	Hypothetical protein
<i>M3_0742</i>	SpyM3_0742	2.1	Hypothetical protein
<i>M3_0894</i>	SpyM3_0894	2.0	Hypothetical protein
<i>M3_0895</i>	SpyM3_0895	2.4	Hypothetical protein
<i>M3_0896</i>	SpyM3_0896	2.4	Hypothetical protein
<i>M3_0897</i>	SpyM3_0897	2.1	Hypothetical protein
<i>M3_0898</i>	SpyM3_0898	2.2	Hypothetical protein
<i>M3_0899</i>	SpyM3_0899	2.1	Hypothetical protein
<i>M3_0900</i>	SpyM3_0900	2.4	Hypothetical protein
<i>M3_1192</i>	SpyM3_1192	2.5	Hypothetical protein
<i>M3_1193</i>	SpyM3_1193	3.6	Hypothetical protein
<i>M3_1195</i>	SpyM3_1195	6.7	Hypothetical protein
<i>M3_1705</i>	SpyM3_1705	2.5	Hypothetical protein
<i>M3_1709</i>	SpyM3_1709	2.3	Hypothetical protein
<i>M3_1743</i>	SpyM3_1743	2080	Hypothetical protein
<i>M3_1828</i>	SpyM3_1828	4.4	Hypothetical protein

<i>M3_1829</i>	SpyM3_1829	3.9	Hypothetical protein
<i>M3_1830</i>	SpyM3_1830	3.8	Hypothetical protein
<i>M3_1831</i>	SpyM3_1831	2.0	Hypothetical protein

Table S2. Genes that are upregulated in  $\Delta SIP$  mutant.

Locus tag	Spy Number <sup>a</sup>	Fold-change <sup>b</sup>	Annotation <sup>c</sup>
<b>Protein synthesis</b>			
<i>rplB</i>	SpyM3_0043	2.3	50S ribosomal protein L2
<i>rplC</i>	SpyM3_0040	2.8	50S ribosomal protein L3
<i>rplD</i>	SpyM3_0041	2.6	50S ribosomal protein L4
<i>rplL</i>	SpyM3_0754	2.6	50S ribosomal protein L7/L12
<i>rplM</i>	SpyM3_1664	3.1	50S ribosomal protein L13
<i>rplQ</i>	SpyM3_0067	3.1	50S ribosomal protein L17
<i>rplS</i>	SpyM3_0474	2.9	50S ribosomal protein L19
<i>rplT</i>	SpyM3_0540	2.4	50S ribosomal protein L20
<i>rplV</i>	SpyM3_0045	2.3	50S ribosomal protein L22
<i>rplW</i>	SpyM3_0042	2.4	50S ribosomal protein L23
<i>rpmB</i>	SpyM3_1629	3.6	50S ribosomal protein L28
<i>rpmF</i>	SpyM3_1816	3.0	50S ribosomal protein L32
<i>rpmG</i>	SpyM3_1817	3.6	50S ribosomal protein L33
<i>rpmJ</i>	SpyM3_0063	2.9	50S ribosomal protein L36
<i>rpsC</i>	SpyM3_0046	2.2	30S ribosomal protein S3
<i>rpsF</i>	SpyM3_1582	2.4	30S ribosomal protein S6
<i>rpsG</i>	SpyM3_0199	2.3	30S ribosomal protein S7
<i>rpsI</i>	SpyM3_1663	4.5	30S ribosomal protein S9
<i>rpsJ</i>	SpyM3_0039	2.9	30S ribosomal protein S10
<i>rpsK</i>	SpyM3_0065	2.5	30S ribosomal protein S11
<i>rpsL</i>	SpyM3_0198	2.5	30S ribosomal protein S12
<i>rpsM</i>	SpyM3_0064	2.6	30S ribosomal protein S13
<i>rpsN.2</i>	SpyM3_1615	2.5	30S ribosomal protein S14
<i>rpsO</i>	SpyM3_1681	3.0	30S ribosomal protein S15
<i>rpsP</i>	SpyM3_0567	2.3	30S ribosomal protein S16
<i>rpsR</i>	SpyM3_1580	3.0	30S ribosomal protein S18
<i>rpsT</i>	SpyM3_0872	3.1	30S ribosomal protein S20
<i>rluD</i>	SpyM3_0786	2.5	Ribosomal large subunit pseudouridine synthase
<i>def</i>	SpyM3_1684	2.4	Peptide deformylase
<b>Amino acid metabolism</b>			
<i>amiC</i>	SpyM3_0618	17.3	Amidase
<i>aroA.2</i>	SpyM3_1279	2.5	Aromatic amino acid biosynthesis
<i>braB</i>	SpyM3_0236	2.9	Branched amino acid transport
<b>DNA synthesis, repair, and metabolism</b>			
<i>purC</i>	SpyM3_0019	8.1	Purine biosynthesis
<i>purF</i>	SpyM3_0021	3.6	Purine biosynthesis
<i>purH</i>	SpyM3_0024	3.1	Purine biosynthesis
<i>purL</i>	SpyM3_0020	3.6	Purine biosynthesis
<i>purM</i>	SpyM3_0022	3.5	Purine biosynthesis
<i>purN</i>	SpyM3_0023	2.9	Purine biosynthesis
<i>pyrB</i>	SpyM3_0560	27.5	Pyrimidine biosynthesis
<i>pyrD</i>			

<i>pyrE</i>	SpyM3_1091	6.1	Pyrimidine biosynthesis
<i>pyrF</i>	SpyM3_0617	30.4	Pyrimidine biosynthesis
<i>pyrG</i>	SpyM3_0616	44.6	Pyrimidine biosynthesis
<i>pyrP</i>	SpyM3_1632	2.4	Pyrimidine biosynthesis
<i>pyrR</i>	SpyM3_0559	37.5	Pyrimidine biosynthesis
<i>guaA</i>	SpyM3_0558	49.1	Pyrimidine biosynthesis
<i>guaB</i>	SpyM3_0845	2.3	GMP synthase
	SpyM3_1857	2.3	Inosine 5'-monophosphate dehydrogenase
<i>nrdE.1</i>			
	SpyM3_1049	4.3	Ribonucleotide-diphosphate reductase $\alpha$ subunit
<i>nrdF.1</i>			
	SpyM3_1050	4.7	Ribonucleotide-diphosphate reductase $\beta$ subunit
<i>nrdG</i>			
	SpyM3_1791	2.4	anaerobic ribonucleotide reductase activator
<i>nrdH</i>			
<i>nrdI.1</i>	SpyM3_1048	4.6	Glutaredoxin-like protein
<i>carA</i>	SpyM3_1706	2.3	Flavoprotein NrdI
	SpyM3_0561	21.5	Carbamoyl phosphate synthase small subunit
<i>carB</i>			
	SpyM3_0562	18.5	Carbamoyl phosphate synthase large subunit
<i>rexA</i>			
	SpyM3_0514	3.6	ATP-dependent exonuclease subunit A
<i>rexB</i>			
	SpyM3_0513	2.8	ATP-dependent exonuclease subunit B
<i>polC</i>			
<i>parC</i>	SpyM3_1687	2.3	DNA polymerase III
<i>parE</i>	SpyM3_0625	2.8	DNA topoisomerase IV-subunit A
<i>rpoA</i>	SpyM3_0624	2.2	DNA topoisomerase IV-subunit B
<i>dyr</i>	SpyM3_0066	2.7	RNA polymerase-alpha subunit
<i>udk</i>	SpyM3_0602	2.6	Dihydrofolate reductase
<i>upp</i>	SpyM3_1042	3.3	Uridine kinase
<i>thyA</i>	SpyM3_0286	3.3	Uracil phosphoribosyl transferase
<i>topA</i>	SpyM3_0601	3.4	Thymidylate synthase
<i>ssb.2</i>	SpyM3_0820	2.4	DNA topoisomerase I
<i>xpt</i>	SpyM3_1581	2.4	Single strand DNA-binding protein2
<i>cdd</i>	SpyM3_0794	4.2	Xanthine phosphoribosyltransferase
	SpyM3_0869	2.4	Cytidine deaminase
<b>Proteases/Peptidases</b>			
<i>pcp</i>			
<i>pepB</i>	SpyM3_0355	2.2	Pyrrolidone-carboxylate peptidase
<i>pepN</i>	SpyM3_1062	3.0	Oligopeptidase
<i>pepO</i>	SpyM3_0875	2.3	Aminopeptidase_N
<i>pepXP</i>	SpyM3_1784	2.4	Endopeptidase
<i>cppA</i>	SpyM3_1603	5.3	x-prolyl dipeptidyl aminopeptidase
<i>clpX</i>	SpyM3_1598	3.5	C3-degrading proteinase
	SpyM3_0604	2.7	ATP-dependent protease
<b>Group A polysaccharide antigen synthesis</b>			
<i>rgpBc</i>			
	SpyM3_0523	2.3	group A polysaccharide antigen synthesis
<i>rgpCc</i>			
	SpyM3_0524	2.1	group A polysaccharide antigen synthesis
<i>rgpDc</i>			
	SpyM3_0525	2.3	group A polysaccharide antigen synthesis
<i>rgpEc</i>			
	SpyM3_0526	2.2	group A polysaccharide antigen synthesis
<i>rgpFc</i>			
			group A polysaccharide antigen

<i>rgpGc</i>	SpyM3_0527	2.8	synthesis
	SpyM3_0528	2.4	group A polysaccharide antigen synthesis
<b>Transporters</b>			
<i>OppD</i>			Oligopeptide ABC transporter ATP-binding subunit
<i>pstB</i>	SpyM3_0218	2.2	
	SpyM3_0877	2.3	Phosphate transporter ATP-binding protein
<i>dppB</i>	SpyM3_1719	2.8	Dipeptide ABC transporter permease
<i>dppC</i>	SpyM3_1720	2.9	Dipeptide ABC transporter permease
<i>dppD</i>	SpyM3_1721	2.6	Dipeptide ABC transporter ATP-binding subunit
<i>dppE</i>	SpyM3_1722	2.7	Dipeptide ABC transporter ATP-binding subunit
<i>potA</i>	SpyM3_0764	2.8	Polyamine transporter complex - subunit A
<i>potB</i>	SpyM3_0765	3.3	Polyamine transporter complex - subunit B
<i>potC</i>	SpyM3_0766	3.2	Polyamine transporter complex - subunit C
<i>potD</i>	SpyM3_0767	3.3	Polyamine transporter complex - subunit D
<i>glpF.2</i>	SpyM3_1600	2.5	Glycerol uptake facilitator protein
<b>Cell wall synthesis</b>			
<i>murB</i>	SpyM3_0763	2.6	UDP-N-acetylpyruvoylglucosamine reductase
<i>murN</i>	SpyM3_0434	2.2	Peptidoglycan branched peptide synthesis protein
<i>pgdA</i>	SpyM3_1044	2.2	Peptidoglycan-N-acetyl glucosamine deacetylase
<i>smc</i>	SpyM3_0376	3.1	Chromosome condensation and segregation protein
<i>divIVA</i>	SpyM3_1167	2.3	Cell division initiation protein
<i>ftsH</i>	SpyM3_0012	2.4	Cell division protein
	SpyM3_0012	2.4	Cell division protein
<b>Enzymes</b>			
<i>acpA</i>	SpyM3_0375	2.8	Double strand RNase
<i>acpP.2</i>	SpyM3_1526	2.9	Acyl carrier protein
<i>ccdA</i>	SpyM3_1269	2.6	Cytochrome c biosynthesis
<i>coaA</i>	SpyM3_0871	2.8	Panthothenate kinase
<i>cobQ</i>	SpyM3_0677	2.5	Cobyric acid synthase
<i>cysE</i>	SpyM3_1674	2.2	Serine acetyl transferase
<i>cysS</i>	SpyM3_1672	3.4	CysteinyI-tRNA synthetase
<i>fabH</i>	SpyM3_1527	2.9	3-oxoacyl-ACP synthase
<i>fhs.1</i>	SpyM3_0853	5.0	Formate-tetrahydrofolate ligase
<i>folD</i>	SpyM3_1157	3.0	Methylene-tetrahydrofolate dehydrogenase
<i>glyQ</i>	SpyM3_1472	2.5	Glycyl-tRNA synthetase
<i>msrA.1</i>	SpyM3_1267	3.0	Bifunctional methionine sulfoxide reductase
<i>mvaS.1</i>	SpyM3_0599	2.2	3-hydroxy-3-methylglutaryl coenzymeA
<i>mvaS.2</i>	SpyM3_0600	2.2	3-hydroxy-3-methylglutaryl coenzyme A synthase

<i>phaB</i>	SpyM3_1529	3.3	Enoyl-coA hydratase
<i>pmi</i>	SpyM3_1566	2.5	Mannose-6-phosphate isomerase
<i>ppc</i>	SpyM3_0430	2.5	Phosphoenolpyruvate carboxylase
<i>sla</i>	SpyM3_1204	2.7	Phospholipase-A2-like protein
<i>spi</i>	SpyM3_1592	2.6	Signal peptidase I
<i>thrS</i>	SpyM3_0365	2.8	Threonine-tRNA ligase
<i>trmU</i>	SpyM3_1840	2.6	tRNA-specific thiouridylase
<b>Transcription regulators</b>			
<i>ropB</i>	SpyM3_1744	3.1	Regulator of Protease B
<i>covS</i>	SpyM3_0245	2.8	Two-component histidine kinase
<b>Hypothetical proteins</b>			
<i>M3_0014</i>	SpyM3_0014	4.0	Hypothetical protein
<i>M3_0025</i>	SpyM3_0025	3.1	Hypothetical protein
<i>M3_0029</i>	SpyM3_0029	2.4	Hypothetical protein
<i>M3_0038</i>	SpyM3_0038	2.9	Hypothetical protein
<i>M3_0072</i>	SpyM3_0072	3.2	Hypothetical protein
<i>M3_0092</i>	SpyM3_0092	2.5	Hypothetical protein
<i>M3_0104</i>	SpyM3_0104	3.5	Hypothetical protein
<i>M3_0212</i>	SpyM3_0212	3.6	Hypothetical protein
<i>M3_0226</i>	SpyM3_0226	2.4	Hypothetical protein
<i>M3_0227</i>	SpyM3_0227	2.8	Hypothetical protein
<i>M3_0228</i>	SpyM3_0228	3.2	Hypothetical protein
<i>M3_0229</i>	SpyM3_0229	2.7	Hypothetical protein
<i>M3_0230</i>	SpyM3_0230	3.3	Hypothetical protein
<i>M3_0237</i>	SpyM3_0237	3.3	Hypothetical protein
<i>M3_0238</i>	SpyM3_0238	2.4	Hypothetical protein
<i>M3_0243</i>	SpyM3_0243	2.2	Hypothetical protein
<i>M3_0254</i>	SpyM3_0254	2.4	Hypothetical protein
<i>M3_0265</i>	SpyM3_0265	2.3	Hypothetical protein
<i>M3_0267</i>	SpyM3_0267	2.2	Hypothetical protein
<i>M3_0268</i>	SpyM3_0268	2.2	Hypothetical protein
<i>M3_0272</i>	SpyM3_0272	3.2	Hypothetical protein
<i>M3_0334</i>	SpyM3_0334	2.2	Hypothetical protein
<i>M3_0340</i>	SpyM3_0340	3.1	Hypothetical protein
<i>M3_0402</i>	SpyM3_0402	2.7	Hypothetical protein
<i>M3_0437</i>	SpyM3_0437	2.4	Hypothetical protein
<i>M3_0515</i>	SpyM3_0515	3.3	Hypothetical protein
<i>M3_0528</i>	SpyM3_0528	2.7	Hypothetical protein
<i>M3_0529</i>	SpyM3_0529	3.6	Hypothetical protein
<i>M3_0530</i>	SpyM3_0530	2.5	Hypothetical protein
<i>M3_0531</i>	SpyM3_0531	2.8	Hypothetical protein
<i>M3_0532</i>	SpyM3_0532	3.5	Hypothetical protein
<i>M3_0541</i>	SpyM3_0541	2.3	Hypothetical protein
<i>M3_0576</i>	SpyM3_0576	2.3	Hypothetical protein
<i>M3_0603</i>	SpyM3_0603	3.4	Hypothetical protein
<i>M3_0605</i>	SpyM3_0605	3.1	Hypothetical protein
<i>M3_0606</i>	SpyM3_0606	2.8	Hypothetical protein
<i>M3_0619</i>	SpyM3_0619	5.4	Hypothetical protein
<i>M3_0620</i>	SpyM3_0620	6.8	Hypothetical protein
<i>M3_0627</i>	SpyM3_0627	3.6	Hypothetical protein
<i>M3_0636</i>	SpyM3_0636	2.5	Hypothetical protein
<i>M3_0637</i>	SpyM3_0637	2.7	Hypothetical protein
<i>M3_0638</i>	SpyM3_0638	2.4	Hypothetical protein
<i>M3_0652</i>	SpyM3_0652	2.4	Hypothetical protein
<i>M3_0653</i>	SpyM3_0653	3.9	Hypothetical protein

M3_0655	SpyM3_0655	4.0	Hypothetical protein
M3_0656	SpyM3_0656	3.5	Hypothetical protein
M3_0774	SpyM3_0774	3.6	Hypothetical protein
M3_0779	SpyM3_0779	2.2	Hypothetical protein
M3_0780	SpyM3_0780	2.4	Hypothetical protein
M3_0783	SpyM3_0783	2.4	Hypothetical protein
M3_0793	SpyM3_0793	5.3	Hypothetical protein
M3_0795	SpyM3_0795	4.8	Hypothetical protein
M3_0797	SpyM3_0797	2.5	Hypothetical protein
M3_0812	SpyM3_0812	2.6	Hypothetical protein
M3_0857	SpyM3_0857	5.6	Hypothetical protein
M3_0860	SpyM3_0860	3.6	Hypothetical protein
M3_0870	SpyM3_0870	3.9	Hypothetical protein
M3_1019	SpyM3_1019	3.4	Hypothetical protein
M3_1020	SpyM3_1020	14.0	Hypothetical protein
M3_1021	SpyM3_1021	3.3	Hypothetical protein
M3_1040	SpyM3_1040	2.5	Hypothetical protein
M3_1060	SpyM3_1060	2.8	Hypothetical protein
M3_1061	SpyM3_1061	3.7	Hypothetical protein
M3_1068	SpyM3_1068	2.8	Hypothetical protein
M3_1069	SpyM3_1069	2.4	Hypothetical protein
M3_1070	SpyM3_1070	2.6	Hypothetical protein
M3_1075	SpyM3_1075	2.4	Hypothetical protein
M3_1077	SpyM3_1077	2.5	Hypothetical protein
M3_1146	SpyM3_1146	2.3	Hypothetical protein
M3_1184	SpyM3_1184	2.2	Hypothetical protein
M3_1264	SpyM3_1264	2.4	Hypothetical protein
M3_1268	SpyM3_1268	2.7	Hypothetical protein
M3_1277	SpyM3_1277	3.0	Hypothetical protein
M3_1388	SpyM3_1388	2.8	Hypothetical protein
M3_1396	SpyM3_1396	2.3	Hypothetical protein
M3_1478	SpyM3_1478	3.2	Hypothetical protein
M3_1507	SpyM3_1507	2.3	Hypothetical protein
M3_1508	SpyM3_1508	2.3	Hypothetical protein
M3_1509	SpyM3_1509	3.0	Hypothetical protein
M3_1510	SpyM3_1510	2.4	Hypothetical protein
M3_1514	SpyM3_1514	4.5	Hypothetical protein
M3_1528	SpyM3_1528	2.9	Hypothetical protein
M3_1587	SpyM3_1587	2.4	Hypothetical protein
M3_1597	SpyM3_1597	3.1	Hypothetical protein
M3_1602	SpyM3_1602	5.3	Hypothetical protein
M3_1606	SpyM3_1606	2.5	Hypothetical protein
M3_1635	SpyM3_1635	2.4	Hypothetical protein
M3_1671	SpyM3_1671	4.3	Hypothetical protein
M3_1673	SpyM3_1673	3.0	Hypothetical protein
M3_1686	SpyM3_1686	2.7	Hypothetical protein
M3_1714	SpyM3_1714	2.3	Hypothetical protein
M3_1792	SpyM3_1792	2.2	Hypothetical protein
M3_1811	SpyM3_1811	2.3	Hypothetical protein
M3_1834	SpyM3_1834	2.6	Hypothetical protein
M3_1843	SpyM3_1843	5.3	Hypothetical protein
M3_1844	SpyM3_1844	2.2	Hypothetical protein
M3_1849	SpyM3_1849	3.0	Hypothetical protein
M3_1850	SpyM3_1850	2.6	Hypothetical protein
M3_1861	SpyM3_1861	3.2	Hypothetical protein

<b>Others</b>			
<i>manM</i>	SpyM3_1512	2.3	Mannose-specific transporter IIC
<i>mecA</i>	SpyM3_0206	2.2	Adaptor protein
<i>ptsI</i>	SpyM3_1046	2.5	PEP:sugar phosphotransferase system
<i>salk</i>	SpyM3_1645	2.5	Salavacin regulon response regulator
<i>salR</i>	SpyM3_1646	2.7	Salavacin regulon sensor histidine kinase
<i>int315.4</i>	SpyM3_1266	2.9	Phage encoded putative integrase
<i>grab</i>	SpyM3_1032	2.7	G-related alpha 2M-binding protein
<i>cpsY</i>	SpyM3_0614	2.3	Transcription regulator

Table S3. Genes that are downregulated in *orf-1\** mutant

Locus tag	Spy Number <sup>a</sup>	Fold-change <sup>b</sup>	Annotation <sup>c</sup>
<b>Virulence factors</b>			
<i>speB</i>	SpyM3_1742	1380	Pyrogenic exotoxin B
<i>spi</i>	SpyM3_1741	1324	Intracellular SpeB inhibitor
<b>Enzymes</b>			
<i>acpA</i>	SpyM3_0375	2.0	Ribonuclease 3
<i>adk</i>	SpyM3_0061	2.6	Adenylate kinase
<i>dys</i>	SpyM3_0602	2.1	Dihydrofolate reductase
<i>hylP.1</i>	SpyM3_0725	2.7	Hyaluronidase
<i>nrdH</i>	SpyM3_1048	2.0	Glutaredoxin-like protein
<i>pheS</i>	SpyM3_0506	2.4	Phenylalanyl-tRNA synthetase
<i>rexA</i>	SpyM3_0514	2.4	ATP-dependent exonuclease A
<i>thrS</i>	SpyM3_0365	2.3	Threonyl-tRNA synthetase
<i>trmU</i>	SpyM3_1840	2.2	tRNA 2-thiouridine synthase
<i>trx.1</i>	SpyM3_0091	2.0	Thioredoxin
<b>Others</b>			
<i>rpsB</i>	SpyM3_1782	2.2	30S ribosomal protein S2
<i>rpsJ</i>	SpyM3_0039	2.5	30S ribosomal protein S10
<b>Hypothetical proteins</b>			
<i>M3_0411</i>	SpyM3_0411	2.1	Hypothetical protein
<i>M3_0439</i>	SpyM3_0439	2.2	Hypothetical protein
<i>M3_0492</i>	SpyM3_0492	2.0	Hypothetical protein
<i>M3_0515</i>	SpyM3_0515	2.5	Hypothetical protein
<i>M3_0603</i>	SpyM3_0603	3.0	Hypothetical protein
<i>M3_0627</i>	SpyM3_0627	4.4	Hypothetical protein
<i>M3_0926</i>	SpyM3_0926	3.3	Hypothetical protein
<i>M3_1068</i>	SpyM3_1068	2.0	Hypothetical protein
<i>M3_1069</i>	SpyM3_1069	2.1	Hypothetical protein
<i>M3_1208</i>	SpyM3_1208	2.3	Hypothetical protein
<i>M3_1212</i>	SpyM3_1212	2.5	Hypothetical protein
<i>M3_1226</i>	SpyM3_1226	2.0	Hypothetical protein
<i>M3_1277</i>	SpyM3_1277	2.2	Hypothetical protein
<i>M3_1278</i>	SpyM3_1278	2.4	Hypothetical protein
<i>M3_1388</i>	SpyM3_1388	2.6	Hypothetical protein
<i>M3_1412</i>	SpyM3_1412	3.9	Hypothetical protein

M3_1413	SpyM3_1413	2.3	Hypothetical protein
M3_1414	SpyM3_1414	2.6	Hypothetical protein
M3_1415	SpyM3_1415	2.5	Hypothetical protein
M3_1417	SpyM3_1415	2.4	Hypothetical protein
M3_1419	SpyM3_1419	2.2	Hypothetical protein
M3_1420	SpyM3_1420	2.2	Hypothetical protein
M3_1421	SpyM3_1421	2.3	Hypothetical protein
M3_1422	SpyM3_1422	2.0	Hypothetical protein
M3_1716	SpyM3_1716	3.4	Hypothetical protein
M3_1717	SpyM3_1717	4.4	Hypothetical protein
M3_1743	SpyM3_1743	1666	Hypothetical protein

Table S4. Genes that are upregulated in *orf-1\** mutant.

Locus tag	Spy Number <sup>a</sup>	Fold-change <sup>b</sup>	Annotation <sup>c</sup>
<b>Virulence factors</b>			
<i>slo</i>	SpyM3_0130	3.6	Streptolysin O
<i>nga</i>	SpyM3_0128	2.4	NAD glycohydrolase
<i>hlyIII</i>	SpyM3_0815	2.2	Putative hemolysin
<b>Transporters</b>			
<i>glnQ</i>	SpyM3_0998	2.3	Glutamine ABC transporter
<i>mtsC</i>	SpyM3_0320	2.2	Manganese transporter permease
<i>opuABC</i>	SpyM3_0144	2.5	Glycine-betaine binding permease
<b>Enzymes</b>			
<i>metB</i>	SpyM3_0133	2.2	Cystathionine beta-lyase
<i>nox.1</i>	SpyM3_0808	2.5	NADH oxidase
<i>phaB</i>	SpyM3_1529	2.3	Enoyl-coA hydratase
<b>Others</b>			
<i>cbp</i>	SpyM3_0098	2.0	Collagen-binding protein
<i>rrf</i>	SpyM3_0327	2.3	Ribosome recycling factor
<i>spoJ</i>	SpyM3_1865	2.3	Chromosome segregation protein
<b>Hypothetical proteins</b>			
M3_0072	SpyM3_0072	2.3	Hypothetical protein
M3_0129	SpyM3_0129	3.0	Hypothetical protein
M3_0163	SpyM3_0163	2.4	Hypothetical protein
M3_0164	SpyM3_0164	2.6	Hypothetical protein
M3_0331	SpyM3_0331	2.3	Hypothetical protein
M3_0377	SpyM3_0377	2.7	Hypothetical protein
M3_0742	SpyM3_0742	2.1	Hypothetical protein
M3_0744	SpyM3_0744	2.0	Hypothetical protein
M3_0979	SpyM3_0979	2.3	Hypothetical protein
M3_1254	SpyM3_1254	3.1	Hypothetical protein
M3_1350	SpyM3_1350	2.2	Hypothetical protein
M3_1547	SpyM3_1547	2.0	Hypothetical protein
M3_1667	SpyM3_1667	2.4	Hypothetical protein
M3_1820	SpyM3_1820	2.0	Hypothetical protein
M3_1821	SpyM3_1821	2.3	Hypothetical protein
M3_1822	SpyM3_1822	2.5	Hypothetical protein
M3_1828	SpyM3_1828	5.0	Hypothetical protein
M3_1829	SpyM3_1829	5.2	Hypothetical protein
M3_1830	SpyM3_1830	5.8	Hypothetical protein

Table S5. Bacterial strains and plasmids used in this study.

Strain or Plasmid	Description	Reference
<b>Strains</b>		
WT	Invasive isolate MGAS10870, serotype M3	(1)
WT:pDC	MGAS10870 <i>trans</i> -complemented with empty vector pDC123, chloramphenicol resistant	(2)
WT:pDC-INT-1	MGAS10870 <i>trans</i> -complemented with plasmid pDC-INT-1, chloramphenicol resistant	This study
WT:pDC-INT-2	MGAS10870 <i>trans</i> -complemented with plasmid pDC-INT-2, chloramphenicol resistant	This study
WT:pDC-INT-3	MGAS10870 <i>trans</i> -complemented with plasmid pDC-INT-3, chloramphenicol resistant	This study
$\Delta ropB$	MGAS10870 $\Delta ropB::aad9$	(3)
$\Delta ropB$ :pDC-orf-1	$\Delta ropB$ mutant <i>trans</i> -complemented with plasmid pDC-orf-1, Chloramphenicol resistant	This study
$\Delta speB$	MGAS10870 $\Delta speB::aad9$	(2)
orf-1*	Isoallelic mutant strain that has the start codon of orf-1 changed to stop codon in parental serotype MGAS10870	This study
orf-1*:pDC	$\Delta orf-1^*$ mutant <i>trans</i> -complemented with empty vector pDC123, Chloramphenicol resistant	This study
orf-1*:pDC-orf-1	$\Delta orf-1^*$ mutant <i>trans</i> -complemented with plasmid pDC-orf-1, Chloramphenicol resistant	This study
orf-2*	Isoallelic mutant strain that has the start codon of orf-2 changed to stop codon in parental serotype MGAS10870	This study
orf-3*	Isoallelic mutant strain that has the start codon of orf-3 changed to stop codon in parental serotype MGAS10870	This study
$\Delta orf-1$	orf-1 deletion mutant in parental serotype MGAS10870	This study
$\Delta eep$	MGAS10870 $\Delta eep::aad9$	This study
$\Delta oppDF$	MGAS10870 $\Delta oppDF::aad9$	This study
	Isoallelic mutant strain that has the in-	

$\Delta dppA$	frame deletion of <i>dppA</i> of <i>dppABCDF</i> operon in parental serotype MGAS10870	This study
$\Delta oppDF/\Delta dppA$	Isoallelic mutant strain that has the in-frame deletion of <i>dppA</i> of <i>dppABCDF</i> operon in $\Delta oppDF$ mutant strain	This study
$\Delta oppDF/\Delta dppA/orf-1^*$	Isoallelic mutant strain that has the start codon of <i>orf-1</i> changed to stop codon in $\Delta oppDF/\Delta dppA$ mutant strain	This study
<i>E. coli</i> DH5 $\alpha$	Host strain for cloning purposes	
<i>E. coli</i> BL21 (DE3)	Host strain for protein overexpression, <i>F-</i> , <i>ompT</i> , <i>hsdSB(rB-mB-)</i> , <i>gal</i> ( $\lambda$ c I 857, <i>ind1</i> , <i>Sam7</i> , <i>nin5</i> , <i>lacUV-T7 gene1</i> ), <i>dcm</i> (DE3)	
<b>Plasmids</b>		
<i>pJL</i>	Low-copy number plasmid capable of replication in GAS and <i>Escherichia coli</i> , Chloramphenicol resistant Used to generate isoallelic GAS mutants	(4)
<i>pDC</i>	Low-copy number plasmid, <i>pDC123</i> , capable of replication in GAS and <i>Escherichia coli</i> , Chloramphenicol resistant	(5)
<i>pDC-INT-1</i>	<i>pDC</i> with the fragment of intergenic region (-772 to -1) between <i>ropB</i> and <i>speB</i>	This study
<i>pDC-INT-2</i>	<i>pDC</i> with the fragment of intergenic region (-772 ~ -268) between <i>ropB</i> and <i>speB</i>	This study
<i>pDC-INT-3</i>	<i>pDC</i> with the fragment of intergenic region (-772 ~ -519) between <i>ropB</i> and <i>speB</i>	This study
<i>pDC-orf-1</i>	<i>pDC</i> with the fragment of intergenic region (-772 ~ -646) between <i>ropB</i> and <i>speB</i>	This study
<i>pDC-orf-1^*</i>	<i>pDC-orf-1</i> that has the start codon of <i>orf-1</i> changed to stop codon	This study
<i>pET28a</i>	Overexpression vector for N-terminally hexahistidine tagged recombinant proteins, Km <sup>R</sup>	Novagen
<i>pET15b</i>	Overexpression vector for N-terminally hexahistidine tagged recombinant proteins, Amp <sup>R</sup>	Novagen

Table S6. Primers and probes used in this study

Primer	Sequence 5' – 3'	Purpose
INT1_Top	CGCATGCTAAGCTTACTAGGATCTAAAAATA CGTTACGTGTG	5' primer for 5' region of INT1 fragment of <i>ropB-speB</i> intergenic region
INT1_Bottom	CATATGAATTCAGCTGCAGGATCTTTTTTATA CCTCTTTCAAAT	3' primer for 5' region of INT1 fragment of <i>ropB-speB</i> intergenic region
INT2_Bottom	CATATGAATTCAGCTGCAGGATCCTACTAGGC AGACTGATAGGC	3' primer for 5' region of INT2 fragment of <i>ropB-speB</i> intergenic region
INT3_Bottom	CATATGAATTCAGCTGCAGGATCCTAGTAGAT GCTCATTTCAGTTGAC	3' primer for 5' region of INT3 fragment of <i>ropB-speB</i> intergenic region
<i>Orf-1</i> _Bottom	CATATGAATTCAGCTGCAGGATCCTACAAAA TAGTAACAATAACCAC	3' primer for 5' region of <i>orf1</i> fragment in <i>ropB-speB</i> intergenic region
pJL_INT_Top	GAATTCCTGCAGCCCGGGGATCAATAACTTT TGAAAACACCATC	5' primer for 5' region of <i>ropB-speB</i> intergenic region to clone intergenic region into pJL for the mutagenesis
pJL_INT_ Bottom	GGCCGCTCTAGAAGTAGTGGATCTGCTGATTT TTGGATAAATG	3' primer for 5' region of <i>ropB-speB</i> intergenic region to clone intergenic region into pJL for the mutagenesis
<i>orf-1*</i> Top	GTAAAAGGAGGCGCCTACTTAGTGGTTATTG TTACTATTTTTG	5' primer for 5' region of <i>orf-1</i> to change the start codon to stop codon
<i>orf-1*</i> Bottom	CAAAAATAGTAACAATAACCACTAAGTAGGCG CCTCCTTTTAAC	3' primer for 5' region of <i>orf-1</i> to change the start codon to stop codon
<i>orf-2*</i> Top	GTAGTTCCTTTTGCAAATAGGTAGTAGATAAAA ATGAG	5' primer for 5' region of <i>orf-2</i> to change the start codon to stop codon
<i>orf-2*</i> Bottom	CTCATTTTTATCTACTACCTATTTGCAAAAGGA ACTAC	3' primer for 5' region of <i>orf-2</i> to change the start codon to stop codon
<i>orf-3*</i> Top	GAAAAAGCCTACGAGTCAACTATAGGACAACC CAAAAAAGACAAAG	5' primer for 5' region of <i>orf-3</i> to change the start codon to stop codon
<i>orf-3*</i> Bottom	CTTTGTCTTTTTTGGGTTGTCCTATAGTTGAC TCGTAGGCTTTTTTC	3' primer for 5' region of <i>orf-3</i> to change the start codon to stop codon

$\Delta orf-1$ Bottom	CATTTTGCAAAGGAAGACTACAACCACATAGTAGGCGCCTCC	3' primer for 5' region of <i>orf-1</i> to delete <i>orf-1</i>
$\Delta orf-1$ Top	GGAGGCGCCTACTATGTGGTTGTAGTTCCTTTTGCAAATG	5' primer for 5' region of <i>orf-1</i> to delete <i>orf-1</i>
$\Delta eep-A$	CGCCTGTCAGGAATTGACAAG	5' primer for 5' region of <i>eep</i>
$\Delta eep-B$	GTTATAGTTATTATAACATGTATTCCTAACATAGATCTCCTTTCAG	3' primer for 5' region of <i>eep</i> with <i>spc</i> sequence overlap
$\Delta eep-C$	CTATTTAAATAACAGATTAATAAAAAATTATAACATGCGCGTCTTTTTCTAATCAAG	5' primer for 5' region of <i>eep</i> with <i>spc</i> sequence overlap
$\Delta eep-D$	CATGGCACCGCCATCTCC	3' primer for 3' region of <i>eep</i>
$\Delta eep-E$	GTTTGGAGTCGCAACAACGCG	5' primer for 5' region of <i>eep</i>
$\Delta eep-F$	CATCACGATACTTAGACT	3' primer for 3' region of <i>eep</i>
$\Delta eep-G$	GTTCCGATGGACCATTACCTC	5' primer for 5' region of <i>eep</i>
$\Delta eep-H$	TGAATAAGCAATAGTATCTTC	3' primer for 3' region of <i>eep</i>
$\Delta eep-spcF$	CTGAAAGGAGATCTATGTTAGGAATACATGTTATAATAACTATAAC	5' primer for <i>spc</i> along with <i>eep</i> overlap sequence
$\Delta eep-spcR$	CTTGATTAGAAAAAGACGCGCATGTTATAATTTTAAATCTGTTATTTAAATAG	3' primer for <i>spc</i> along with <i>eep</i> overlap sequence
$\Delta oppDF-A$	GACTTTTCAAGCGTTATATTTG	5' primer for 5' region of <i>oppDF</i>
$\Delta oppDF-B$	GTTATAGTTATTATAACATGTATTCATTTAACTCCTATCTATGTGA	3' primer for 5' region of <i>oppDF</i> with <i>spc</i> sequence overlap
$\Delta oppDF-C$	CTATTTAAATAACAGATTAATAAAAAATTATAAATTGTAAGAGATGCACTGAC	5' primer for 5' region of <i>oppDF</i> with <i>spc</i> sequence overlap
$\Delta oppDF-D$	GTATACGATATCTTTACTGTCATTG	3' primer for 3' region of <i>oppDF</i>
$\Delta oppDF-E$	TGTACTACTGGATGGATTGGTGTGCG	5' primer for 5' region of <i>oppDF</i>
$\Delta oppDF-F$	TGGCTTGTTACATGCAGGAAGCTC	3' primer for 3' region of <i>oppDF</i>
$\Delta oppDF-G$	CACTTTTACTAGGAGATATTGTCATG	5' primer for 5' region of <i>oppDF</i>
$\Delta oppDF-H$	CTGTGCTGACAGATTTATTCTC	3' primer for 3' region of <i>oppDF</i>
$\Delta oppDF-spcF$	TCACATAGATAGGAGTTAAATGAATACATGTTATAATAACTATAAC	5' primer for <i>spc</i> along with <i>oppDF</i> overlap sequence
$\Delta oppDF-spcR$	GTCAGTGCATCTCTTTTACAATTTATAATTTTTTAAATCTGTTATTTAAATAG	3' primer for <i>spc</i> along with <i>oppDF</i> overlap sequence
$\Delta dppA-A$	GAATTCCTGCAGCCCGGGGATCGCTATTCCAAATAGATTGAATCCTC	5' primer for 5' region of <i>dppA</i>
$\Delta dppA-B$	CTAAAATAAGCCCAGTCAAAAATAACG	3' primer for 5' region of <i>dppA</i>
$\Delta dppA-C$	CGTTATTTTTGACTGGGCTTATTTAGCGCGTT	5' primer for 5' region of

	TAGTTAATACAGCGAC	<i>dppA</i>
$\Delta$ <i>dppA-D</i>	GGCCGCTCTAGAACTAGTGGATCGGTAACATA AGGTGCTTAATCCG	3' primer for 3' region of <i>dppA</i>
<i>pET-28a ropB</i> <i>top</i>	GGACAGCAAATGGGTCGCGGATCCATGGAAA TTGGTGAAACCGTTG	5' primer for 5' region of <i>ropB</i>
<i>pET-28a ropB</i> <i>bottom</i>	TCGACGGAGCTCGAATTCGGATCTCAGGACA GTTTATGTTTAATG	3' primer for 3' region of <i>ropB</i>
<i>tufA</i> qRTFwd	CAACTCGTCACTATGCGCACAT	5' primer for <i>tufA</i> qRT-PCR
<i>tufA</i> qRTRev	GAGCGGCACCAGTGATCAT	3' primer for <i>tufA</i> qRT-PCR
<i>tufA</i> probe C	CTCCAGGACACGCGGACTACGTTAAAAA	Probe for <i>tufA</i> qRT-PCR
<i>speB</i> qRTFwd	ACTCTACCAGCGGATCATTTG	5' primer for <i>speB</i> qRT-PCR
<i>speB</i> qRTRev	CAGCGGTACCAGCATAAGTAG	3' primer for <i>speB</i> qRT-PCR
<i>speB</i> probe	TGCTTCCTTCATGGAAAGTTATGTCGAACA	Probe for <i>speB</i> qRT-PCR
<i>ropB</i> qRTFwd	AAGATAGTAAGCCAACAAAGGA	5' primer for <i>ropB</i> qRT-PCR
<i>ropB</i> qRTRev	TGACAAATAAGTCCGCTCTG	3' primer for <i>ropB</i> qRT-PCR
<i>ropB</i> probe	TTGGTCAAGGTGTTATTAGCAACTCTTACTGA GGAA	Probe for <i>ropB</i> qRT-PCR
<i>orf-3</i> qRTFwd	CTTGGTGTTGTGGACCCTATC	5' primer for <i>orf-3</i> qRT-PCR
<i>orf-3</i> qRTRev	TAGGCAGACTGATAGGCAAGA	3' primer for <i>orf-3</i> qRT-PCR
<i>orf-3</i> probe	CAGCTAGCAAACAATAGGTTGTGCTTGAC	Probe for <i>orf-3</i> qRT-PCR
<i>orf-1</i> probe	ATAGTAGGCGCCTCCTTTTAAAC	Probe for <i>orf-1</i> Northern blot
<i>Probe1-fwd</i>	ATGTCAAGCCTTCCTAGTTG	5' primer for 5' region of probe 1 used in EMSA
<i>Probe1-rev</i>	CAAAAATAGTAACAATAACCACTAAGTAGGCG CCTCCTTTTAAAC	3' primer for 3' region of probe 1 and probe 2 used in EMSA
<i>Probe2-fwd</i>	CGCATGCTAAGCTTACTAGGATCTAAAAAATA CGTTACGTGTG	5' primer for 5' region of probe 2 used in EMSA
<i>Probe3-fwd</i>	TAGATACGGCAGAAG	5' primer for 5' region of probe 3 used in EMSA
<i>Probe3-rev</i>	CACCTCCTTACTTAG	3' primer for 3' region of probe 3 used in EMSA
<i>pET-15b speB</i> <i>top</i>	GGGAATTCATATGTTTGCTCGTAACGAAAAA GAAGCA	5' primer for 5' region of <i>speB</i>
<i>pET-15b speB</i> <i>bottom</i>	CGCCGCTCGAGCTAAGGTTTGATGCCTACAA CAGCA	3' primer for 3' region of <i>speB</i>

Table S7. Preparation of Chemically-Defined Medium

<b>Component</b>	<b>grams/liter</b>
Chemically Defined Medium A*	17.12
NaHCO <sub>3</sub>	2.5
Carbon source (Glucose)	10
L-cysteine HCl	0.5

Bring to volume, filter sterilize (0.22 µm pore size), and store at 4° C, protected from light.

CDM is typically good for about a week, if stored at 4°C; discard when precipitates form.

\*Chemically Defined Medium A (recipe below) was originally formulated by SAFC Biosciences (taken over and subsequently discontinued by Sigma Aldrich).

**\*Chemically Defined Medium A recipe**

<b><i>I. Amino Acids</i></b>	<b><i>grams/liter</i></b>
DL-Alanine	0.1
L-Arginine	0.1
L-Aspartic Acid	0.1
L-Cystine, 2HCl	0.0652
L-Glutamic Acid	0.1
L-Glutamine	0.2
Glycine	0.1
L-Histidine	0.1
Hydroxy L-Proline	0.1
L-Isolueicine	0.1
L-Leucine	0.1
L-Lysine HCl	0.1249
L-Methionine	0.1

L-Phenylalanine	0.1
L-Proline	0.1
L-Serine	0.1
L-Threonine	0.2
L-Tryptophan	0.1
L-Tyrosine, 2Na, 2H <sub>2</sub> O	0.1442
L-Valine	0.1
<b>II. Bases</b>	<b>grams/liter</b>
Adenine Sulfate, 2H <sub>2</sub> O	0.02
Guanine, HCl, H <sub>2</sub> O	0.02
Uracil	0.02
<b>III. Salts</b>	<b>grams/liter</b>
Calcium Chloride, Anhydrous	0.005066
Magnesium Sulfate, Anhydrous	0.3419
Manganous Sulfate, H <sub>2</sub> O	0.005
Potassium Phosphate, Dibasic, Anhydrous	0.2
Potassium Phosphate, monobasic, Anhydrous	1
Sodium Acetate Anhydrous	2.7126
Sodium Phosphate, Dibasic, Anhydrous	7.35
Sodium Phosphate, monobasic, H <sub>2</sub> O	3.195
<b>IV. Iron</b>	<b>grams/liter</b>
Ferric Nitrate, 9 H <sub>2</sub> O	0.001
Ferrous Sulfate, 7 H <sub>2</sub> O	0.005
<b>V. Vitamins</b>	<b>grams/liter</b>

Beta-NAD, 3 H <sub>2</sub> O	0.0025
Biotin	0.0002
Cyanocobalamin	0.0001
D-Calcium Pantothenate	0.002
Folic Acid	0.0008
Niacinamide	0.001
Para-Aminobenzoic Acid	0.0002
Pyridoxal, HCl	0.001
Pyridoxamine, 2HCl	0.001
Riboflavin	0.002
Thiamine, HCl	0.001

## Supplemental Materials and Methods

**Bacterial strains, plasmids and growth conditions.** Bacterial strains and plasmids used in this study are listed in supplementary table S3. Strain MGAS10870 is a previously described invasive serotype M3 isolate whose genome has been fully sequenced (1). MGAS10870 is representative of serotype M3 strains that cause invasive infections and has wild-type sequences for all major regulatory genes (1). *Escherichia coli* DH5 $\alpha$  strain was used as the host for plasmid constructions and BL21(DE3) strain was used for recombinant protein overexpression. GAS was grown routinely on Trypticase Soy agar containing 5% sheep blood (BSA; Becton Dickinson) or in Todd-Hewitt broth containing 0.2% (w/v) yeast extract (THY; DIFCO). When required, spectinomycin or chloramphenicol was added to a final concentration of 100  $\mu\text{g/ml}$  or 5  $\mu\text{g/ml}$ , respectively. All GAS growth experiments were done in triplicate on three separate occasions for a total of nine replicates. Overnight cultures were inoculated into fresh media to achieve an initial absorption at 600 nm ( $A_{600}$ ) of 0.03. Bacterial growth was monitored by measuring the optical density at  $A_{600}$ . The *Escherichia coli* strain used for protein overexpression was grown in Luria-Bertani broth (LB broth; Fisher).

**Creation of isoallelic strains.** Isoallelic strains containing either single codon changes or inactivation of entire coding region were generated as previously described (3). A DNA fragment with approximately 600 bp on either side of the coding region of interest was amplified using the primers listed in supplementary table S4 and cloned into the multi-cloning site of the temperature-sensitive plasmid pJL1055 (5). The resultant plasmids were electroporated into group A streptococci and colonies with plasmid incorporated into the GAS chromosome were selected for subsequent plasmid curing. DNA sequencing was then performed to ensure that no spurious mutations were introduced.

**Construction of *trans*-complementation plasmids.** To complement the isoallelic mutant strains, either the different fragments of the *speB-ropB* intergenic region or the coding sequence of *SIP* gene together with the native promoter region were cloned into the *E. coli*-GAS shuttle vector *pDC123* (4). Using the primers listed in supplementary table S4, the respective fragments were amplified by PCR from GAS genomic DNA, digested with *Bgl*III and *Nde*I, and ligated into digested vector *pDC123*. The inserts were verified by DNA sequencing and electroporated into the appropriate GAS strains.

**Northern blot analysis.** Northern blotting analysis was performed as previously described (6). Membranes were hybridized in ULTRAhyb Ultrasensitive Hybridization Buffer (Thermo Fisher) at 42 °C with <sup>32</sup>P-end-labeled DNA oligonucleotides. Signals were visualized with a Typhoon phosphorimager (GE healthcare) and band intensities were quantified using the GelQuant software (BiochemLabSolutions).

**Transcript level analysis.** GAS strains were grown to the indicated A<sub>600</sub> and incubated with two volumes of RNeasy Protect (Qiagen) for 10 min at room temperature. RNA isolation and purification were performed with an RNeasy kit (Qiagen). After quality control analysis, cDNA was synthesized from the purified RNA using Superscript III (Invitrogen) and Taqman quantitative RT-PCR was performed with an ABI 7500 Fast System (Applied Biosystems). Comparison of transcript levels was performed by the  $\Delta C_T$  method of analysis using *tufA* as the endogenous control gene (7). The Taqman primers and probes used are listed in Supplementary table S4.

**Western immunoblot analysis of SpeB in the culture supernatant.** For the purpose of raising rabbit polyclonal anti-SpeB antibodies, we overexpressed and purified the mature

form of SpeB (SpeB<sub>M</sub>). Briefly, the coding region of *speB* of strain MGAS10870 without its secretion signal sequence (amino acids 1-27) was cloned into plasmid pET-15b using the primers listed in supplementary table S4. Protein was overexpressed in *E. coli* strain BL21(DE3). Cells were grown at 37°C till the A<sub>600</sub> reaches 0.5 and induced with 0.5 mM IPTG at 37°C for 3 hours. Cells were resuspended in buffer A (20 mM Tris HCl pH 8.0, 0.2 M NaCl, 5% glycerol, and 1 mM TCEP) and lysed by a cell lyser (Constant systems). The N-terminal hexa-histidine tagged zymogen form of SpeB was purified by affinity chromatography using a Ni-NTA agarose column. Purified recombinant SpeB zymogen was incubated at 4°C for 2 days to facilitate its autocatalytic conversion into SpeB<sub>M</sub>. Finally, SpeB<sub>M</sub> was purified by size exclusion chromatography with superdex 75G column. The protein was purified to > 95% homogeneity and the sequence identity of the purified SpeB<sub>M</sub> was confirmed by mass spectrometry-based identification of the N-terminal amino acids.

Purified SpeB<sub>M</sub> was used to produce rabbit polyclonal anti-SpeB antibodies commercially (Pacific Immunologicals). Briefly, purified SpeB<sub>M</sub> (100µg) mixed with Freund's complete adjuvant was injected subcutaneously to each of two rabbits. Two additional immunizations with SpeB<sub>M</sub> mixed in Freund's incomplete adjuvant were carried out every 3 weeks. Serum was collected and SpeB-specific antibodies were affinity purified using SpeB<sub>M</sub>. Specific reactivity with SpeB was assessed by western blotting and detected only in the post-immunization serum.

Cells were grown to indicated growth phase and harvested by centrifugation. The cell-free culture supernatant was prepared by filtration with 0.22 µm membrane and the filtrate was concentrated two-fold by speed-vac drying. Equal volumes of the samples were resolved on a 15% SDS-PAGE gel, transferred to a nitrocellulose membrane, and probed with polyclonal anti-SpeB rabbit antibodies. SpeB was detected with a secondary antibody

conjugated with horseradish peroxidase and visualized by chemiluminescence using the SuperSignal West Pico Rabbit IgG detection kit (Thermo Scientific).

**SpeB protease activity assay.** Analysis of SpeB protease activity was assessed by casein hydrolysis and zone of clearance on skim milk agar plates. GAS growth was stabbed on milk agar plates and protease activity was analyzed following overnight incubation at 37°C.

**Synthetic peptide addition assay.** Synthetic peptides of high purity (>90% purity) obtained from Lifetein (Lifetein LLC, NC) were suspended in 100% DMSO to prepare a 10 mM stock solution. Stock solutions were aliquoted and stored at -20°C until use. Working stocks were prepared by diluting the stock solution in 25% DMSO.

**Secretome swapping experiments.** To assess the presence or absence of the regulatory factor in the stationary growth phase culture supernatant of GAS that induces *speB* expression, the indicated strains were grown to stationary phase ( $A_{600} > 1.5$ ). Cell-free culture supernatants were prepared by centrifugation and filtering through 0.22  $\mu\text{m}$  membrane filter. The cell pellets of the wild type GAS grown to mid-exponential growth phase ( $A_{600} \sim 0.8$ ) were resuspended in the secretomes prepared from the stationary growth phase of the indicated strains and incubated at 37°C for 1 h. Transcript level analyses was performed by qRT-PCR as described above.

**Fluorescence measurements.** To demonstrate the cytosolic internalization of exogenously added FITC-SIP, GAS cells were grown to early stationary phase of growth ( $A_{600} \sim 1.7$ ;  $3.04 \times 10^8$  colony-forming units/ml) and incubated with the indicated concentrations of FITC-SIP-1 for 1h at 37 °C. Cells were harvested by centrifugation, washed twice with phosphate-

buffered saline (PBS), and resuspended in equal volume of PBS. Cells were lysed by fastprep (MP Biomedicals) and lysates were clarified by centrifugation at 13,000 rpm at 4°C for 30 minutes. Samples were analyzed in 100 µl volume using an excitation and emission wavelengths of 490 nm and 520 nm, respectively. Readings were taken using a Biotek microplate reader (Biotek) and fluorescence measurements in relative fluorescence units (RFU) were reported.

**Confocal fluorescence microscopy.** To demonstrate the internalization of FITC-SIP, GAS cells were grown to early stationary phase of growth ( $A_{600} = 1.7$ ;  $3.04 \times 10^8$  colony-forming units/ml) and incubated with FITC-SIP-1 for 1h at 37 °C. Cells were harvested by centrifugation, washed twice with PBS, and images were taken using a laser scanning confocal microscope (Olympus, Fluo-View™ FV1000) at 100X magnification.

**Protein overexpression and purification.** The coding region of either the full-length or C-terminal domain (RopB-CTD) (amino acids 56-280) of *ropB* gene of strain MGAS10870 was cloned into plasmid pET-28a and protein was overexpressed in *E. coli* strain BL21 (DE3). Protein overexpression and purification for both full-length RopB and RopB-CTD were carried out as described previously (2, 8). The protein was purified to >95% homogeneity and concentrated to a final concentration of ~ 20 mg/ml.

**Fluorescence polarization assay.** Fluorescence polarization-based RopB-ligand binding experiments were performed with a Biotek microplate reader (Biotek) using the intrinsic fluorescence of fluorescein labelled DNA or synthetic peptides. The polarization (P) of the labelled DNA or synthetic peptides increases as a function of protein binding and equilibrium dissociation constants were determined from plots of millipolarization ( $P \times 10^{-3}$ ) against

protein concentration. For RopB-DNA-binding studies, 1 nM 5'-fluoresceinated oligoduplex in binding buffer (20 mM Tris-HCl pH 8.5, 200 mM NaCl, 1 mM TCEP and 25% DMSO) was titrated against increasing concentrations of purified RopB and the resulting change in polarization measured. Samples were excited at 490 nm and emission measured at 530 nm. The RopB-peptide-binding studies were performed in a peptide-binding buffer composed of 20mM potassium phosphate pH 6.0, 75mM NaCl, 2% DMSO, 1mM EDTA and 0.0005% Tween 20. All data were plotted using Kaleidagraph and the resulting plots were fitted with the equation  $P = \{(P_{\text{bound}} - P_{\text{free}})[\text{protein}]/(K_D + [\text{protein}])\} + P_{\text{free}}$ , where  $P$  is the polarization measured at a given protein concentration,  $P_{\text{free}}$  is the initial polarization of the free ligand,  $P_{\text{bound}}$  is the maximum polarization of specifically bound ligand and  $[\text{protein}]$  is the protein concentration. Non-linear least squares analysis was used to determine  $P_{\text{bound}}$ , and  $K_D$ . The binding constant reported is the average value from at least three independent experimental measurements.

**Electrophoretic mobility shift assay.** Probes containing different fragments of the promoter sequences of *speB* was generated by polymerase chain reaction using the primers listed in the Supplementary table S4. Binding reactions were carried out in 20  $\mu\text{l}$  volume of binding buffer (20 mM Tris-HCl pH 8.0, 0.2 M NaCl, 1 mM Tris (2-carboxyethyl) phosphine hydrochloride (TCEP), and 5% glycerol) containing 50 nM of probe and increasing concentrations of recombinant RopB. After 15 minutes incubation at 37°C, the reactions mixtures were resolved on a 10% native polyacrylamide gel supplemented with 5% glycerol (native PAGE) for 90 minutes at 100V at 4°C in Tris Borate (TB) buffer with 5% glycerol. The gels were stained with ethidium bromide and analyzed on a BioRad Gel Electrophoresis System.

**Size exclusion chromatography.** Size exclusion chromatography was used to determine the oligomerization state of recombinant RopB in the presence and absence of synthetic peptides. A Superdex-200 column (GE healthcare) was calibrated using cytochrome C (Mr 12,400), carbonic anhydrase (Mr 29,000), bovine serum albumin (Mr 66,000), alcohol dehydrogenase (Mr 150,000) and  $\beta$ -amylase (200,000). The  $K_{Average}$  ( $K_{ave}$ ) was calculated using the equation  $K_{ave} = (V_E - V_O)/(V_T - V_O)$ , where  $V_T$ ,  $V_E$  and  $V_O$  are the total column volume, elution volume and void volume of the column, respectively. A standard graph was obtained by plotting the logarithm of the molecular weight (Mr) versus the  $K_{ave}$  (Graphpad prism). The  $K_{ave}$  of each marker and the experimental samples were the average value of two or more experiments.

**Analysis of RopB oligomerization state.** The oligomerization state of recombinant RopB in the presence and absence of synthetic peptides was analyzed by blue-native polyacrylamide gel electrophoresis. Apo- or peptide-bound RopB fractionated by size exclusion chromatography were run on a 4-16% NativePAGE™ Novex Bis-Tris gel (Thermo Fisher Scientific) according to the manufacturer's instructions. NativeMark™ unstained molecular mass ladder (ThermoFisher Scientific) was used as molecular weight marker to determine the oligomeric state of RopB.

**Mass spectrometry analysis.** All reagents were prepared in 50 mM HEPES (pH 8.5). For samples containing RopB, cysteine reduction was performed using dithiothreitol, followed by alkylation with iodacetamide, and digestion with trypsin. For the sample containing only the SIP-1, these steps were omitted. For all samples a clean-up step was performed using OASIS HLB  $\mu$ Elution Plate (Waters). Samples were analysed on a Q Exactive Plus

instrument (Thermo Scientific). Peptide separation was performed using the UltiMate 3000 RSLC nano LC system (Dionex) equipped with a trapping cartridge ( $\mu$ -Precolumn C18 PepMap 100, 5 $\mu$ m, 300  $\mu$ m i.d. x 5 mm, 100 Å) and an analytical column (Acclaim PepMap 100 75  $\mu$ m x 50 cm C<sub>18</sub>, 3  $\mu$ m, 100 Å) over a 60-minute gradient and online injected into the mass spectrometer. MS scan resolution was set to 70,000. The ion filling time was set to a maximum of 10 ms with a target of  $3 \times 10^6$ . Acquisition was performed in data dependent mode (DDA). Selection and fragmentation of singly charged (1+) precursor ions was enabled. MS2 scan resolution was set to 17,500, with a 100 ms fill time and a target of  $2 \times 10^5$  ions. HCD normalized collision energy was set to 26. SIP-1 identification from the RopB+SIP-1 complex sample was performed based on the precursor mass and comparison with the MS2 spectrum of SIP-1 obtained from the single peptide, SIP-1, experiment.

**RNA-seq analysis.** GAS strains were grown in THY medium to stationary phase of growth and a total of 5 biological replicates per strain were used. RNA isolation and purification were performed using an RNeasy (Qiagen) mini kit according to the manufacturer's protocol. RNA was analyzed for quality and concentration with an Agilent 2100 Bioanalyzer. The ribosomal RNA was then removed using a Ribo-zero treatment kit (Epicenter) according to manufacturer's protocol and further purified using the Min-Elute RNA purification kit (Qiagen). The ribosomally depleted RNA was then used to synthesize adaptor tagged cDNA libraries using the ScriptSeq V2 RNA-seq library preparation kit (Epicenter). cDNA libraries were then run on a NextSeq using the Illumina v2 reagent kit (Illumina). Approximately 10 million reads were obtained per sample and the reads were mapped to the MGAS315 genome (1) using the CLC-Genomics WorkBench, version 5 (CLC Bio). For RNA-seq analysis, the total number of reads per gene between the replicates was normalized by TPKM [(transcripts/kilobase of gene)/(million reads aligning to the genome)]. Using the TPKM values, pair-wise comparisons

were carried out between the two samples to identify the differentially expressed genes. Genes with 2-fold difference and  $P < 0.05$  after applying Bonferroni's correction considered to be statistically significant.

**Animal virulence studies.** Mouse experiments were performed according to protocols approved by the Houston Methodist Hospital Research Institute Institutional Animal Care and Use Committee. These studies were carried out in strict accordance with the recommendations in the Guide for the Care and Use of Laboratory Animals, 8<sup>th</sup> edition. Virulence of the isogenic mutant GAS strains was assessed using three mouse models. For intraperitoneal infection, 10 female 3-4 week-old CD1 mice (Harlan Laboratories) were used for each GAS strain. Animals were inoculated intraperitoneally with  $1 \times 10^7$  CFUs and survival was monitored daily. Data were graphically displayed as a Kaplan-Meier survival curve and analyzed using the log-rank test. For intramuscular infection, 10 female 3-4 week-old CD1 mice (Harlan Laboratories) were inoculated in the right hindlimb with  $1 \times 10^7$  CFU of each strain and monitored for near mortality. Results were graphically displayed as a Kaplan-Meier survival curve and analyzed using the log-rank test. For subcutaneous infection, 10 female 4- to 5-week-old, immunocompetent SKH1-hrBR hairless mice (Charles River BRF, Houston, TX) were inoculated subcutaneously with  $1 \times 10^7$  CFUs of each strain and lesion areas were measured daily. Data were graphically displayed as mean  $\pm$  SEM lesion area over time (Prism4) and analyzed using ANOVA (XLStat). For histopathology, infected hindlimbs were examined at 24 and 48 h post-inoculation. Tissues from excised lesions were fixed in 10% phosphate-buffered formalin, decalcified, serially sectioned, and embedded in paraffin using standard automated instruments. Hematoxylin and eosin and Gram-stained sections were examined in a blinded fashion with a BX5 microscope and photographed with a

DP70 camera (Olympus). Micrographs of tissues taken from the inoculation sites that showed pathology characteristic of each strain were selected for publication.

**Statistical analysis.** Prism (GraphPad Software 7.0) was used for statistical analyses. All GAS growth experiments for transcript level analyses were done in triplicate on three separate occasions for a total of nine replicates. The protein-peptide and protein-DNA binding experiments were done on three separate occasions to ensure reproducibility. For near mortality, values are shown as Kaplan-Meier survival curves, and statistical significance was determined using the log-rank test. For lesion area measurements in the subcutaneous mouse model of infection, statistical significance was determined using a Two-way ANOVA (XLStat).

## References

1. Beres SB, *et al.* (2010) Molecular complexity of successive bacterial epidemics deconvoluted by comparative pathogenomics. *Proc. Natl. Acad. Sci. USA* **107**:4371-4376.
2. Shelburne III SA, *et al.* (2011) An amino-terminal signal peptide of Vfr protein negatively influences RopB-dependent SpeB expression and attenuates virulence in *Streptococcus pyogenes*. *Mol. Microbiol.* **82**:1481-1495.
3. Carroll RK, *et al.* (2011) Naturally occurring single amino acid replacements in a regulatory protein alter streptococcal gene expression and virulence in mice. *J. Clin. Invest.* **121**:1956-1968.
4. Li J, Kasper DL, Ausubel FM, Rosner B, & Michel JL (1997) Inactivation of the  $\alpha$  C protein antigen gene, *bca*, by a novel shuttle/suicide vector results in attenuation of virulence and immunity in group B *Streptococcus*. *Proc. Natl. Acad. Sci. USA* **94**:13251-13256.
5. Chaffin DO & Rubens CE (1998) Blue/white screening of recombinant plasmids in Gram-positive bacteria by interruption of alkaline phosphatase gene (*phoZ*) expression. *Gene* **219**:91-99.
6. Fröhlich KS, Haneke K, Papenfort K, & Vogel J (2016) The target spectrum of SdsR small RNA in Salmonella. *Nucl. Acids Res.* **44**:10406-10422.
7. Sanson M, *et al.* (2015) Adhesin competence repressor (AdcR) from *Streptococcus pyogenes* controls adaptive responses to zinc limitation and contributes to virulence. *Nucl. Acids Res.* **43**:418-432.

8. Makthal N, *et al.* (2016) Structural and functional analysis of RopB: a major virulence regulator in *Streptococcus pyogenes*. *Mol. Microbiol.* **99**:1119-1133.

## CHAPTER 2

**Signaling by a Conserved Quorum Sensing Pathway Contributes to Growth *Ex Vivo* and Oropharyngeal Colonization of Human Pathogen Group A *Streptococcus*.**

**Makthal N, Do H, VanderWal AR, Olsen RJ, Musser JM, Kumaraswami M.**

Published: March 12<sup>th</sup> 2018. *Infect Immun* 86:e00169-18.



## Signaling by a Conserved Quorum Sensing Pathway Contributes to Growth *Ex Vivo* and Oropharyngeal Colonization of Human Pathogen Group A Streptococcus

Nishanth Makthal,<sup>a</sup> Hackwon Do,<sup>a</sup> Arica R. VanderWal,<sup>a</sup> Randall J. Olsen,<sup>a,b</sup> James M. Musser,<sup>a,b</sup>  Muthiah Kumaraswami<sup>a</sup>

<sup>a</sup>Center for Molecular and Translational Human Infectious Diseases Research, Houston Methodist Research Institute, and Department of Pathology and Genomic Medicine, Houston Methodist Hospital, Houston, Texas, USA

<sup>b</sup>Department of Pathology and Laboratory Medicine, Weill Medical College of Cornell University, New York, New York, USA

**ABSTRACT** Bacterial virulence factor production is a highly coordinated process. The temporal pattern of bacterial gene expression varies in different host anatomic sites to overcome niche-specific challenges. The human pathogen group A streptococcus (GAS) produces a potent secreted protease, SpeB, that is crucial for pathogenesis. Recently, we discovered that a quorum sensing pathway comprised of a leaderless short peptide, SpeB-inducing peptide (SIP), and a cytosolic global regulator, RopB, controls *speB* expression in concert with bacterial population density. The SIP signaling pathway is active *in vivo* and contributes significantly to GAS invasive infections. In the current study, we investigated the role of the SIP signaling pathway in GAS-host interactions during oropharyngeal colonization. The SIP signaling pathway is functional during growth *ex vivo* in human saliva. SIP-mediated *speB* expression plays a crucial role in GAS colonization of the mouse oropharynx. GAS employs a distinct pattern of SpeB production during growth *ex vivo* in saliva that includes a transient burst of *speB* expression during early stages of growth coupled with sustained levels of secreted SpeB protein. SpeB production aids GAS survival by degrading LL37, an abundant human antimicrobial peptide. We found that SIP signaling occurs during growth in human blood *ex vivo*. Moreover, the SIP signaling pathway is critical for GAS survival in blood. SIP-dependent *speB* regulation is functional in strains of diverse *emm* types, indicating that SIP signaling is a conserved virulence regulatory mechanism. Our discoveries have implications for future translational studies.

**KEYWORDS** colonization, group A streptococcus, pathogenesis, quorum sensing, virulence regulation

**B**acterial pathogens colonize different host anatomic sites with various ecologies and encounter unique challenges in each tissue microenvironment. The host employs niche-specific anatomic barriers, antimicrobial defense mechanisms, and nutritional immune mechanisms to inhibit bacterial proliferation. Successful pathogens have sensory mechanisms to monitor environmental cues and mount tailored transcriptional responses to adapt to new environments. One such sensory program in Gram-positive bacteria, known as quorum sensing, uses secreted bacterial peptide signals to monitor the population density and mediate the spatiotemporal regulation of virulence factor production (1, 2). The quorum sensing pathway involves signal production, secretion, and sensing by neighboring bacteria and population-wide modulation of gene expression (1–3). Quorum sensing pathways control several bacterial traits, including virulence, biofilm formation, antibiotic resistance, sporulation, and

Received 2 March 2018 Accepted 4 March 2018

Accepted manuscript posted online 12 March 2018

**Citation** Makthal N, Do H, VanderWal AR, Olsen RJ, Musser JM, Kumaraswami M. 2018. Signaling by a conserved quorum sensing pathway contributes to growth *ex vivo* and oropharyngeal colonization of human pathogen group A streptococcus. *Infect Immun* 86:e00169-18. <https://doi.org/10.1128/IAI.00169-18>.

**Editor** Nancy E. Freitag, University of Illinois at Chicago

**Copyright** © 2018 American Society for Microbiology. All Rights Reserved.

Address correspondence to Muthiah Kumaraswami, [mkumaraswami@houstonmethodist.org](mailto:mkumaraswami@houstonmethodist.org).

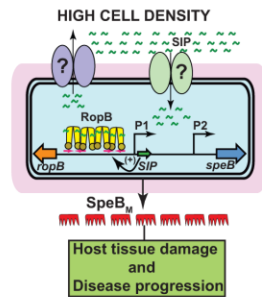


**FIG 1** Proposed model for mechanism of SIP-dependent intercellular communication and GAS virulence regulation. At a high cell density, SIP is produced, secreted, and reimported into the cytosol. The high-affinity RopB-DNA interactions and RopB polymerization aided by SIP binding lead to upregulation of SIP gene expression, which results in the robust induction of SIP production by a positive-feedback mechanism. Finally, the SIP-dependent upregulation of *speB* leads to the abundant secretion of the mature form of SpeB protease (SpeB<sub>M</sub>), which facilitates host tissue damage and disease dissemination by cleavage of various host and GAS proteins. The *ropB* and *speB* genes are divergently transcribed. The block arrows indicate the coding regions of *ropB*, *speB*, and the gene for SIP. The angled arrows above the line indicate two transcription start sites for *speB*, designated P1 and P2. The pseudo inverted repeats containing the RopB-binding site within the *speB* promoter are marked by arrows and colored in red.

genetic competence (2–7). Virulence regulation by quorum sensing has been studied extensively *in vitro*. However, bacterial growth in laboratory medium does not fully recapitulate the growth in the complex host environment in which the signaling occurs during infection. Thus, elucidation of the niche-specific contribution of quorum sensing pathways during infection is critical to understand the dynamics of quorum sensing regulatory pathways *in vivo*. In addition, knowledge of the spatiotemporal pattern of signaling *in vivo* may lead to interference strategies targeting the quorum sensing pathways for antimicrobial or vaccine development.

*Streptococcus pyogenes*, also known as group A streptococcus (GAS), is a versatile human pathogen that colonizes diverse host anatomic sites. GAS causes a range of disease manifestations (8, 9), including mild pharyngitis and skin infections and life-threatening invasive infections, such as necrotizing fasciitis and streptococcal toxic shock syndrome. GAS also causes acute rheumatic fever (ARF), rheumatic heart disease (RHD), and poststreptococcal glomerulonephritis (10–12). Despite the significant morbidity and mortality associated with GAS infections worldwide (10, 13), disease prevention efforts are significantly hampered by the lack of a licensed human GAS vaccine (14, 15). Thus, continued study of virulence regulatory pathways is warranted to identify additional molecular targets and aid vaccine development.

A secreted cysteine protease known as SpeB is a major virulence factor that is crucial for GAS pathogenesis in multiple anatomic sites (16–20). SpeB is produced abundantly during infection, and its protease activity contributes significantly to host tissue damage and disease dissemination (16, 17, 21, 22). Consistent with this, inactivation of SpeB attenuates virulence in several animal models of infection (18–21, 23, 24). Recently, we discovered that a noncanonical GAS quorum sensing pathway controls *speB* expression in coordination with bacterial population density (4, 25). A GAS-encoded leaderless peptide signal designated SpeB-inducing peptide (SIP) and an intracellular peptide-sensing global transcription regulator known as regulator of protease B (RopB) form a peptide signal and receptor pair and activate *speB* expression during high bacterial population density (4). The 8-amino-acid SIP is produced during high bacterial population density, secreted, and reimported into the bacterial cytosol and engages in direct interactions with cytosolic RopB (4) (Fig. 1). SIP binding induces allosteric changes in RopB, resulting in high-affinity interactions with the operator sequences located within the *speB* promoter and RopB oligomerization (Fig. 1). Subsequently, the transcription-

ally competent association between RopB-SIP and the *speB* promoter induces robust *speB* expression (3, 4) (Fig. 1). Importantly, the SIP signaling pathway is active during invasive infection in mouse models, and each component of the SIP signaling pathway is critical for GAS pathogenesis (4).

Pharyngitis is the most common form of GAS disease. Oropharyngeal GAS colonization is a major predisposing factor for the development of immunopathological consequences, such as ARF and RHD (12, 26–28). Saliva is the first line of host defense in the oral cavity and contains several innate and adaptive immune factors that control microbial growth (29). However, GAS successfully proliferates and persists in human saliva, and GAS transmission between hosts typically occurs through saliva (30–34). Similarly, development of systemic infection requires that GAS survive in human blood. Previous studies indicated that SpeB is critical for GAS survival *ex vivo* in human saliva and blood (30). However, the regulatory mechanisms controlling SpeB biogenesis, their contributions to GAS survival *ex vivo* in human saliva and blood, and their role in oropharyngeal GAS colonization remain unknown. Here we used biochemical analyses, *ex vivo* gene expression studies, mouse infection studies, and immunologic methods to demonstrate that the SIP signaling pathway is active during GAS growth *ex vivo* in human saliva and blood and controls *speB* expression. We discovered that GAS has a distinct *speB* expression profile during growth *ex vivo* in human saliva, which may be crucial for pathogen survival in the human host. Importantly, the SIP signaling pathway is functional among strains of diverse GAS *emm* types and contributes to GAS persistence in human saliva and mouse oropharyngeal GAS colonization. In summary, our findings reveal a ubiquitous role for SIP-mediated SpeB production in GAS pathogenesis in multiple host niches and suggest new therapeutic strategies.

## RESULTS

**Kinetics of *speB* transcripts during GAS growth *ex vivo* in human saliva.** To determine the *speB* expression pattern during GAS growth *in vitro*, we analyzed GAS growth kinetics and the *speB* transcript level in GAS grown in Todd-Hewitt broth containing 0.2% (wt/vol) yeast extract (THY). The initial induction of *speB* expression occurred only during high bacterial population density ( $6.9 \times 10^8$  CFU/ml; 695-fold induction in *speB* expression), and the *speB* transcript level persisted at higher levels during stationary phase of GAS growth (Fig. 2A). Next, we assessed growth kinetics and *speB* transcript levels during GAS growth *ex vivo* in human saliva. GAS growth increased during the first 16 h and reached a maximum population density ( $\sim 10^7$  CFU/ml) at 16 h postinoculation (Fig. 2B). Subsequently, GAS entered into a phase of persistence and sustained viability at a lower population density ( $\sim 10^5$  CFU/ml) until 6 days postinoculation (Fig. 2B). Correlation of *speB* transcript levels with GAS growth in saliva showed a density-dependent pattern of *speB* expression (Fig. 2B). Compared to the starting time point, the initial induction of *speB* expression occurred at 12 h postinoculation ( $2.4 \times 10^6$  CFU/ml; 1,169-fold induction of *speB* expression). *speB* transcript levels peaked at 16 h postinoculation, corresponding to the highest GAS population density in saliva ( $1.1 \times 10^7$  CFU/ml; 2,533-fold induction of *speB* expression) (Fig. 2B). *speB* transcript levels decreased drastically by 48 h postinoculation and remained at basal levels as the number of GAS CFU in saliva declined (Fig. 2B).

We next compared the kinetics of *speB* transcript levels in GAS grown in saliva and nutrient-rich laboratory (THY) medium. Under both growth conditions, GAS upregulated *speB* expression in concert with an increase in the bacterial population density (Fig. 2A and B). However, significant differences in the *speB* expression profiles were observed between the two growth conditions. In saliva, initial induction of *speB* expression occurred at a much lower population density ( $2.4 \times 10^6$  CFU/ml; 1,169-fold induction in *speB* expression) relative to GAS growth in laboratory medium ( $6.9 \times 10^8$  CFU/ml; 695-fold induction in *speB* expression) (Fig. 2A and B). Importantly, even at a much higher bacterial population density ( $4.3 \times 10^8$  CFU/ml; no induction in *speB* expression), no upregulation of *speB* expression was observed during *in vitro* growth (Fig. 2A). Further, in saliva, *speB* expression increased at between 12 and 24 h postin-

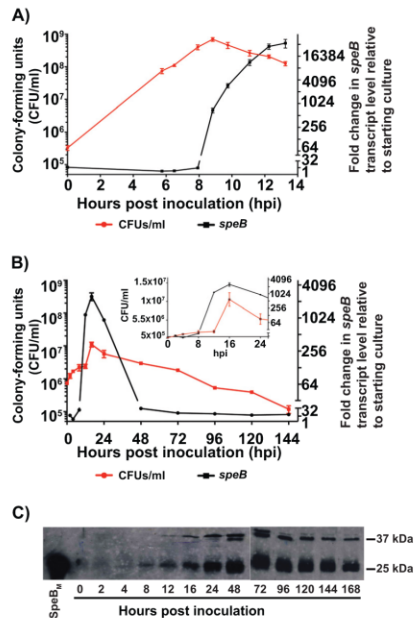


**FIG 2** GAS growth and *speB* transcript level kinetics in human saliva. The MGAS10870 strain was grown to mid-exponential phase ( $A_{600\text{nm}} \sim 0.4$ ), washed twice in sterile PBS, and suspended in human saliva at a starting bacterial population density of  $\sim 10^5$  CFU/ml. Samples were collected at the indicated time points to determine the number of CFU, *speB* transcript levels, and SpeB protein levels. (A and B) The kinetics of GAS growth and *speB* transcript levels in THY medium (A) and human saliva (B) are shown. The left y axis represents the growth curve, as determined by assessing the number of CFU by plating serial dilutions of 100- $\mu$ l aliquots collected at the indicated time points. The right y axis represents the fold change in *speB* transcript levels at the indicated time points, as measured by qRT-PCR. The fold change in transcript levels relative to the level in the starting culture (time point = 0 h) is shown. (Inset) The exponential phase of GAS growth in saliva is shown. The data graphed are means  $\pm$  standard deviations for three biological replicates. (C) Western immunoblot analysis of secreted SpeB during growth in human saliva. The cell-free saliva samples were resolved on a 15% SDS-polyacrylamide gel and transferred to nitrocellulose membranes. The membranes were probed with anti-SpeB polyclonal rabbit antibody and visualized with chemiluminescence. The mature form of purified recombinant SpeB (SpeB<sub>6</sub>; 25 kDa) was used as a marker. The masses of the molecular mass markers are shown in kilodaltons.

oculation, and the induction of *speB* expression was transient (Fig. 2B). In contrast, during GAS growth in laboratory medium, the transcript levels of *speB* continued to increase along with the increase in bacterial population density.

Finally, to understand the downstream consequences of the transient induction of *speB* expression on GAS growth in saliva, we assessed secreted SpeB protein levels by Western immunoblotting. The secreted SpeB protease levels resembled the *speB* expression profile, as SpeB was initially detected at 12 h postinoculation and reached maximal levels at 24 h postinoculation in saliva (Fig. 2C). However, unlike the *speB* transcript profile, the secreted SpeB protease levels persisted in saliva during the entire 6-day study period (Fig. 2C). Collectively, these data suggest that GAS employs a pattern of *speB* expression during growth *ex vivo* in human saliva distinct from the pattern of growth *in vitro*, and early induction of *speB* expression and sustained secreted SpeB protease levels may contribute to GAS survival in human saliva.

**SIP signaling is active during *ex vivo* growth in human saliva.** To test the hypothesis that the SIP signaling pathway controls *speB* expression during GAS growth *ex vivo* in human saliva, we performed synthetic SIP (SIP; MWLLLLLFL) addition experiments using the isogenic *SIP\** mutant strain. In this mutant, the start codon of SIP was replaced with a stop codon, thereby disrupting the translation of SIP (4) (see Fig. S1 in

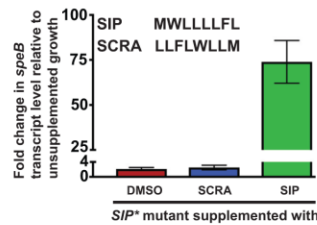


**FIG 3** SIP signaling occurs during GAS growth in human saliva. Addition of synthetic SIP restores *speB* expression in the isogenic *SIP\** mutant strain during growth in human saliva. Scrambled peptide (SCRA), with a length and amino acid composition identical to those of SIP but with the order of the amino acid sequence being varied, was used as a negative control. The *SIP\** mutant strain was grown to late exponential phase ( $A_{600} \sim 1.5$ ) in THY, washed in sterile PBS, resuspended in an equal volume of human saliva, and incubated for 30 min. Cells were supplemented with either 500 nM the indicated peptides or the solvent used in peptide stock solutions (DMSO) and incubated for an additional 30 min at 37°C. Transcript levels of *speB* were assessed by qRT-PCR. The fold change in *speB* transcript levels relative to the level in unsupplemented GAS growth is shown. The data graphed are means  $\pm$  standard deviations for three biological replicates.

the supplemental material). Thus, in the *SIP\** mutant strain endogenous SIP production is defective and *speB* expression is dependent on exogenously added synthetic SIP (4). A scrambled peptide (SCRA; LLFLWLLM) with an amino acid composition identical to that of SIP but in which the order of the sequence was varied was used as a negative control (4). The *SIP\** mutant strain was grown to late exponential growth phase ( $A_{600} \sim 1.5$ ) in THY medium, washed with phosphate-buffered saline (PBS), and suspended in an equal volume of fresh human saliva. After 30 min of incubation, cells were supplemented with either synthetic SIP or SCRA and *speB* transcript levels were measured by quantitative reverse transcription-PCR (qRT-PCR). Consistent with our hypothesis, addition of SIP caused the significant induction of *speB* expression. In contrast, SCRA failed to induce *speB* expression (Fig. 3). These results suggest that SIP signaling occurs during GAS growth in human saliva and that SIP is responsible for the upregulation of *speB* expression in saliva.

#### The SIP signaling pathway promotes GAS growth ex vivo in human saliva.

Given that SIP-dependent upregulation of *speB* expression occurs during GAS growth in saliva, we hypothesized that the SIP signaling pathway is required for optimal growth in saliva. To test this hypothesis, we compared the growth kinetics of the wild-type (WT) parental strain with that of the isogenic  $\Delta$ *speB*,  $\Delta$ *ropB*, or *SIP\** mutant strain. All four strains had similar growth kinetics during growth in laboratory medium (4). However, compared to the growth of the WT parental strain, all three mutant strains were significantly impaired in growth in saliva. In addition, the mutant strains persisted at a significantly lower population density (Fig. 4A). Importantly, the defective growth of the isogenic *SIP\** mutant strain in saliva was restored to the WT-like phenotype in the *trans*-complemented strain (*SIP\**::pDC-SIP) (Fig. 4A and S1). Collectively, these data suggest that gene regulation by the SIP signaling pathway contributes significantly to the ability of GAS to persist in saliva.

#### The SIP signaling pathway contributes significantly to mouse oropharyngeal GAS colonization.

We next tested the hypothesis that the SIP signaling pathway contributes to GAS colonization of the mouse oropharynx. Although GAS is a human-only pathogen, the murine model of oropharyngeal GAS colonization has been extensively used to investigate GAS survival at the oropharynx (35–39). Mice were infected intranasally with  $10^8$  CFU of each GAS strain. The mouse oropharynx was swabbed daily, and GAS colonization was determined by assessing the number of CFU in throat swabs. Significantly fewer mice were colonized by the isogenic  $\Delta$ *ropB*,  $\Delta$ *speB*, and *SIP\** mutant strains than by the WT parental strain (Fig. 4B) ( $P < 0.0001$ ). However, the defective colonization by the *SIP\** mutant strain was restored to WT colonization levels in the *trans*-complemented (*SIP\**::pDC-SIP) strain (Fig. 4B) ( $P < 0.0001$ ). Together, these

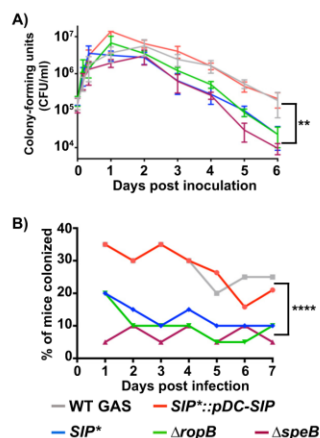


**FIG 4** The SIP signaling pathway aids bacterial survival in human saliva and contributes significantly to GAS colonization of the mouse oropharynx. (A) Growth curves of the indicated strains in human saliva. GAS grown to stationary phase ( $A_{600} \sim 1.7$ ) in laboratory medium was washed with sterile PBS and resuspended in human saliva. Growth was monitored by plating serial dilutions of 100- $\mu$ l aliquots at the indicated time points postinoculation. Colonies were counted to determine the number of CFU. The data graphed are means  $\pm$  standard deviations for three biological replicates.  $P$  values (\*\*,  $P < 0.01$ ) for the indicated strains were determined by comparison to WT GAS. (B) The SIP signaling pathway contributes significantly to GAS colonization of the mouse oropharynx. The percentage of mice with GAS isolated from the oropharynx at the indicated time points is shown. Adult outbred CD-1 mouse (20 mice per group) nostrils were inoculated with  $2 \times 10^8$  CFU of the indicated GAS strains. The mouse oropharynx was swabbed daily, and the swabs were plated on streptococcal selective agar (SSA). The plates were incubated for 48 h, and beta-hemolytic colonies were counted.  $P$  values (\*\*\*\*,  $P < 0.0001$ ) for the indicated strains were determined by comparison to WT GAS.

data suggest that the SIP signaling pathway contributes significantly to the ability of GAS to colonize the mouse oropharynx.

**SIP signaling occurs during growth *ex vivo* in human blood, and inactivation of the SIP signaling pathway results in decreased GAS survival in blood.** We previously demonstrated that inactivation of SIP attenuated GAS virulence in a mouse model of bacteremia (4). This result led us to hypothesize that the SIP signaling pathway is critical for GAS survival in human blood and systemic disease pathogenesis. To test this hypothesis, we first assessed whether the SIP signaling pathway controls SpeB biogenesis during growth in human blood *ex vivo*. To test this hypothesis, the isogenic  $SIP^*$  mutant strain was grown to late exponential phase ( $A_{600} \sim 1.5$ ) in THY, washed with sterile PBS, and suspended in an equal volume of fresh human blood *ex vivo*. Consistent with our observations with GAS growth in saliva, the addition of synthetic SIP caused robust induction of *speB* expression in the  $SIP^*$  mutant during growth *ex vivo* in blood (Fig. 5A). Restoration of *speB* expression in the  $SIP^*$  mutant was specific for the amino acid sequence of inferred native SIP, as the scrambled peptide (SCRA) failed to induce *speB* expression (Fig. 5A). Collectively, these data indicate that SIP signaling is responsible for the induction of *speB* expression during GAS growth in blood *ex vivo*.

Next, we assessed the contribution of the SIP signaling pathway to GAS survival in human blood. The parental WT and isogenic mutant GAS strains were grown in human blood for 3 h, and bacterial growth was assessed by counting the number of CFU. Compared to the WT strain, the  $\Delta ropB$ ,  $\Delta speB$ , and  $SIP^*$  mutant strains were defective in their ability to proliferate in blood (Fig. 5B). However, the WT-like growth phenotype in blood was restored in the  $SIP^*$  mutant strain complemented with pDC-SIP, suggesting that provision of SIP *in trans* is sufficient to reverse the defective phenotype of the  $SIP^*$  mutant (Fig. 5B). Together, these results suggest that SIP-dependent gene regulation is crucial for GAS survival *ex vivo* in human blood and may contribute to GAS virulence during systemic infection.

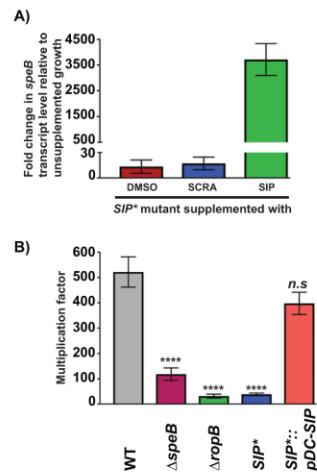


**FIG 5** SIP signaling occurs during GAS growth in human blood and contributes significantly to GAS growth in human blood. (A) Addition of synthetic SIP restores *speB* expression in the isogenic SIP\* mutant strain during growth in human blood. The fold change in *speB* transcript levels relative to unsupplemented bacterial growth is shown. The data graphed are means  $\pm$  standard deviations for three biological replicates. (B) Bactericidal assay of the indicated GAS strains. Bacteria were grown to mid-exponential phase ( $A_{600nm} \sim 0.4$ ) in THY, and approximately 100 CFU of each GAS strain was inoculated into 300  $\mu$ l of fresh human blood. After 3 h of incubation at 37°C, the multiplication factors were calculated by dividing the numbers of CFU per milliliter obtained after 3 h of incubation by the starting inoculum. The *P* values (n.s., not significant [ $P > 0.5$ ]; \*\*\*\*,  $P < 0.0001$ ) for the indicated strains were determined by comparison to WT GAS. The data graphed are means  $\pm$  standard deviations for three biological replicates.

**SIP-dependent *speB* expression contributes to GAS resistance against LL37-mediated cytotoxicity.** Antimicrobial peptides such as LL37 are abundant in human saliva and blood. LL37 mediates its cytotoxicity by inducing bacterial membrane lysis (40–43). Given that SIP-dependent gene regulation is crucial for GAS survival in human saliva and blood *ex vivo*, we hypothesized that the SIP signaling pathway contributes to GAS resistance against LL37-induced cytotoxicity. To test this hypothesis, GAS grown to stationary phase was washed and incubated with LL37 in phosphate buffer for 45 min. The bacterial resistance to LL37-mediated cytotoxicity was assessed by comparing the survival of untreated and LL37-treated GAS. Consistent with the role of SpeB as an LL37-degrading protease (41, 44), the SpeB-producing WT and *trans*-complemented GAS strains exhibited significant resistance against LL37 treatment (Fig. 6). Conversely, the isogenic  $\Delta$ *speB*,  $\Delta$ *ropB*, and SIP\* mutant strains, which cannot produce SpeB, were killed significantly more efficiently by LL37 than the SpeB-producing strains (Fig. 6) ( $P < 0.005$ ). These data indicate that the resistance to LL37-mediated cytotoxicity conferred by SIP-dependent *speB* expression contributes to GAS survival.

**The SIP signaling mechanism is conserved among diverse GAS *emm* types.** Genes encoding RopB, SIP, and SpeB are highly conserved among *emm* types, suggesting that the SIP signaling pathway is a conserved virulence regulatory mechanism among genetically diverse strains (4). To test the hypothesis that the SIP signaling mechanism is functional in various GAS *emm* types, we performed a synthetic SIP addition experiment using genetically diverse GAS strains that belong to M-protein serotypes M1, M3, M12, M59, and M89 (45–49). The genomes of the strains used have been sequenced and have WT alleles for all known major regulatory genes, including *ropB*, *mga*, and *covRS*. The strains of all tested *emm* types encode the same inferred SIP amino acid sequence.

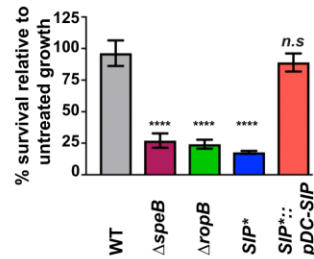


**FIG 6** SIP-dependent gene regulation confers GAS resistance against LL37-mediated cytotoxicity. GAS strains grown to stationary phase of growth in THY ( $A_{600} \sim 1.7$ ) were washed with PBS and incubated with 2.5  $\mu\text{M}$  synthetic LL37 in phosphate buffer for 45 min at 37°C. The antimicrobial effect of LL37 was assessed by calculating the ratio of the number of surviving cells in the LL37-treated group to the total number of bacteria incubated in the mock-treated group. Statistical significance was determined by *t* test. *P* values (n.s., not significant [ $P > 0.5$ ]; \*\*\*\*,  $P < 0.0001$ ) for the indicated strains were determined by comparison to the WT.

Expression of *speB* occurs predominantly during the stationary phase of GAS growth in THY medium (4, 23, 25, 50). Thus, we tested whether the addition of the synthetic peptide containing the amino acid sequence of SIP decouples the growth phase dependency of *speB* expression and causes the early onset of *speB* expression in these different strains. Consistent with our previous observations in the GAS M3 serotype (4), SIP-specific induction of *speB* expression occurred during the exponential phase of growth in all tested strains (Fig. 7). Thus, SIP-dependent upregulation of *speB* expression is a conserved regulatory mechanism among diverse GAS *emm* types commonly causing human infections.

**SIP is produced *in vivo* in infected humans.** Next, we tested the hypothesis that SIP is produced during human infection and evokes production of anti-SIP antibodies by measuring anti-SIP antibody titers by enzyme-linked immunosorbent assay (ELISA). A random 9-amino-acid peptide derived from an unrelated GAS protein was used as a nonspecific control. Serum samples from 5 convalescing patients with previous invasive GAS infections and 5 pediatric patients with culture-positive GAS pharyngitis were assessed. All tested serum samples from patients with either invasive or pharyngeal GAS infections had anti-SIP antibody titers of a 1:1,000 dilution. However, even at a 1:100 dilution, the serum samples failed to react with the nonspecific control peptide.

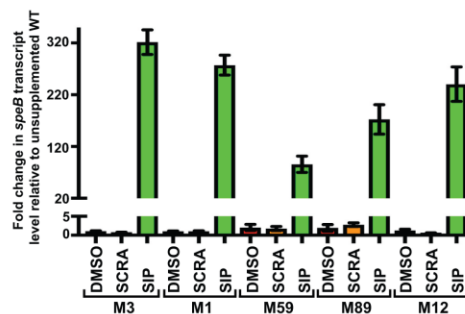


**FIG 7** The SIP signaling pathway is conserved among several GAS M-protein serotypes. WT GAS isolates belonging to M-protein serotypes M1 (MGAS2221), M3 (MGAS10870), M59 (MGAS15249), M89 (MGAS26844), and M12 (MGAS9429) were grown to mid-exponential phase ( $A_{600} \sim 0.4$ ). Cells were subsequently incubated with either 500 nM synthetic SIP or scrambled peptide (SCRA) for an additional 60 min. The transcript levels of *speB* were assessed by qRT-PCR, and the fold change in *speB* expression relative to that in DMSO-supplemented growth is shown.

Collectively, the human serologic data provide evidence that SIP is produced *in vivo* in infected humans.

## DISCUSSION

The antivirulence approach is an emerging paradigm to combat bacterial infections by targeting either the virulence factors or regulatory networks controlling virulence factor production for antimicrobial development (51–53). The ideal target for an antivirulence strategy must be active during infection and during the time of treatment and participate in disease pathogenesis (51–53). Thus, knowledge of the spatiotemporal pattern of virulence factor production *in vivo* is a crucial prerequisite for successful antivirulence targeting studies. Given that the SIP signaling pathway is active in the host and that SIP-mediated SpeB production is critical for GAS virulence in invasive animal models of infection (4), the SIP signaling pathway is an attractive target for antivirulence strategies to treat GAS infections. However, the contribution of the SIP signaling pathway to GAS survival in the oropharynx, the primary route of GAS entry into the host, remains unknown. In this study, we demonstrated that the SIP signaling pathway is the primary regulatory mechanism controlling *speB* expression during GAS growth *ex vivo* in saliva. Importantly, SIP-mediated *speB* regulation is critical for bacterial survival in human saliva and contributes significantly to oropharyngeal GAS colonization. Collectively, our results suggest that the SIP signaling pathway is active during GAS infection and participates in disease pathogenesis in multiple host niches, including the oropharynx (4, 23).

GAS employs a temporal pattern of *speB* expression during growth *ex vivo* in saliva that is distinct from the kinetics of the *speB* transcript profile during GAS growth *in vitro* (Fig. 2A and B). GAS triggers a transient but robust induction of *speB* expression during the early stages of growth in saliva (Fig. 2B), resulting in the accumulation of large amounts of extracellular SpeB protease (Fig. 2C). Early induction of SpeB protease production in saliva is likely an adaptive strategy to achieve sufficient quantities of SpeB protease in saliva before the onset of host innate immune responses. Given that human saliva contains several antimicrobial mechanisms (29, 40), the protease activity of SpeB may aid GAS survival in saliva by negating the cytotoxicity of host immune factors. Consistent with this, SIP-dependent SpeB production aids GAS survival in the presence of LL37 (Fig. 6), indicating that SpeB-mediated cleavage of LL37 likely contributes to GAS evasion of LL37-mediated cytotoxicity.

The temporal pattern of SpeB biogenesis during GAS growth in human saliva also has significant implications for future translational studies targeting the SIP signaling pathway for antimicrobial development. SIP signaling occurs only during the early stages of GAS growth *ex vivo* in saliva and is relatively inactive during the later stages of growth in saliva (Fig. 2B). Thus, the therapeutic targeting of the SIP signaling pathway to treat oropharyngeal GAS infections may be more effective during early stages of GAS infection. Alternatively, prophylactic targeting of the SIP signaling pathway may be a viable option, as anti-SIP antibodies are likely to be disruptive to SIP signaling and SpeB production. Furthermore, SpeB is present in relative abundance for a prolonged period during GAS growth *ex vivo* in saliva. Importantly, SpeB-producing strains demonstrated a better ability to persist in saliva and colonize the mouse oropharynx. Thus, targeting SpeB for antimicrobial development may be an effective strategy to treat oropharyngeal GAS infections.

GAS reaches a maximum population density of only  $10^7$  CFU/ml, which is  $2 \log_{10}$ -fold less than the bacterial population density observed during GAS growth *in vitro* (Fig. 2A and B). Our observations are consistent with the GAS population densities reported in prior *ex vivo* growth studies in saliva or the GAS burden during acute pharyngitis in human patients (30–33). During growth *in vitro*, the SIP-mediated upregulation of *speB* expression occurs only at population densities greater than  $10^8$  CFU/ml (Fig. 2B). Although GAS does not reach such high population densities during growth in human saliva, it has the ability to induce *speB* expression at significantly lower population densities ( $\sim 10^6$  CFU/ml) (Fig. 2A). These results suggest that additional mechanisms or

signals in saliva may contribute to the upregulation of *speB* expression. To address the niche-specific distinction in the regulation of *speB* expression in saliva, we considered two possibilities. First, the host uses salivary glycoproteins to promote GAS aggregation as a defense mechanism to prevent bacterial attachment to epithelial surfaces and eliminate GAS from the oral cavity (54). Thus, it is possible that GAS may reach locally high bacterial population densities within a confined environment, such as bacterial aggregates, which leads to the local accumulation of SIP and induction of *speB* expression. Consistent with this, *Staphylococcus aureus* at a relatively low population density within a confined space, such as phagosomes, senses the accumulating extracellular peptide signal and activates the quorum sensing regulon (55, 56). Alternatively, additional bacterial or host-derived molecules present in saliva may act as inducers that provide the initial impetus toward the activation of the SIP signaling pathway, which leads to the autoinduction of the endogenous SIP signaling pathway and upregulation of *speB* expression. In accordance with this, *Pseudomonas aeruginosa* uses the excess aromatic amino acids in the sputum from cystic fibrosis patients as precursors for the synthesis of a quorum sensing signal molecule and activates the quorum sensing regulon (57). Additional investigations are required to elucidate the mechanistic basis for *speB* expression at relatively low GAS population densities in saliva.

The GAS genome encodes four different peptide-signaling systems comprised of sensor-peptide pairs, namely, ComR-ComS, SilAB-SilCR, Rgg-SHP, and RopB-SIP (4, 58–60). The ComRS system is involved in the regulation of genetic competence in streptococci, but its role in GAS remains elusive (61, 62). Although the SilCR signaling pathway participates in GAS pathogenesis, it is not conserved among GAS *emm* serotypes and is encoded by less than 25% of the sequenced GAS genomes (59, 60). The Rgg-SHP quorum sensing system is conserved among GAS *emm* serotypes, but its contribution to GAS pathogenesis is not fully understood (58, 59). In contrast, the RopB-SIP signaling pathway is highly conserved in all the sequenced GAS genomes, is functional in diverse GAS *emm* serotypes, and is critical for GAS disease pathogenesis in multiple host anatomic sites (4, 22) (Fig. 7). These properties of the SIP signaling pathway, combined with the observed immunological recognition of SIP by the host immune system, make the SIP signaling pathway a potential candidate for GAS vaccine development.

In conclusion, we demonstrate that GAS employs a combination of early activation of the SIP signaling pathway and timely SpeB production for successful persistence in saliva and colonization of the mouse oropharynx. The critical differences in the SIP signaling profile observed between GAS growth *in vitro* and *ex vivo* also underscore the significance of the need to study bacterial virulence regulatory programs under conditions that simulate their natural environment. In summary, in addition to elucidating the molecular details of niche-specific virulence regulation by the SIP signaling pathway, the results from this study also provide the scaffold for future translational studies targeting the SIP signaling pathway to treat or prevent pharyngeal GAS infections.

## MATERIALS AND METHODS

**Bacterial strains, plasmids, and growth conditions.** The bacterial strains and plasmids used in this study are listed in Table S1 in the supplemental material. Strain MGAS10870 is a previously described invasive serotype M3 isolate whose genome has been fully sequenced (46). MGAS10870 is representative of serotype M3 strains that cause invasive infections and has wild-type sequences for all known major regulatory genes (46). The *Escherichia coli* DH5 $\alpha$  strain was used as the host for plasmid constructions. GAS was grown routinely on Trypticase soy agar containing 5% sheep blood (BSA; Becton Dickinson) or in Todd-Hewitt broth containing 0.2% (wt/vol) yeast extract (THY; Difco). When required, chloramphenicol was added to a final concentration of 5  $\mu$ g/ml. All GAS growth experiments were done in triplicate on three separate occasions for a total of nine replicates. Overnight cultures were inoculated into fresh medium to achieve an initial absorption at 600 nm ( $A_{600}$ ) of 0.03. Bacterial growth was monitored by measuring the  $A_{600}$ . The *E. coli* strain was grown in Luria-Bertani (LB) broth (Fisher).

**Collection of human saliva.** Saliva from adult volunteers was collected on ice under a protocol approved by the Institutional Review Board at Houston Methodist Research Institute (approval number Pro00003833) using the method described previously with minor modifications (30). Dithiothreitol (DTT; Gold Biotechnology) was added at a final concentration of 2.5 mmol to the saliva pool, and the mixture was incubated on ice for 30 min. The saliva was clarified by centrifugation at 23,000  $\times$  g for 1 h, followed

by filtration through a 0.22- $\mu$ m-pore-size membrane filter (Corning, NY). Pooled saliva was stored frozen at  $-20^{\circ}\text{C}$ . Saliva from at least four donors was pooled to minimize the potential effects of donor variation.

**GAS growth in human saliva.** The ability of GAS strains to grow and persist in human saliva was evaluated as described previously (30). Briefly, human saliva was collected from healthy volunteers and pooled as described above. GAS was grown overnight in Todd-Hewitt broth supplemented with 0.2% yeast extract (THY; BD Biosciences, Sparks, MD), diluted 1:100 with fresh THY, and grown to the growth phase indicated above. The bacterial cells were pelleted, washed twice with sterile PBS, and suspended in saliva at  $\sim 1 \times 10^5$  CFU/ml. Aliquots were removed at the time points indicated above and in the figures. Samples were serially diluted 10-fold in sterile PBS and plated in duplicate on Trypticase soy agar plates supplemented with 5% sheep blood (BD Biosciences). The plates were incubated overnight, and colonies were counted to determine the number of CFU. All incubations were at  $37^{\circ}\text{C}$  with 5%  $\text{CO}_2$ . Each experiment was performed in triplicate on three separate occasions.

**Mouse oropharyngeal infection.** All animal experiments were conducted under a protocol approved by the Houston Methodist Research Institute Institutional Animal Care and Use Committee (approval number AUP-1215-0069). Twenty 3- to 4-week-old female CD1 mice (Harlan Laboratories) were inoculated intranasally with  $2 \times 10^8$  CFU of the appropriate GAS strain in 50  $\mu$ l phosphate-buffered saline (PBS). Mouse throats were swabbed prior to inoculation to ensure the absence of beta-hemolytic bacteria and daily thereafter for a total of 7 days to assess GAS colonization. Throat swab specimens were vortexed in 300  $\mu$ l sterile PBS at 1,000 rpm on a high-speed microplate shaker (Illumina, San Diego, CA), and the numbers of CFU per milliliter were determined by serial diluting 1:10 in PBS, plated on group A streptococcal selective agar with 5% sheep blood (SSA; Becton Dickinson), and grown overnight at  $37^{\circ}\text{C}$ , and the beta-hemolytic colonies were counted.

**GAS growth studies in human blood.** Whole blood was drawn from consenting, healthy, nonimmune donors in sodium heparin tubes (Becton Dickinson) under a Houston Methodist Research Institute Institutional Review Board-approved experimental protocol (approval number Pro00004933). GAS growth in blood was performed as described previously (63). Indicated GAS strains were grown in THY at  $37^{\circ}\text{C}$  in 5%  $\text{CO}_2$  to mid-exponential phase ( $A_{600} \sim 0.4$ ) and harvested. The cells were washed twice and suspended in an equal volume of sterile PBS. Approximately 20 to 100 CFU of each GAS strain was inoculated into 300  $\mu$ l of fresh human blood. Samples were incubated for 3 h at  $37^{\circ}\text{C}$  in 5%  $\text{CO}_2$  with end-to-end rotation. The numbers of CFU per milliliter were determined by serially diluting the samples 1:10 in PBS, plating the samples, and growing the samples overnight at  $37^{\circ}\text{C}$  in 5%  $\text{CO}_2$ , and the beta-hemolytic colonies were counted. Multiplication factors were calculated by dividing the number of CFU per milliliter determined after 3 h of incubation by the starting inoculum. Each experiment was performed in triplicate on separate occasions.

**GAS RNA isolation and gene transcript analysis from human saliva and blood.** One volume of GAS strains grown in human saliva or human blood was collected in 2 volumes of RNeasy Protect (Qiagen) at the time points indicated above, incubated at room temperature for 10 min, and harvested by centrifugation. Bacterial cell pellets grown in blood were suspended in 10 volumes of ammonium chloride lysing solution (Becton Dickinson), incubated for 10 min on ice, and separated from lysed erythrocytes by centrifugation at  $3,000 \times g$  at  $4^{\circ}\text{C}$  for 10 min. RNA was isolated from the GAS growth in saliva or blood and purified using an RNeasy kit (Qiagen) according to the manufacturer's instructions.  $A_{260}/A_{280}$  ratios were used to assess RNA integrity. cDNA was synthesized from purified RNA using SuperScript III reverse transcriptase (Invitrogen). TaqMan PCR was performed with an ABI 7500 Fast system (Applied Biosystems). Comparison of transcript levels was performed by the  $\Delta C_T$  threshold cycle ( $C_T$ ) method of analysis using *tufA* as the endogenous control gene (64). The sequences of the probes and primers used in the TaqMan PCR are listed in Table S2.

**Western immunoblot analysis.** MGAS10870 was grown in human saliva to the time points indicated above, and supernatant was collected by centrifugation. The culture supernatant was filtered through a 0.22- $\mu$ m-pore-size filter (Millipore), and the filtrate was concentrated by drying with a Speed-Vac. Equal volumes of concentrated supernatant sample were resolved on a 15% SDS-polyacrylamide gel, transferred to a nitrocellulose membrane (Bio-Rad), and probed with polyclonal anti-SpeB rabbit antibodies. Secondary antibody conjugated with horseradish peroxidase was used to detect SpeB and visualized with chemiluminescence using a SuperSignal West Pico rabbit IgG detection kit (Thermo Scientific).

**Synthetic peptide addition assay during GAS growth in human saliva and human blood.** Synthetic peptides of high purity ( $>90\%$  purity) obtained from Peptide 2.0 (Chantilly, VA) were suspended in 100% dimethyl sulfoxide (DMSO) to prepare a 10 mM stock solution. Stock solutions were aliquoted and stored at  $-20^{\circ}\text{C}$  until use. Working stocks were prepared by diluting the stock solution in 25% DMSO.

**LL37 cytotoxicity assays.** GAS strains were grown to stationary phase in THY ( $A_{600} \sim 1.7$ ), washed with PBS, and suspended in 10 mM sodium phosphate buffer (pH 6.8). Similar starting numbers of CFU per milliliter of each strain were preincubated at  $37^{\circ}\text{C}$  for an additional 2 h. Subsequently, LL37 was added to a final concentration of 2.5  $\mu\text{M}$ , the culture was incubated for 45 min, and bacterial killing was assessed by counting the numbers of CFU per milliliter. The LL37 cytotoxicity was assessed by calculating the ratio of the number of surviving cells in the LL37-treated group to the number of bacteria incubated in the mock-treated group.

**Analysis of *in vivo* SIP expression by ELISA.** ELISA was used to determine if SIP is expressed during human GAS infection. Synthetic SIP was used to coat MaxiSorp ELISA plates (Nunc) at 0.5  $\mu\text{g}/\text{well}$  at  $4^{\circ}\text{C}$  overnight. A synthetic 9-mer peptide derived from an unrelated GAS cytosolic protein (CvfA, SpyM3\_1376) with an amino acid sequence of YALISIRLK was used as a nonspecific control. Convalescent-phase human serum samples were collected from 5 patients with previous invasive GAS infections under a protocol

approved by the Houston Methodist Research Institute Institutional Review Board. Acute-phase human serum samples from 5 pediatric patients with acute GAS pharyngitis were also collected. A serial 2-fold dilution of the serum samples was used, and secondary horseradish peroxidase (HRP)-conjugated anti-human immunoglobulin antibody (Millipore Sigma Inc.) was used to detect bound primary antibody. The absorbance of the plates at 420 nm ( $A_{420}$ ) was read. An  $A_{420}$  reading greater than at least thrice the value of the PBS negative control was considered a positive reaction.

**Statistical analysis.** Repeated-measure analysis of variance (ANOVA) was used to test the differences in nasopharyngeal colonization between strains. Paired Student's *t* test was used to compare the ability of GAS strains to survive in human saliva or blood by comparing the  $\log_{10}$  number of CFU per milliliter of the indicated strains on day 6 or multiplication factors after 3 h of incubation, respectively. Statistical significance was assigned at a two-sided *P* value of 0.05, using Bonferroni's adjustment for multiple comparisons when appropriate. GraphPad Prism software was used for statistical calculations.

#### SUPPLEMENTAL MATERIAL

Supplemental material for this article may be found at <https://doi.org/10.1128/IAI.00169-18>.

**SUPPLEMENTAL FILE 1**, PDF file, 1.3 MB.

**SUPPLEMENTAL FILE 2**, PDF file, 0.1 MB.

**SUPPLEMENTAL FILE 3**, PDF file, 0.1 MB.

#### ACKNOWLEDGMENTS

This work was supported by funds from the Fondren Foundation to J.M.M. and National Institutes of Health grant 1R01AI109096-01A1 to M.K. H.D. was supported by the Basic Science Research Program through the National Research Foundation of Korea (NRF), funded by the Ministry of Education (2017R1A6A3A03008353).

We declare no conflict of interest.

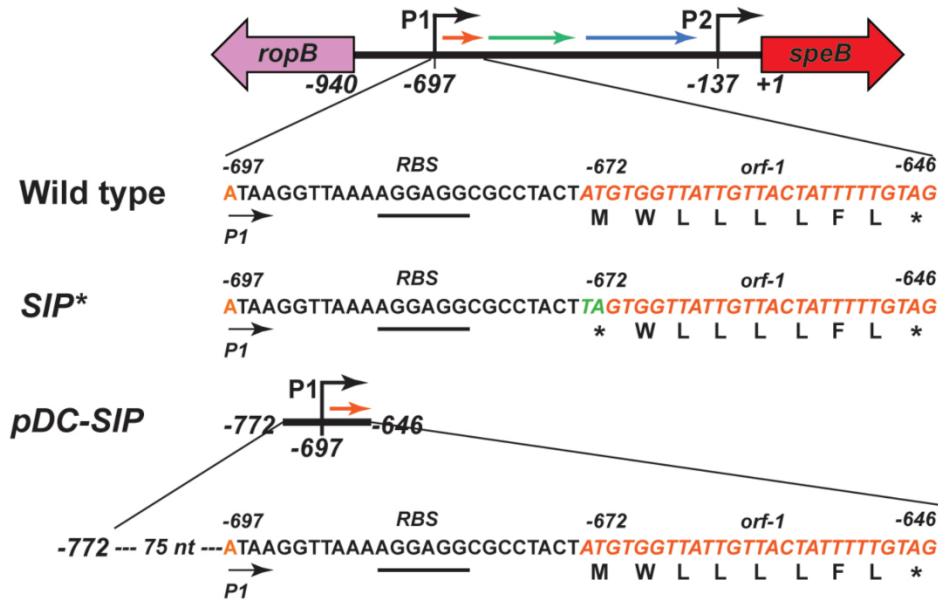
#### REFERENCES

1. Thoendel M, Kavanaugh JS, Flack CE, Horswill AR. 2011. Peptide signaling in the staphylococci. *Chem Rev* 111:117–151. <https://doi.org/10.1021/cr100370n>.
2. Dunny GM, Leonard BAB. 1997. Cell-cell communication in gram-positive bacteria. *Annu Rev Microbiol* 51:527–564. <https://doi.org/10.1146/annurev.micro.51.1.527>.
3. Do H, Kumaraswami M. 2016. Structural mechanisms of peptide recognition and allosteric modulation of gene regulation by the RRNPP family of quorum-sensing regulators. *J Mol Biol* 428:2793–2804. <https://doi.org/10.1016/j.jmb.2016.05.026>.
4. Do H, Makthal N, VanderWal AR, Rettel M, Savitski MM, Peschek N, Papenfort K, Olsen RJ, Musser JM, Kumaraswami M. 2017. Leaderless secreted peptide signaling molecule alters global gene expression and increases virulence of a human bacterial pathogen. *Proc Natl Acad Sci U S A* 114:E8498–E8507. <https://doi.org/10.1073/pnas.1705972114>.
5. Peregó M, Hoch JA. 1996. Cell-cell communication regulates the effects of protein aspartate phosphatases on the phosphorelay controlling development in *Bacillus subtilis*. *Proc Natl Acad Sci U S A* 93:1549–1553.
6. Perchat S, Dubois T, Zouhir S, Gominet M, Poncet S, Lemy C, Aumont-Nicaise M, Deutscher J, Gohar M, Nessler S. 2011. A cell-cell communication system regulates protease production during sporulation in bacteria of the *Bacillus cereus* group. *Mol Microbiol* 82:619–633. <https://doi.org/10.1111/j.1365-2958.2011.07839.x>.
7. Slamti L, Lereclus D. 2002. A cell-cell signaling peptide activates the PlcR virulence regulon in bacteria of the *Bacillus cereus* group. *EMBO J* 21:4550–4559. <https://doi.org/10.1093/emboj/cdf450>.
8. Olsen RJ, Shelburne SA, Musser JM. 2009. Molecular mechanisms underlying group A streptococcal pathogenesis. *Cell Microbiol* 11:1–12. <https://doi.org/10.1111/j.1462-5822.2008.01225.x>.
9. Cunningham MW. 2000. Pathogenesis of group A streptococcal infections. *Clin Microbiol Rev* 13:470–511. <https://doi.org/10.1128/CMR.13.4.470-511.2000>.
10. Ralph AP, Carapetis JR. 2012. Group A streptococcal diseases and their global burden, p 1–27. In Chhatwal SG (ed), *Host-pathogen interactions in streptococcal diseases*. Springer, Berlin, Germany.
11. Carapetis JR, Beaton A, Cunningham MW, Guilherme L, Karthikeyan G, Mayosi BM, Sable C, Steer A, Wilson N, Wyber R, Zuhlke L. 2016. Acute rheumatic fever and rheumatic heart disease. *Nat Rev Dis Primers* 2:15084. <https://doi.org/10.1038/nrdp.2015.84>.
12. Carapetis JR, Steer AC, Mulholland EK, Weber M. 2005. The global burden of group A streptococcal diseases. *Lancet Infect Dis* 5:685–694. [https://doi.org/10.1016/S1473-3099\(05\)70267-X](https://doi.org/10.1016/S1473-3099(05)70267-X).
13. Sanyahumbi AS, Colquhoun S, Wyber R, Carapetis JR. 2016. Global disease burden of group A streptococcus. In Ferretti JJ, Stevens DL, Fischetti VA (ed), *Streptococcus pyogenes: basic biology to clinical manifestations*. University of Oklahoma Health Sciences Center, Oklahoma City, OK.
14. Dale JB, Batzloff MR, Cleary PP, Courtney HS, Good MF, Grandi G, Halperin S, Margarit IY, McNeil S, Pandey M. 2016. Current approaches to group A streptococcal vaccine development. In Ferretti JJ, Stevens DL, Fischetti VA (ed), *Streptococcus pyogenes: basic biology to clinical manifestations*. University of Oklahoma Health Sciences Center, Oklahoma City, OK.
15. Steer AC, Carapetis JR, Dale JB, Fraser JD, Good MF, Guilherme L, Moreland NJ, Mulholland EK, Schodel F, Smeesters PR. 2016. Status of research and development of vaccines for *Streptococcus pyogenes*. *Vaccine* 34:2953–2958. <https://doi.org/10.1016/j.vaccine.2016.03.073>.
16. Carroll RK, Musser JM. 2011. From transcription to activation: how group A *Streptococcus*, the flesh-eating pathogen, regulates SpeB cysteine protease production. *Mol Microbiol* 81:588–601. <https://doi.org/10.1111/j.1365-2958.2011.07709.x>.
17. Carroll RK, Shelburne SA, Olsen RJ, Suber B, Sahasrabhojane P, Kumaraswami M, Beres SB, Shea PR, Flores AR, Musser JM. 2011. Naturally occurring single amino acid replacements in a regulatory protein alter streptococcal gene expression and virulence in mice. *J Clin Invest* 121:1956–1968. <https://doi.org/10.1172/JCI45169>.
18. Lukomski S, Burns EH, Wyde PR, Podbielski A, Rurangirwa J, Moore-Poveda DK, Musser JM. 1998. Genetic inactivation of an extracellular cysteine protease (SpeB) expressed by *Streptococcus pyogenes* decreases resistance to phagocytosis and dissemination to organs. *Infect Immun* 66:771–776.
19. Lukomski S, Montgomery CA, Rurangirwa J, Geske RS, Barrish JP, Adams GJ, Musser JM. 1999. Extracellular cysteine protease produced by *Streptococcus pyogenes* participates in the pathogenesis of invasive skin infection and dissemination in mice. *Infect Immun* 67:1779–1788.
20. Lukomski S, Sreevatsan S, Amberg C, Reichardt W, Woischnik M, Podbielski A, Musser JM. 1997. Inactivation of *Streptococcus pyogenes* extracellular cysteine protease significantly decreases mouse lethality of se-

- rotype M3 and M49 strains. *J Clin Invest* 99:2574–2580. <https://doi.org/10.1172/JCI119445>.
21. Olsen RJ, Sitkiewicz I, Ayeras AA, Gonulal VE, Cantu C, Beres SB, Green NM, Lei B, Humbird T, Greaver J. 2010. Decreased necrotizing fasciitis capacity caused by a single nucleotide mutation that alters a multiple gene virulence axis. *Proc Natl Acad Sci U S A* 107:888–893. <https://doi.org/10.1073/pnas.0911811107>.
  22. Olsen RJ, Raghuram A, Cantu C, Hartman MH, Jimenez FE, Lee S, Ngo A, Rice KA, Saddington D, Spillman H, Valson C, Flores AR, Beres SB, Long SW, Nasser W, Musser JM. 2015. The majority of 9,729 group A streptococcus strains causing disease secrete SpeB cysteine protease: pathogenesis implications. *Infect Immun* 83:4750–4758. <https://doi.org/10.1128/IAI.00989-15>.
  23. Shelburne SA, III, Olsen RJ, Makthal N, Brown NG, Sahasrabhojane P, Watkins EM, Palzkill T, Musser JM, Kumaraswami M. 2011. An amino-terminal signal peptide of Vfr protein negatively influences RopB-dependent SpeB expression and attenuates virulence in *Streptococcus pyogenes*. *Mol Microbiol* 82:1481–1495. <https://doi.org/10.1111/j.1365-2958.2011.07902.x>.
  24. Svensson MD, Scaramuzzino DA, Sjöbring U, Olsén A, Frank C, Bessen DE. 2000. Role for a secreted cysteine proteinase in the establishment of host tissue tropism by group A streptococci. *Mol Microbiol* 38:242–253. <https://doi.org/10.1046/j.1365-2958.2000.02144.x>.
  25. Makthal N, Gavagan M, Do H, Olsen RJ, Musser JM, Kumaraswami M. 2016. Structural and functional analysis of RopB: a major virulence regulator in *Streptococcus pyogenes*. *Mol Microbiol* 99:1119–1133. <https://doi.org/10.1111/mmi.13294>.
  26. Eisenberg M. 1993. Rheumatic heart disease in the developing world: prevalence, prevention, and control. *Eur Heart J* 14:122–128. <https://doi.org/10.1093/eurheartj/14.1.122>.
  27. Kumar P, Garhwal S, Chaudhary V. 1992. Rheumatic heart disease: a school survey in a rural area of Rajasthan. *Indian Heart J* 44:245–246.
  28. Wannemaker LW. 1973. The chain that links the heart to the throat. *Circulation* 48:9–18. <https://doi.org/10.1161/01.CIR.48.1.9>.
  29. Amerongen AVN, Veerman ECL. 2002. Saliva—the defender of the oral cavity. *Oral Dis* 8:12–22. <https://doi.org/10.1034/j.1601-0825.2002.1o816.x>.
  30. Shelburne SA, Granville C, Tokuyama M, Sitkiewicz I, Patel P, Musser JM. 2005. Growth characteristics of and virulence factor production by group A *Streptococcus* during cultivation in human saliva. *Infect Immun* 73:4723–4731. <https://doi.org/10.1128/IAI.73.8.4723-4731.2005>.
  31. Hamburger M, Jr. 1944. Studies on the transmission of hemolytic streptococcus infections. I. Cross infections in army hospital wards. *J Infect Dis* 1944:58–70.
  32. Hamburger M, Jr. 1944. Studies on the transmission of hemolytic streptococcus infections. II. Beta hemolytic streptococci in the saliva of persons with positive throat cultures. *J Infect Dis* 1944:71–78.
  33. Hamburger M, Robertson O. 1948. Expulsion of group A hemolytic streptococci in droplets and droplet nuclei by sneezing, coughing and talking. *Am J Med* 4:690–701. [https://doi.org/10.1016/S0002-9343\(48\)90392-1](https://doi.org/10.1016/S0002-9343(48)90392-1).
  34. Ross P. 1971. Beta-haemolytic streptococci in saliva. *J Hyg (Lond)* 69:347–353.
  35. Alam FM, Turner CE, Smith K, Wiles S, Srisakandan S. 2013. Inactivation of the CovR/S virulence regulator impairs infection in an improved murine model of *Streptococcus pyogenes* naso-pharyngeal infection. *PLoS One* 8:e61655. <https://doi.org/10.1371/journal.pone.0061655>.
  36. Ji Y, Carlson B, Kondagunta A, Cleary PP. 1997. Intranasal immunization with C5a peptidase prevents nasopharyngeal colonization of mice by the group A *Streptococcus*. *Infect Immun* 65:2080–2087.
  37. Shelburne SA, III, Sahasrabhojane P, Suber B, Keith DB, Davenport MT, Horstmann N, Kumaraswami M, Olsen RJ, Brennan RG, Musser JM. 2011. Niche-specific contribution to streptococcal virulence of a MalR-regulated carbohydrate binding protein. *Mol Microbiol* 81:500–514. <https://doi.org/10.1111/j.1365-2958.2011.07708.x>.
  38. Shelburne SA, Keith D, Horstmann N, Sumbly P, Davenport MT, Graviss EA, Brennan RG, Musser JM. 2008. A direct link between carbohydrate utilization and virulence in the major human pathogen group A *Streptococcus*. *Proc Natl Acad Sci U S A* 105:1698–1703. <https://doi.org/10.1073/pnas.0711767105>.
  39. Watson ME, Jr, Neely MN, Caparon MG. 2016. Animal models of *Streptococcus pyogenes* infection. In Ferretti JJ, Stevens DL, Fischetti VA (ed), *Streptococcus pyogenes: basic biology to clinical manifestations*. University of Oklahoma Health Sciences Center, Oklahoma City, OK.
  40. Davidopoulou S, Diza E, Menexes G, Kalfas S. 2012. Salivary concentration of the antimicrobial peptide LL-37 in children. *Arch Oral Biol* 57:865–869. <https://doi.org/10.1016/j.archoralbio.2012.01.008>.
  41. Johansson L, Thulin P, Sendi P, Hertzén E, Linder A, Åkesson P, Low DE, Agerberth B, Norrby-Teglund A. 2008. Cathelicidin LL-37 in severe *Streptococcus pyogenes* soft tissue infections in humans. *Infect Immun* 76:3399–3404. <https://doi.org/10.1128/IAI.01392-07>.
  42. Malcolm J, Sherriff A, Lappin DF, Ramage G, Conway DI, Macpherson LMD, Culshaw S. 2014. Salivary antimicrobial proteins associate with age-related changes in streptococcal composition in dental plaque. *Mol Oral Microbiol* 29:284–293. <https://doi.org/10.1111/omi.12058>.
  43. Zanetti M. 2004. Cathelicidins, multifunctional peptides of the innate immunity. *J Leukoc Biol* 75:39–48. <https://doi.org/10.1189/jlb.0403147>.
  44. Schmidtchen A, Frick I-M, Andersson E, Tapper H, Björck L. 2002. Proteinases of common pathogenic bacteria degrade and inactivate the antibacterial peptide LL-37. *Mol Microbiol* 46:157–168. <https://doi.org/10.1046/j.1365-2958.2002.03146.x>.
  45. Zhu L, Olsen RJ, Nasser W, Beres SB, Vuopio J, Kristinsson KG, Gottfredsson M, Porter AR, DeLeo FR, Musser JM. 2015. A molecular trigger for intercontinental epidemics of group A *Streptococcus*. *J Clin Invest* 125:3545–3559. <https://doi.org/10.1172/JCI82478>.
  46. Beres SB, Carroll RK, Shea PR, Sitkiewicz I, Martinez-Gutierrez JC, Low DE, McGeer A, Willey BM, Green K, Tyrrell GJ, Goldman TD, Feldgarden M, Birren BW, Fofanov Y, Boos J, Wheaton WD, Honisch C, Musser JM. 2010. Molecular complexity of successive bacterial epidemics deconvoluted by comparative pathogenomics. *Proc Natl Acad Sci U S A* 107:4371–4376. <https://doi.org/10.1073/pnas.0911295107>.
  47. Beres SB, Musser JM. 2007. Contribution of exogenous genetic elements to the group A *Streptococcus* metagenome. *PLoS One* 2:e800. <https://doi.org/10.1371/journal.pone.0000800>.
  48. Nasser W, Beres SB, Olsen RJ, Dean MA, Rice KA, Long SW, Kristinsson KG, Gottfredsson M, Vuopio J, Raisanen K, Caugant DA, Steinbakk M, Low DE, McGeer A, Darenberg J, Henriques-Normark B, Van Beneden CA, Hoffmann S, Musser JM. 2014. Evolutionary pathway to increased virulence and epidemic group A *Streptococcus* disease derived from 3,615 genome sequences. *Proc Natl Acad Sci U S A* 111:E1768–E1776. <https://doi.org/10.1073/pnas.1403138111>.
  49. Fittipaldi N, Beres SB, Olsen RJ, Kapur V, Shea PR, Watkins ME, Cantu CC, Laucirica DR, Jenkins L, Flores AR, Lovgren M, Ardanuy C, Liñares J, Low DE, Tyrrell GJ, Musser JM. 2012. Full-genome dissection of an epidemic of severe invasive disease caused by a hypervirulent, recently emerged clone of group A *Streptococcus*. *Am J Pathol* 180:1522–1534. <https://doi.org/10.1016/j.ajpath.2011.12.037>.
  50. Neely MN, Lyon WR, Runft DL, Caparon M. 2003. Role of RopB in growth phase expression of the SpeB cysteine protease of *Streptococcus pyogenes*. *J Bacteriol* 185:5166–5174. <https://doi.org/10.1128/JB.185.17.5166-5174.2003>.
  51. Dickey SW, Cheung GY, Otto M. 2017. Different drugs for bad bugs: antivirulence strategies in the age of antibiotic resistance. *Nat Rev Drug Discov* 16:457–471. <https://doi.org/10.1038/nrd.2017.23>.
  52. Heras B, Scanlon MJ, Martin JL. 2015. Targeting virulence not viability in the search for future antibacterials. *Br J Clin Pharmacol* 79:208–215. <https://doi.org/10.1111/bcp.12356>.
  53. Rasko DA, Sperandio V. 2010. Anti-virulence strategies to combat bacteria-mediated disease. *Nat Rev Drug Discov* 9:117–128. <https://doi.org/10.1038/nrd3013>.
  54. Courtney H, Hasty D. 1991. Aggregation of group A streptococci by human saliva and effect of saliva on streptococcal adherence to host cells. *Infect Immun* 59:1661–1666.
  55. Carnes EC, Lopez DM, Donegan NP, Cheung A, Gresham H, Timmins GS, Brinker CJ. 2010. Confinement-induced quorum sensing of individual *Staphylococcus aureus* bacteria. *Nat Chem Biol* 6:41–45. <https://doi.org/10.1038/nchembio.264>.
  56. Pang YY, Schwartz J, Thoendel M, Ackermann LW, Horswill AR, Nauseef WM. 2010. agr-dependent interactions of *Staphylococcus aureus* USA300 with human polymorphonuclear neutrophils. *J Innate Immun* 2:546. <https://doi.org/10.1159/000319855>.
  57. Palmer KL, Aye LM, Whiteley M. 2007. Nutritional cues control *Pseudomonas aeruginosa* multicellular behavior in cystic fibrosis sputum. *J Bacteriol* 189:8079–8087. <https://doi.org/10.1128/JB.01138-07>.
  58. Chang JC, LaSarre B, Jimenez JC, Aggarwal C, Federle MJ. 2011. Two group A streptococcal peptide pheromones act through opposing Rgg regulators to control biofilm development. *PLoS Pathog* 7:e1002190. <https://doi.org/10.1371/journal.ppat.1002190>.
  59. Jimenez JC, Federle MJ. 2014. Quorum sensing in group A *Streptococcus*

- cus. *Front Cell Infect Microbiol* 4:127. <https://doi.org/10.3389/fcimb.2014.00127>.
60. Belotserkovsky I, Baruch M, Peer A, Dov E, Ravins M, Mishalian I, Persky M, Smith Y, Hanski E. 2009. Functional analysis of the quorum-sensing streptococcal invasion locus (sil). *PLoS Pathog* 5:e1000651. <https://doi.org/10.1371/journal.ppat.1000651>.
61. Mashburn-Warren L, Morrison DA, Federle MJ. 2012. The cryptic competence pathway in *Streptococcus pyogenes* is controlled by a peptide pheromone. *J Bacteriol* 194:4589–4600. <https://doi.org/10.1128/JB.00830-12>.
62. Mashburn-Warren L, Morrison DA, Federle MJ. 2010. A novel double-tryptophan peptide pheromone controls competence in *Streptococcus* spp. via an Rgg regulator. *Mol Microbiol* 78:589–606. <https://doi.org/10.1111/j.1365-2958.2010.07361.x>.
63. Lancefield RC. 1959. Persistence of type-specific antibodies in man following infection with group A streptococci. *J Exp Med* 110:271–292. <https://doi.org/10.1084/jem.110.2.271>.
64. Sanson M, Makthal N, Flores AR, Olsen RJ, Musser JM, Kumaraswami M. 2015. Adhesin competence repressor (AdcR) from *Streptococcus pyogenes* controls adaptive responses to zinc limitation and contributes to virulence. *Nucleic Acids Res* 43:418–432. <https://doi.org/10.1093/nar/gku1304>.

1 Supplementary figure S1



2

3 Figure S1. Schematics showing the organization of genetic elements in GAS strains and  
 4 *trans*-complementation plasmid used in this study. The *ropB* and *speB* genes are divergently  
 5 transcribed. The angled arrows above the line indicate two transcription start sites for *speB*,  
 6 designated P1 and P2. The intergenic region with three predicted open reading frames are  
 7 shown as horizontal arrows. Numbers indicate the nucleotide positions relative to the first  
 8 nucleotide of *speB* start codon. Nucleotides corresponding to transcription start site P1 is  
 9 highlighted in orange. Inferred ribosomal binding site (RBS) located upstream of *SIP* is  
 10 underlined and labeled. Nucleotide sequences of *SIP* are italicized and colored in orange.  
 11 Amino acid sequence corresponding to each codon of *SIP* is given below. \* indicates stop  
 12 codon. Substitution of *SIP* start codon with stop codon in *SIP\** strain is highlighted in green.

13  
 14  
 15  
 16

1 Table S2. Primers and probes used in this study

Primer	Sequence 5' – 3'	Purpose
<i>tufA</i> qRTFwd	CAACTCGTCACTATGCGCACAT	5' primer for <i>tufA</i> qRT-PCR
<i>tufA</i> qRTRev	GAGCGGCACCAGTGATCAT	3' primer for <i>tufA</i> qRT-PCR
<i>tufA</i> probe C	CTCCAGGACACGCGGACTACGTTAAAAA	Probe for <i>tufA</i> qRT-PCR
<i>speB</i> qRTFwd	ACTCTACCAGCGGATCATTG	5' primer for <i>speB</i> qRT-PCR
<i>speB</i> qRTRev	CAGCGGTACCAGCATAAGTAG	3' primer for <i>speB</i> qRT-PCR
<i>speB</i> probe	TGCTTCCTTCATGGAAAGTTATGTCGAACA	Probe for <i>speB</i> qRT-PCR

2

3

4

5

6

7

8

9

10

11

12

13

14

15

16

17

18

19

20

21

1 Table S1. Bacterial strains and plasmids used in this study.

Strain or Plasmid	Description	Reference
<b>Strains</b>		
WT	Invasive isolate MGAS10870, serotype M3	(1)
WT:pDC	MGAS10870 <i>trans</i> -complemented with empty vector pDC123, chloramphenicol resistant	(2)
MGAS2221	Invasive isolate, serotype M1	(3)
MGAS15249	Invasive isolate, serotype M59	(4)
MGAS26844	Invasive isolate, serotype M89	(5)
MGAS9429	Pharyngeal isolate, serotype M12	(6)
$\Delta ropB$	MGAS10870 $\Delta ropB::aad9$	(7)
$\Delta speB$	MGAS10870 $\Delta speB::aad9$	(2)
SIP*	Isoallelic mutant strain that has the start codon of SIP changed to stop codon in parental serotype MGAS10870	(8)
SIP*:pDC	SIP* mutant <i>trans</i> -complemented with empty vector pDC123, Chloramphenicol resistant	(8)
SIP*:pDC-SIP	SIP* mutant <i>trans</i> -complemented with plasmid pDC-SIP, Chloramphenicol resistant	(8)
<i>E. coli</i> DH5 $\alpha$	Host strain for cloning purposes	
<b>Plasmids</b>		
pJL	Low-copy number plasmid capable of replication in GAS and <i>Escherichia coli</i> , Chloramphenicol resistant Used to generate isoallelic GAS mutants	(9)
pDC	Low-copy number plasmid, pDC123, capable of replication in GAS and <i>Escherichia coli</i> , Chloramphenicol resistant	(10)
pDC-SIP	pDC with the fragment of intergenic region (-772 ~ -646) between <i>ropB</i> and <i>speB</i>	(8)

2

3

4

1 **References**

- 2
- 3 1. **Beres SB, Carroll RK, Shea PR, Sitkiewicz I, Martinez-Gutierrez JC, Low DE, McGeer A, Willey BM, Green K, Tyrrell GJ, Goldman TD, Feldgarden M, Birren BW, Fofanov Y, Boos J, Wheaton WD, Honisch C, Musser JM.** 2010. Molecular complexity of successive bacterial epidemics deconvoluted by comparative pathogenomics. *Proc Natl Acad Sci USA* **107**:4371-4376.
- 6 2. **Shelburne III SA, Olsen RJ, Makthal N, Brown NG, Sahasrabhojane P, Watkins EM, Palzkill T, Musser JM, Kumaraswami M.** 2011. An amino-terminal signal peptide of Vfr protein negatively influences RopB-dependent SpeB expression and attenuates virulence in *Streptococcus pyogenes*. *Mol Microbiol* **82**:1481-1495.
- 11 3. **Nasser W, Beres SB, Olsen RJ, Dean MA, Rice KA, Long SW, Kristinsson KG, Gottfredsson M, Vuopio J, Raisanen K, Caugant DA, Steinbakk M, Low DE, McGeer A, Darenberg J, Henriques-Normark B, Van Beneden CA, Hoffmann S, Musser JM.** 2014. Evolutionary pathway to increased virulence and epidemic group A *Streptococcus* disease derived from 3,615 genome sequences. *Proc Natl Acad Sci U S A* **111**:E1768-1776.
- 16 4. **Fittipaldi N, Beres SB, Olsen RJ, Kapur V, Shea PR, Watkins ME, Cantu CC, Laucirica DR, Jenkins L, Flores AR, Lovgren M, Ardanuy C, Liñares J, Low DE, Tyrrell GJ, Musser JM.** 2012. Full-Genome Dissection of an Epidemic of Severe Invasive Disease Caused by a Hypervirulent, Recently Emerged Clone of Group A *Streptococcus*. *Am J Pathol* **180**:1522-1534.
- 21 5. **Zhu L, Olsen RJ, Nasser W, Beres SB, Vuopio J, Kristinsson KG, Gottfredsson M, Porter AR, DeLeo FR, Musser JM.** 2015. A molecular trigger for intercontinental epidemics of group A *Streptococcus*. *J Clin Invest* **125**:3545-3559.
- 26 6. **Beres SB, Musser JM.** 2007. Contribution of exogenous genetic elements to the group A *Streptococcus* metagenome. *PLoS One* **2**:e800.
- 28 7. **Carroll RK, Shelburne SA, Olsen RJ, Suber B, Sahasrabhojane P, Kumaraswami M, Beres SB, Shea PR, Flores AR, Musser JM.** 2011. Naturally occurring single amino acid replacements in a regulatory protein alter streptococcal gene expression and virulence in mice. *J Clin Invest* **121**:1956-1968.
- 31 8. **Do H, Makthal N, VanderWal AR, Rettel M, Savitski MM, Peschek N, Papenfort K, Olsen RJ, Musser JM, Kumaraswami M.** 2017. Leaderless secreted peptide signaling molecule alters global gene expression and increases virulence of a human bacterial pathogen. *Proc Natl Acad Sci USA* **114**:E8498-E8507.
- 34 9. **Li J, Kasper DL, Ausubel FM, Rosner B, Michel JL.** 1997. Inactivation of the  $\alpha$  C protein antigen gene, *bca*, by a novel shuttle/suicide vector results in attenuation of virulence and immunity in group B *Streptococcus*. *Proc Natl Acad Sci USA* **94**:13251-13256.
- 37 10. **Chaffin D, Rubens C.** 1998. Blue/white screening of recombinant plasmids in Gram-positive bacteria by interruption of alkaline phosphatase gene (*phoZ*) expression. *Gene* **219**:91-99.
- 40
- 41
- 42
- 43
- 44
- 45
- 46
- 47
- 48

## DISCUSSION

The emergence of bacterial multidrug resistance against existing antibiotics and lack of new antibiotics in the pipeline pose a major threat to public health (5, 148-150). Thus, novel targeting strategies are urgently required to identify new antimicrobial targets to combat complicated infections caused by multidrug resistant bacteria. In this regard, the toxins produced by bacteria or signaling pathways controlling toxin production are ideal targets for antimicrobial development as they contribute significantly to disease pathogenesis. An ideal antimicrobial target must be expressed during infection, participate in disease pathogenesis, and accessible in the host for therapeutic targeting (151-153). Given that cysteine protease SpeB is produced abundantly during human GAS infection (99, 100), and SpeB protease activity is a key contributor to GAS pathogenesis due to its role in various bacterial processes during infection (1, 2, 68, 72, 73, 96, 154), it is a plausible candidate for antimicrobial targeting studies. Consistent with this, SpeB protease has been previously targeted for vaccine and antimicrobial development (104, 106). Although preclinical protection studies showed significant promise, the success has not translated to clinical trials (155). In this study, we have discovered that GAS produces a novel quorum-sensing signal, a leaderless peptide SIP, which acts as an intercellular signal to control the expression of *speB* in concert with high bacterial population density. Contrary to all the characterized bacterial peptide signals, SIP amino acid sequence lacks several classical features that are required for peptide secretion and maturation. Nevertheless, SIP functions as an effective intercellular signal (chapter 1). In addition to SIP identification, we have deduced several mechanistic steps in the SIP signaling pathway that includes production of SIP in its mature form, and secretion and reinternalization of SIP to GAS cytosol by yet to be identified mechanisms. The reinternalized SIP is recognized by its cognate receptor, transcription regulator RopB, in the

cytosol. Binding of SIP induces allosteric changes in RopB that are crucial for activation of *speB* gene expression. Importantly, we showed that the SIP signaling pathway is active *in vivo* and contributes significantly to GAS virulence in mouse models of infection. We also showed that SIP signaling occurs during GAS growth *ex vivo* in human saliva and blood, and SIP-mediated *speB* expression is important for GAS survival in both saliva and blood. Given that SIP-dependent gene regulation is the primary signaling pathway that controls *speB* expression during infection, we propose that the molecular components of peptide signaling pathway may present alternate targets for therapeutic or prophylactic possibilities to treat GAS infections. However, further investigations are required to identify various components of this pathway for successful antimicrobial targeting.

## 1. Mechanism of SIP export

Without exception, the bacterial quorum sensing signals must be secreted to coordinate population-wide gene regulation (120, 126, 133-135). Gram-positive bacteria typically use oligopeptides as secreted signals, commonly referred to as peptide signals or auto-inducing peptides. The peptide signals are initially produced as inactive pre-peptides (125). Biogenesis of active (mature) peptide signals is a multi-step process involving secretion and proteolytic processing of the inactive pre-peptides. (4, 156). Generally, the peptide signals have three regions: the amino-terminus segment (n-region) rich in positively-charged amino acids, central core part (h-region) containing hydrophobic amino acids, and the C-terminus (c-region) fragment that has the protease recognition and cleavage region (107, 157). The basic n-region contains the characteristic secretion signal sequence that directs the translocation of the peptide signal to

bacterial membrane for secretion via the general secretory pathway (Sec) (4, 156, 158). The membrane-bound signal peptidase I then cleaves the secretion signal sequence as the peptide signals emerge from the Sec pathway (158). The c-region of the peptide signal typically contains one or more protease cleavage sites that are processed in the membrane by the intramembrane protease, enhanced expression of pheromone (Eep), and various secreted proteases (4, 125, 159). The extracellular peptide signals are subjected to additional processing by the secreted proteases before releasing the active (mature) peptide signal (127).

The biogenesis of mature SIP is unique compared to the hall marks of characterized bacterial peptide signals in other gram-positive bacteria. SIP is encoded in GAS genome as an 8-amino acid peptide in its mature form. SIP lacks the amino acid sequence characteristics in the n-region required for secretion (Fig. 3A of chapter 1). The lack of secretion signal sequence raises an important question – is SIP secreted? However, we demonstrated that the cell-free culture supernatant from peptide-producing WT GAS growth has regulatory activity, whereas the cell-free culture supernatant obtained from the peptide non-producing *sip*\* (start codon ATG mutated to stop codon TAG to disrupt the translation) mutant does not have the regulatory activity (Fig. 3D of chapter 1). These results showed that only the SIP-producing strains contain regulatory activity in the secreted component of GAS growth, thus establishing direct causation between the presence of intact *sip* gene in GAS genome and extracellular regulatory activity. Our efforts to provide direct evidence demonstrating the extracellular presence of SIP by mass-spectrometry are unsuccessful so far, likely due to the hydrophobic nature of SIP. In conclusion, despite the lack of a secretion signal sequence, SIP is secreted.

SIP amino acid sequence also lacks protease cleavage sites in the c-region (Fig. 3A of chapter 1). SIP does not require proteolytic processing by Eep as the genetic inactivation of *eep* in

*Δeep* mutant did not affect *speB* expression (Fig. 3B and 3C of chapter 1), indicating that SIP is produced in its mature form.

The dedicated PptAB exporter was previously shown to be required for the export of SHP, cognate peptide signals of Rgg regulators in *Streptococcus* (160, 161). However, our findings indicated that PptAB is not required for SIP signaling (unpublished data). Collectively, our analyses demonstrate that SIP is the founding member of a new class of leaderless peptide signals and is likely exported out of GAS cytosol by a yet-to-be identified novel secretion pathway.

## **2. Import of extracellular SIP to the GAS cytoplasm**

The general paradigm of bacterial peptide signaling requires that the secreted mature peptide signals are recognized either extracellularly by the membrane-bound sensor kinase of two component systems or by the cytosolic transcription regulators (4, 125). The members of RRNPP family regulators are cytosolic peptide receptors that differentially regulate target gene expression upon their interactions with the cognate peptide signals (4, 125). Invariably, the import of cognate peptide signals of RRNPP family regulators into the cytosol is mediated by the membrane-bound peptide permeases, oligopeptide permeases (Opp) or dipeptide permeases (Dpp) (4, 125, 162-164). Both Opp and Dpp permeases are five subunit complexes that belong to the family of ATP-binding cassette (ABC) transporters (165-170). Typically, the *opp* and *dpp* genes are transcribed as a five-gene operon and highly conserved across Gram-positive bacteria (165-170). Opp mediates the uptake of longer peptides (up to 35 residues), independent of their amino acid composition (165-168), whereas Dpp permeases import dipeptides into the bacterial cytosol (171). As in other bacteria, two different five-gene operons, *oppABCDF* and *dppABCDE*, encoding Opp and Dpp

permeases, respectively, are present in the GAS genome. Previously, both Opp and Dpp permeases were implicated in the regulation of *speB* expression (164, 172). The role of peptide permeases in *speB* regulation combined with our discovery of SIP suggested that Opp or Dpp may influence *speB* expression due to their role in SIP reimport. However, our results revealed that genetic inactivation of *opp* ( $\Delta oppDF$ ), or *dpp* ( $\Delta dppA$ ) permeases in GAS M3 serotype did not affect *speB* expression (Fig. 3B of chapter 1). Given that the two permeases are highly conserved, we considered the possibility that the two importers may be functionally redundant, and inactivation of one importer may be compensated by the presence of second importer. To test this possibility, we generated a  $\Delta oppDF/\Delta dppA$  double mutant strain and measured *speB* transcript levels. Surprisingly, *speB* gene expression in the  $\Delta oppDF/\Delta dppA$  double mutant strain was comparable to that of WT GAS (Fig. 3B of chapter 1). Furthermore, addition of synthetic SIP to  $\Delta oppDF/\Delta dppA$  mutant restored WT-like *speB* expression in the  $\Delta oppDF/\Delta dppA/\Delta sip$  strain (Fig. 3B of chapter 1). Collectively, these observations suggest that Opp/Dpp permeases are not involved in SIP reimport. Importantly, the lack of a role for peptide permeases in SIP reimport raises a fundamental question: is SIP imported back to GAS cytoplasm? Our supplementation studies with fluorescein isothiocyanate (FITC)-labelled SIP unambiguously demonstrated that exogenously added SIP is internalized in GAS cytosol (Fig. 3F of chapter 1). Thus, it is likely that novel mechanisms are involved in SIP import. However, additional investigations will be required to fully elucidate the molecular details of SIP transport mechanisms.

### **3. Binding of SIP to RopB and its implications in *speB* expression**

Despite the vast differences in the biogenesis, secretion and import mechanism between SIP and other RRNPP family signaling peptides, our results indicate that the underlying molecular

mechanism by which SIP influences *speB* regulation is consistent with the other members of the family. Typically, the mature peptide signals are 5 – 8 amino acid long, highly hydrophobic and modulate the expression of target genes by binding to their respective regulators with a high degree of specificity (4). Consistent with this, our protein-peptide binding studies (chapter 1) indicate that the intact SIP in its native order of amino acid sequence is engaged in high affinity and sequence-specific interactions with RopB (dissociation constant  $K_d \sim 2.6$  nM). Truncation of SIP by single amino acid disrupted RopB binding (Fig. 4A and 4B of chapter 1), indicating that full-length SIP is required for RopB interactions. The *in vitro* observations were recapitulated *in vivo* as single amino acid truncation of SIP failed to induce *speB* expression in *sip\** mutant strain (Fig. 2B of chapter 1). Thus we conclude that the binding of SIP to RopB regulator is a crucial step for the activation of *speB* expression. These findings were further corroborated by our structural studies in which we delineated the chemical basis for SIP recognition by RopB (173). We showed that SIP binds to the concave surface in the C-terminal domain of RopB. The SIP binding pocket is composed of hydrophobic and aromatic amino acids as well as asparagines that are characteristics of TPR domains (4). Importantly, the SIP-contacting RopB residues are crucial for the *in vivo* expression of SpeB and GAS virulence (173). Collectively, these results demonstrate that SIP recognition by RopB is crucial for the transcription regulation of *speB*.

The influence of environmental pH on the expression of *speB* is known for several decades (2). Caparon and group have reported that the *speB* expression was maximum when the *in vitro* culture medium was acidified to pH 6.0 and repressed at pH 7.5 (110). GAS auto-acidifies its growth conditions due to lactic acid production (from pH 7.5 during exponential growth phase to pH 6.0 during stationary phase) (2). Interestingly, the auto-acidification coincides with both high GAS population density and the onset of *speB* expression. These observations suggest the presence

of an interplay between environmental pH and SIP signaling. In accordance with this, our recent findings demonstrated that the binding affinity of SIP to RopB is sensitive to pH and high affinity interactions are favored under below neutral pH conditions (pH 6.0) (accepted manuscript). These results suggest that environmental pH controls SIP recognition by RopB. Compared to binding affinity ( $K_d$  value) in pH 6.0, the affinity was significantly reduced in buffer with pH 7.5 and pH 9.0 by 23-fold and 177-fold, respectively (data not shown). Intriguingly, when environmental acidification occurs, GAS cytosol also acidified (pH 5.8), indicating that the cytosolic environment during high population density is the conducive for high affinity RopB-SIP interactions. We further demonstrated that a pH-sensing histidine switch is present in RopB that monitors environment pH and controls SIP binding to the pocket in RopB (173).

In addition to pH, other GAS factors such as the two-component CovRS system, major transcription regulator Mga, transcription regulator CcpA also (Fig. 5 of Introduction) regulate SpeB production. However, how all these factors work, either individually or in tandem, to tightly modulate the production of SpeB is poorly understood (2). Given that SIP is the primary mechanism controlling *speB* expression and environmental pH is integrated into SIP pathway, it is possible that other GAS factors may exert their influence on *speB* expression by modulating SIP signaling pathway. Such discoveries would significantly advance our current understanding of the complex signaling peptide functions in GAS, and other pathogenic bacteria.

#### **4. Allosteric changes in RopB upon SIP binding**

Typically, the RRNPP family cognate peptides induce allosteric changes upon binding to their respective regulator, and these conformational changes in the regulators are crucial to the

target gene regulation (4). Among the RRNPP regulators, the binding of activation peptide cCF10 disrupts PrgX tetramerization, which is crucial for the activation of gene expression. On the other hand, in *Bacillus cereus*, the binding of NrpX peptide to NrpR induces NrpR tetramerization which represents the transcriptionally active state of NrpR (132, 174). Similarly, the binding of PapR to PlcR releases the otherwise masked N-terminal DNA binding domain of PlcR which leads to promoter binding and gene regulation (175). Our results indicate that SIP induces unique allosteric changes in RopB to activate *speB* expression. SIP facilitates high-affinity RopB-DNA interactions and subsequent polymerization of RopB on *speB* promoter to control gene expression. Although two different promoter sequences P1 and P2 have been implicated to be involved in starting the transcription of *speB* (114), the role of P2 has been in question for several years now. Hence, we included the probe containing the sequence of P2 in our EMSA experiment to deduce its role in RopB regulatory activity. Our results show that both apo-RopB and RopB-SIP complex do not bind to the probe containing the promoter sequence of P2 (Fig. S6D of chapter 1) and these findings are consistent with the recent re-annotation of P2 promoter as a Rnase Y processing site of *speB* mRNA (116). Importantly, we show that SIP promotes RopB binding to two binding sites, site 1 and site 2, in *speB* promoter. The two sites are located upstream of P1 and are separated by a 121-bp-long spacer region (Fig. 4 and S6 of chapter 1). SIP also induces RopB oligomerization on the promoter sequences, however the DNA binding event precedes RopB oligomerization (Fig. 4I and S9 of chapter 1). Based on these findings, we propose that SIP promotes high affinity interactions between RopB and the two binding sites in P1. Using these interactions as nucleation event, RopB polymerizes between the spacer region of the two sites and the polymerization event of RopB results in the activation of *speB* transcription. Our future structural studies will be directed to

identify SIP-induced allosteric changes in RopB that contribute to RopB-DNA interactions and RopB oligomerization on DNA.

## 5. Role of SIP in GAS pathogenesis

The production/protease activity of SpeB has been extensively studied (2). The role of SpeB in GAS disease pathogenesis in animal models of infection and during natural human infections is well established (71, 72, 74, 75, 94, 95). Our *in vitro* analyses demonstrate that SIP signaling pathway is the primary regulatory mechanism controlling *speB* expression. However, the findings in the laboratory medium do not fully recapitulate the conditions encountered by GAS in the complex host environment (2). This led us to ask a three-part question (i) whether SIP is produced during GAS infection, ii) whether SIP signaling pathway is active during GAS infection in the host, and iii) whether SIP signaling pathway contributes to GAS pathogenesis. Our findings in chapter 2 show that the serum samples obtained from 5 convalescing patients with prior invasive GAS infections and 5 pediatric patients with GAS pharyngitis had anti-SIP antibodies, suggesting that SIP is produced by GAS in the host during infection (Table 1 of chapter 2). To answer the second and third part of the question, we compared the *in vivo speB* expression levels in mice infected subcutaneously with one of the following strains: WT, *sip\** mutant, and *sip\** mutant *trans*-complemented with *sip*. We have used WT GAS strain grown to late-exponential phase in the laboratory medium as the reference. We observed a ~ 3000-fold increase in *speB* transcript levels in WT GAS compared to the reference. However, the *sip\** mutant strain had *speB* transcript levels comparable to that of reference (Fig. 6A of chapter 1), indicating that SIP signaling pathway is active and controls *speB* expression *in vivo* during infection. Overall, these results (Fig. 1D of

chapter 1) demonstrate that SIP is produced during infection and intercellular SIP signaling pathway activates GAS virulence gene regulation in the complex host environment.

GAS is a versatile pathogen that infects several host niches. Given the variations in the complex host milieu at different host anatomical sites, it is remarkable that GAS possess mechanisms to colonize and establish infections in diverse host environments (12, 19). In this regard, we raised the question whether SIP signaling pathway contributes to GAS pathogenesis at different host anatomical sites (Fig. 5 of chapter 1).

The host oropharynx is the most common site for GAS colonization and pharyngitis is the common form of GAS disease manifestation (13, 176). GAS employs unique transcriptional program to survive in human saliva and colonize oropharynx. Among the GAS genes upregulated during growth in saliva, *SpeB* is critical for optimum GAS growth *ex vivo* in human saliva (77, 177). This is not surprising considering the fact that saliva is the first line of host defense and contains antimicrobial peptides such as LL37 to control pathogen growth (76, 178). Using the *ex vivo* growth conditions, we demonstrated that addition of synthetic SIP activates *speB* expression in the *sip\** mutant during growth *ex vivo* in human saliva and blood. These observations suggest that SIP signaling occurs during growth in human body fluids and SIP signaling pathway is the primary regulatory mechanism that controls *speB* expression. Furthermore, when comparing the growth kinetics of WT, *sip\**, and trans-complemented strains for survival in human saliva and oropharyngeal colonization, the SIP non-producing strains were significantly impaired in growth *ex vivo* in human saliva and oropharyngeal colonization compared to SIP-producing strains (Fig. 4A and Fig. 5B of chapter 2). Given that the oropharynx is the primary route of GAS entry, our discovery that the SIP-mediated *speB* regulation is critical for GAS colonization in the host is of

particular importance as this can lead to translational strategies targeting SIP signaling pathway to control GAS survival in the oropharynx (Fig. 4B of chapter 2).

## 6. General model of quorum sensing mediated regulation of SpeB

The ability of bacterial pathogens to sense environmental cues and mediate spatiotemporal regulation of virulence factors is crucial for successful survival in the host (107, 120, 121, 179, 180). In this regard, GAS employs multilayered regulatory mechanisms to coordinate *speB* expression in concert with high bacterial population density. We have previously demonstrated that the transcription of *speB* is negatively influenced by the N-terminal secretion signal peptide of virulence factor related (Vfr) protein during low bacterial population density (107). Although the exact identity of the peptide sequence was not determined, our results indicated that the mature peptide resides in the N-terminal 40 amino acids of Vfr and modulates *speB* expression by binding to RopB (107). Based on these observations, we propose the following model (Fig. 6E of chapter 1) for population density-dependent regulation of *speB* expression. The mature Vfr peptide produced during low GAS population density binds to RopB and negatively influences *speB* expression. Conversely, during high GAS population density, the expression of *vfr* is downregulated and *sip* expression is induced. Once SIP reaches the threshold concentration, it binds to RopB and induces RopB-dependent activation of *speB* expression (Fig. 6E of chapter 1). SIP production also activates the positive feedback loop causing robust induction of *sip* and *speB* expression. Similar mode of gene regulation was observed in PrgX from *Enterococcus faecalis*. As in RopB, PrgX has two cognate peptides, an inhibitory peptide, iCF10 and an activation peptide, cCF10. Both peptides compete to bind to the PrgX protein and modulate the gene regulation activity of PrgX (181).

## 7. Perspectives and future directions

The Rgg/Rap/NprR/PlcR/PrgX proteins constitute the founding members of RRNPP family of regulators in gram-positive bacteria. However, bioinformatics analyses of bacterial genomes suggest that a large number of RRNPP homologs exist in different bacteria (125, 129). The cognate signaling peptides of the prototypical RRNPP family regulators have been identified. However, the cognate signaling peptides for most of these homologs are yet to be identified. RopB forms a subfamily of Rgg regulators. A major challenge in identifying the cognate peptide signals for RopB-like regulators is that the sORFs encoding non-canonical SIP-like bacterial peptide signals that are produced in its mature form. Thus, identification of such bacterial peptide signals using the criteria for classical bacterial peptide signals can be unsuccessful (125, 182). In this regard, our discovery of SIP provides a roadmap for the identification of SIP-like leaderless peptide signals and accelerate the discovery of the similar leaderless peptide signals in other bacteria. Furthermore, identification of SIP also underscores the complexities associated with bacterial intercellular communication pathways and expands the repertoire of bacterial languages.

In pathogenic bacteria, quorum sensing pathways play a significant role in the regulation of crucial traits such as virulence, sporulation, biofilm formation, and antibiotic resistance (71, 133-135, 183). Although we have elucidated the identity of the peptide signal controlling virulence gene regulation in GAS, several steps of this pathway remain poorly understood. Specifically, the molecular mechanisms by which SIP is secreted and brought back to the GAS cytosol are unknown. Thus, investigations into other aspects of SIP signaling will establish the basic principles of leaderless peptide signaling and will likely identify previously unknown therapeutic targets and strategies.

**REFERENCES**

1. Patterson MJ. 1996. Streptococcus, Medical Microbiology 4th edition. University of Texas Medical Branch at Galveston.
2. Carroll RK, Musser JM. 2011. From transcription to activation: how group A streptococcus, the flesh-eating pathogen, regulates SpeB cysteine protease production. *Molecular microbiology* 81:588-601.
3. DeLano WL. 2002. The PyMOL molecular graphics system. <http://www.pymol.org>.
4. Do H, Kumaraswami M. 2016. Structural mechanisms of peptide recognition and allosteric modulation of gene regulation by the RRNPP family of quorum-sensing regulators. *Journal of molecular biology* 428:2793-2804.
5. Davies J, Davies D. 2010. Origins and evolution of antibiotic resistance. *Microbiol Mol Biol Rev* 74:417-433.
6. Ventola CL. 2015. The antibiotic resistance crisis: part 1: causes and threats. *Pharmacy and therapeutics* 40:277.
7. Neu HC. 1992. The crisis in antibiotic resistance. *Science* 257:1064-1073.
8. Cohen NR, Lobritz MA, Collins JJ. 2013. Microbial persistence and the road to drug resistance. *Cell host & microbe* 13:632-642.
9. Li B, Webster TJ. 2018. Bacteria antibiotic resistance: New challenges and opportunities for implant-associated orthopedic infections. *Journal of Orthopaedic Research®* 36:22-32.
10. Spellberg B, Gilbert DN. 2014. The future of antibiotics and resistance: a tribute to a career of leadership by John Bartlett. *Clinical infectious diseases* 59:S71-S75.
11. Todar K. 2008. Streptococcus pyogenes and streptococcal disease. Online Textbook of Bacteriology.
12. Olsen RJ, Shelburne SA, Musser JM. 2009. Molecular mechanisms underlying group A streptococcal pathogenesis. *Cellular microbiology* 11:1-12.
13. Carapetis JR, Steer AC, Mulholland EK, Weber M. 2005. The global burden of group A streptococcal diseases. *The Lancet infectious diseases* 5:685-694.
14. Nelson DC, Garbe J, Collin M. 2011. Cysteine proteinase SpeB from Streptococcus pyogenes—a potent modifier of immunologically important host and bacterial proteins. *Biological chemistry* 392:1077-1088.
15. Cunningham MW. 2000. Pathogenesis of group A streptococcal infections. *Clinical microbiology reviews* 13:470-511.
16. Ferretti J, Köhler W. 2016. History of streptococcal research, Streptococcus pyogenes: Basic Biology to Clinical Manifestations [Internet]. University of Oklahoma Health Sciences Center.
17. Ebell M, Smith M, Barry H, Ives K, Carey M. 2001. The rational clinical examination. Does this patient have strep throat? *JAMA* [Internet].
18. Wessels MR. 2011. Streptococcal pharyngitis. *New England Journal of Medicine* 364:648-655.
19. Walker MJ, Barnett TC, McArthur JD, Cole JN, Gillen CM, Henningham A, Sriprakash K, Sanderson-Smith ML, Nizet V. 2014. Disease manifestations and pathogenic mechanisms of group A Streptococcus. *Clinical microbiology reviews* 27:264-301.
20. Steer AC, Carapetis JR, Dale JB, Fraser JD, Good MF, Guilherme L, Moreland NJ, Mulholland EK, Schodel F, Smeesters PR. 2016. Status of research and development of vaccines for Streptococcus pyogenes. *Vaccine* 34:2953-2958.
21. Cole C, Gazewood J. 2007. Diagnosis and treatment of impetigo. *American family physician* 75.

22. Makthal N, Nguyen K, Do H, Gavagan M, Chandrangsu P, Helmann JD, Olsen RJ, Kumaraswami M. 2017. A critical role of zinc importer AdcABC in group A streptococcus-host interactions during infection and its implications for vaccine development. *EBioMedicine* 21:131-141.
23. Maurice J. 2013. Rheumatic heart disease back in the limelight. *The Lancet* 382:1085-1086.
24. Lee JL, Naguwa SM, Cheema GS, Gershwin ME. 2009. Acute rheumatic fever and its consequences: a persistent threat to developing nations in the 21st century. *Autoimmunity reviews* 9:117-123.
25. Hajar R. 2016. Rheumatic fever and rheumatic heart disease a historical perspective. *Heart views: the official journal of the Gulf Heart Association* 17:120.
26. Carapetis JR, Currie BJ. 1999. Mortality due to acute rheumatic fever and rheumatic heart disease in the Northern Territory: a preventable cause of death in aboriginal people. *Australian and New Zealand journal of public health* 23:159-163.
27. Bisno A. 2010. Nonsuppurative poststreptococcal sequelae: rheumatic fever and glomerulonephritis, p 2611–2622. Mandell, Douglas, and Bennett's principles and practice of infectious diseases, 7th ed Livingstone Elsevier, Philadelphia, PA.
28. Smeesters PR, Mardulyn P, Vergison A, Leplae R, Van Melderen L. 2008. Genetic diversity of Group A Streptococcus M protein: implications for typing and vaccine development. *Vaccine* 26:5835-5842.
29. Lamagni TL, Darenberg J, Luca-Harari B, Siljander T, Efstratiou A, Henriques-Normark B, Vuopio-Varkila J, Bouvet A, Creti R, Ekelund K. 2008. Epidemiology of severe Streptococcus pyogenes disease in Europe. *Journal of clinical microbiology* 46:2359-2367.
30. O'loughlin RE, Roberson A, Cieslak PR, Lynfield R, Gershman K, Craig A, Albanese BA, Farley MM, Barrett NL, Spina NL. 2007. The epidemiology of invasive group A streptococcal infection and potential vaccine implications: United States, 2000–2004. *Clinical Infectious Diseases* 45:853-862.
31. Sanson M, Makthal N, Flores AR, Olsen RJ, Musser JM, Kumaraswami M. 2014. Adhesin competence repressor (AdcR) from Streptococcus pyogenes controls adaptive responses to zinc limitation and contributes to virulence. *Nucleic acids research* 43:418-432.
32. Davies HD, McGeer A, Schwartz B, Green K, Cann D, Simor AE, Low DE, Group OGASS. 1996. Invasive group A streptococcal infections in Ontario, Canada. *New England Journal of Medicine* 335:547-554.
33. Organization WH. 2005. The current evidence for the burden of group A streptococcal diseases. Geneva: World Health Organization,
34. Gastanaduy A, Huwe B, Kaplan E, Mckay C, Wannamaker L. 1980. Failure of penicillin to eradicate group A streptococci during an outbreak of pharyngitis. *The Lancet* 316:498-502.
35. Kaplan EL, Johnson DR. 2001. Unexplained reduced microbiological efficacy of intramuscular benzathine penicillin G and of oral penicillin V in eradication of group A streptococci from children with acute pharyngitis. *Pediatrics* 108:1180-1186.
36. Cunningham MW, Antone SM, Gulizia JM, McManus BM, Fischetti VA, Gauntt CJ. 1992. Cytotoxic and viral neutralizing antibodies crossreact with streptococcal M protein, enteroviruses, and human cardiac myosin. *Proceedings of the National Academy of Sciences* 89:1320-1324.
37. Hynes W. 2004. Virulence factors of the group A streptococci and genes that regulate their expression. *Front Biosci* 9:3399-3433.
38. Dale JB, Beachey EH. 1986. Sequence of myosin-crossreactive epitopes of streptococcal M protein. *Journal of Experimental Medicine* 164:1785-1790.
39. Sela S, Aviv A, Tovi A, Burstein I, Caparon MG, Hanski E. 1993. Protein F: an adhesin of Streptococcus pyogenes binds fibronectin via two distinct domains. *Molecular microbiology* 10:1049-1055.
40. Terao Y. 2012. The virulence factors and pathogenic mechanisms of Streptococcus pyogenes. *Journal of Oral Biosciences* 54:96-100.

41. Berggård K, Johnsson E, Morfeldt E, Persson J, Stålhammar-Carlemalm M, Lindahl G. 2001. Binding of human C4BP to the hypervariable region of M protein: a molecular mechanism of phagocytosis resistance in *Streptococcus pyogenes*. *Molecular microbiology* 42:539-551.
42. Horstmann RD, Sievertsen HJ, Knobloch J, Fischetti VA. 1988. Antiphagocytic activity of streptococcal M protein: selective binding of complement control protein factor H. *Proceedings of the National Academy of Sciences* 85:1657-1661.
43. Johnsson E, Berggård K, Kotarsky H, Hellwage J, Zipfel PF, Sjöbring U, Lindahl G. 1998. Role of the hypervariable region in streptococcal M proteins: binding of a human complement inhibitor. *The Journal of Immunology* 161:4894-4901.
44. Dale JB, Washburn RG, Marques MB, Wessels MR. 1996. Hyaluronate capsule and surface M protein in resistance to opsonization of group A streptococci. *Infection and immunity* 64:1495-1501.
45. Moses AE, Wessels MR, Zalcmán K, Albertí S, Natanson-Yaron S, Menes T, Hanski E. 1997. Relative contributions of hyaluronic acid capsule and M protein to virulence in a mucoid strain of the group A *Streptococcus*. *Infection and immunity* 65:64-71.
46. Hynes W, Sloan M. 2016. Secreted extracellular virulence factors, *Streptococcus pyogenes*: Basic Biology to Clinical Manifestations [Internet]. University of Oklahoma Health Sciences Center.
47. Timmer AM, Timmer JC, Pence MA, Hsu L-C, Ghochani M, Frey TG, Karin M, Salvesen GS, Nizet V. 2009. Streptolysin O promotes group A *Streptococcus* immune evasion by accelerated macrophage apoptosis. *Journal of Biological Chemistry* 284:862-871.
48. Ginsburg I. 1999. Is streptolysin S of group A streptococci a virulence factor? *Apmis* 107:1051-1059.
49. Buchanan JT, Simpson AJ, Aziz RK, Liu GY, Kristian SA, Kotb M, Feramisco J, Nizet V. 2006. DNase expression allows the pathogen group A *Streptococcus* to escape killing in neutrophil extracellular traps. *Current Biology* 16:396-400.
50. Ofek I, Bergner-Rabinowitz S, Ginsburg I. 1970. Oxygen-stable Hemolysins of Group A *Streptococci* VII. The Relation of the Leukotoxic Factor to Streptolysin S. *Journal of Infectious Diseases* 122:517-522.
51. Frick I-M, Shannon O, Åkesson P, Mörgelin M, Collin M, Schmidtchen A, Björck L. 2011. Antibacterial activity of the contact and complement systems is blocked by SIC, a protein secreted by *Streptococcus pyogenes*. *Journal of Biological Chemistry* 286:1331-1340.
52. Frick IM, Åkesson P, Herwald H, Mörgelin M, Malmsten M, Nägler DK, Björck L. 2006. The contact system—a novel branch of innate immunity generating antibacterial peptides. *The EMBO journal* 25:5569-5578.
53. Proft T, Fraser JD. 2016. Streptococcal superantigens: biological properties and potential role in disease, *Streptococcus pyogenes*: basic biology to clinical manifestations [Internet]. University of Oklahoma Health Sciences Center.
54. Fraser JD, Proft T. 2008. The bacterial superantigen and superantigen-like proteins. *Immunological reviews* 225:226-243.
55. Hytönen J, Haataja S, Gerlach D, Podbielski A, Finne J. 2001. The SpeB virulence factor of *Streptococcus pyogenes*, a multifunctional secreted and cell surface molecule with streptadhesin, laminin-binding and cysteine protease activity. *Molecular microbiology* 39:512-519.
56. Chiang-Ni C, Wu J-J. 2008. Effects of streptococcal pyrogenic exotoxin B on pathogenesis of *Streptococcus pyogenes*. *Journal of the Formosan Medical Association* 107:677-685.
57. TONGS MS. 1919. ECTOENZYMES OF STREPTOCOCCI. *JAMA* 73:1277-1279.
58. Elliott SD. 1945. A proteolytic enzyme produced by group A streptococci with special reference to its effect on the type-specific M antigen. *Journal of experimental medicine* 81:573-592.

59. Kim YB, Watson DW. 1970. A purified group A streptococcal pyrogenic exotoxin: physicochemical and biological properties including the enhancement of susceptibility to endotoxin lethal shock. *Journal of Experimental Medicine* 131:611-628.
60. Gerlach D, Reichardt W, Fleischer B, Schmidt K-H. 1994. Separation of mitogenic and pyrogenic activities from so-called erythrogenic toxin type B (streptococcal proteinase). *Zentralblatt für Bakteriologie* 280:507-514.
61. Bohach GA, Hauser AR, Schlievert PM. 1988. Cloning of the gene, *speB*, for streptococcal pyrogenic exotoxin type B in *Escherichia coli*. *Infection and immunity* 56:1665-1667.
62. Björck L, Åkesson P, Bohus M, Trojnar J, Abrahamson M, Olafsson I, Grubb A. 1989. Bacterial growth blocked by a synthetic peptide based on the structure of a human proteinase inhibitor. *Nature* 337:385.
63. Kapur V, Majesky MW, Li L-L, Black RA, Musser JM. 1993. Cleavage of interleukin 1 beta (IL-1 beta) precursor to produce active IL-1 beta by a conserved extracellular cysteine protease from *Streptococcus pyogenes*. *Proceedings of the National Academy of Sciences* 90:7676-7680.
64. Wolf BB, Gibson CA, Kapur V, Hussaini IM, Musser JM, Gonias SL. 1994. Proteolytically active streptococcal pyrogenic exotoxin B cleaves monocytic cell urokinase receptor and releases an active fragment of the receptor from the cell surface. *Journal of Biological Chemistry* 269:30682-30687.
65. Gerlach D, Knöll H, Köhler W, Ozegowski J-H, Hribalova V. 1983. Isolation and characterization of erythrogenic toxins V. Communication: identity of erythrogenic toxin type B and streptococcal proteinase precursor. *Zentralblatt für Bakteriologie, Mikrobiologie und Hygiene 1 Abt Originale A, Medizinische Mikrobiologie, Infektionskrankheiten und Parasitologie* 255:221-233.
66. Kellner A, Robertson T. 1954. Myocardial necrosis produced in animals by means of crystalline streptococcal proteinase. *The Journal of experimental medicine* 99:495.
67. Chaussee MS, Liu J, Stevens DL, Ferretti JJ. 1996. Genetic and phenotypic diversity among isolates of *Streptococcus pyogenes* from invasive infections. *Journal of Infectious Diseases* 173:901-908.
68. Olsen RJ, Raghuram A, Cantu C, Hartman MH, Jimenez FE, Lee S, Ngo A, Rice KA, Saddington D, Spillman H. 2015. The majority of 9,729 group A streptococcus strains causing disease secrete SpeB cysteine protease: pathogenesis implications. *Infection and immunity* 83:4750-4758.
69. Yu C, Ferretti JJ. 1991. Frequency of the erythrogenic toxin B and C genes (*speB* and *speC*) among clinical isolates of group A streptococci. *Infection and immunity* 59:211-215.
70. Carroll RK, Shelburne SA, Olsen RJ, Suber B, Sahasrabhojane P, Kumaraswami M, Beres SB, Shea PR, Flores AR, Musser JM. 2011. Naturally occurring single amino acid replacements in a regulatory protein alter streptococcal gene expression and virulence in mice. *The Journal of clinical investigation* 121:1956-1968.
71. Makthal N, Gavagan M, Do H, Olsen RJ, Musser JM, Kumaraswami M. 2016. Structural and functional analysis of RopB: a major virulence regulator in *S. streptococcus pyogenes*. *Molecular microbiology* 99:1119-1133.
72. Hollands A, Aziz RK, Kansal R, Kotb M, Nizet V, Walker MJ. 2008. A naturally occurring mutation in *ropB* suppresses SpeB expression and reduces M1T1 group A streptococcal systemic virulence. *PLoS One* 3:e4102.
73. Olsen RJ, Laucirica DR, Watkins ME, Feske ML, Garcia-Bustillos JR, Vu C, Cantu C, Shelburne III SA, Fittipaldi N, Kumaraswami M. 2012. Polymorphisms in regulator of protease B (RopB) alter disease phenotype and strain virulence of serotype M3 group A *Streptococcus*. *Journal of Infectious Diseases* 205:1719-1729.
74. Lukomski S, Sreevatsan S, Amberg C, Reichardt W, Woischnik M, Podbielski A, Musser JM. 1997. Inactivation of *Streptococcus pyogenes* extracellular cysteine protease significantly decreases

- mouse lethality of serotype M3 and M49 strains. *The Journal of clinical investigation* 99:2574-2580.
75. Olsen RJ, Sitkiewicz I, Ayeras AA, Gonulal VE, Cantu C, Beres SB, Green NM, Lei B, Humbird T, Greaver J. 2010. Decreased necrotizing fasciitis capacity caused by a single nucleotide mutation that alters a multiple gene virulence axis. *Proceedings of the National Academy of Sciences* 107:888-893.
  76. Amerongen AN, Veerman E. 2002. Saliva—the defender of the oral cavity. *Oral diseases* 8:12-22.
  77. Shelburne SA, Granville C, Tokuyama M, Sitkiewicz I, Patel P, Musser JM. 2005. Growth characteristics of and virulence factor production by group A *Streptococcus* during cultivation in human saliva. *Infection and immunity* 73:4723-4731.
  78. Hamburger Jr M. 1944. Studies on the Transmission of Hemolytic *Streptococcus* Infections: I. Cross Infections in Army Hospital Wards. *The Journal of Infectious Diseases*:58-70.
  79. Hamburger Jr M. 1944. Studies on the transmission of hemolytic streptococcus infections: II. Beta hemolytic streptococci in the saliva of persons with positive throat cultures. *The Journal of Infectious Diseases*:71-78.
  80. Hamburger Jr M, Robertson O. 1948. Expulsion of group A hemolytic streptococci in droplets and droplet nuclei by sneezing, coughing and talking. *The American journal of medicine* 4:690-701.
  81. Ross P. 1971. Beta-haemolytic streptococci in saliva. *Epidemiology & Infection* 69:347-353.
  82. Collin M, Olsén A. 2001. Effect of SpeB and EndoS from *Streptococcus pyogenes* on human immunoglobulins. *Infection and Immunity* 69:7187-7189.
  83. Collin M, Olsén A. 2001. EndoS, a novel secreted protein from *Streptococcus pyogenes* with endoglycosidase activity on human IgG. *The EMBO journal* 20:3046-3055.
  84. Noris M, Remuzzi G. Overview of complement activation and regulation, p 479-492. *In* (ed), Elsevier,
  85. Egesten A, Olin AI, Linge HM, Yadav M, Mörgelin M, Karlsson A, Collin M. 2009. SpeB of *Streptococcus pyogenes* differentially modulates antibacterial and receptor activating properties of human chemokines. *PLoS One* 4:e4769.
  86. Herwald H, Collin M, Müller-Esterl W, Björck L. 1996. Streptococcal cysteine proteinase releases kinins: a virulence mechanism. *Journal of Experimental Medicine* 184:665-673.
  87. Nyberg P, Rasmussen M, Björck L. 2004.  $\alpha$ 2-Macroglobulin-proteinase complexes protect *Streptococcus pyogenes* from killing by the antimicrobial peptide LL-37. *Journal of Biological Chemistry* 279:52820-52823.
  88. Schmidtchen A, Frick IM, Björck L. 2001. Dermatan sulphate is released by proteinases of common pathogenic bacteria and inactivates antibacterial  $\alpha$ -defensin. *Molecular microbiology* 39:708-713.
  89. Chen Z, Itzek A, Malke H, Ferretti JJ, Kreth J. 2012. Dynamics of speB mRNA transcripts in *Streptococcus pyogenes*. *Journal of bacteriology* 194:1417-1426.
  90. Berge A, Björck L. 1995. Streptococcal cysteine proteinase releases biologically active fragments of streptococcal surface proteins. *Journal of Biological Chemistry* 270:9862-9867.
  91. Raeder R, Woischnik M, Podbielski A, Boyle M. 1998. A secreted streptococcal cysteine protease can cleave a surface-expressed M1 protein and alter the immunoglobulin binding properties. *Research in microbiology* 149:539-548.
  92. Berge A, Kihlberg B-M, Sjöholm AG, Björck L. 1997. Streptococcal protein H forms soluble complement-activating complexes with IgG, but inhibits complement activation by IgG-coated targets. *Journal of Biological Chemistry* 272:20774-20781.
  93. Wexler DE, Cleary PP. 1985. Purification and characteristics of the streptococcal chemotactic factor inactivator. *Infection and immunity* 50:757-764.

94. Kuo C-F, Wu J-J, Lin K-Y, Tsai P-J, Lee S-C, Jin Y-T, Lei H-Y, Lin Y-S. 1998. Role of streptococcal pyrogenic exotoxin B in the mouse model of group A streptococcal infection. *Infection and immunity* 66:3931-3935.
95. Olsen RJ, Watkins ME, Cantu CC, Beres SB, Musser JM. 2011. Virulence of serotype M3 Group A Streptococcus strains in wax worms (*Galleria mellonella* larvae). *Virulence* 2:111-119.
96. Terao Y, Mori Y, Yamaguchi M, Shimizu Y, Ooe K, Hamada S, Kawabata S. 2008. Group A streptococcal cysteine protease degrades C3 (C3b) and contributes to evasion of innate immunity. *Journal of Biological Chemistry* 283:6253-6260.
97. Kapur V, Topouzis S, Majesky MW, Li L-L, Hamrick MR, Hamill RJ, Patti JM, Musser JM. 1993. A conserved Streptococcus pyogenes extracellular cysteine protease cleaves human fibronectin and degrades vitronectin. *Microbial pathogenesis* 15:327-346.
98. Tsai P-J, Lin Y-S, Kuo C-F, Lei H-Y, Wu J-J. 1999. Group A Streptococcus induces apoptosis in human epithelial cells. *Infection and immunity* 67:4334-4339.
99. Johansson L, Thulin P, Sendi P, Hertzén E, Linder A, Åkesson P, Low DE, Agerberth B, Norrby-Teglund A. 2008. Cathelicidin LL-37 in severe Streptococcus pyogenes soft tissue infections in humans. *Infection and immunity* 76:3399-3404.
100. Norrby-Teglund A, Pauksens K, Holm SE, Norgren M. 1994. Relation between low capacity of human sera to inhibit streptococcal mitogens and serious manifestation of disease. *Journal of Infectious Diseases* 170:585-591.
101. Eriksson BK, Andersson J, Holm SE, Norgren M. 1999. Invasive group A streptococcal infections: T1M1 isolates expressing pyrogenic exotoxins A and B in combination with selective lack of toxin-neutralizing antibodies are associated with increased risk of streptococcal toxic shock syndrome. *The Journal of infectious diseases* 180:410-418.
102. Holm SE, Norrby A, Bergholm A-M, Norgren M. 1992. Aspects of pathogenesis of serious group A streptococcal infections in Sweden, 1988–1989. *Journal of Infectious Diseases* 166:31-37.
103. Gubba S, Low DE, Musser JM. 1998. Expression and Characterization of Group A Streptococcus Extracellular Cysteine Protease Recombinant Mutant Proteins and Documentation of Seroconversion during Human Invasive Disease Episodes. *Infection and immunity* 66:765-770.
104. Ulrich RG. 2008. Vaccine based on a ubiquitous cysteinyl protease and streptococcal pyrogenic exotoxin A protects against Streptococcus pyogenes sepsis and toxic shock. *Journal of immune based therapies and vaccines* 6:8.
105. Morefield G, Touhey G, Lu F, Dunham A, HogenEsch H. 2014. Development of a recombinant fusion protein vaccine formulation to protect against Streptococcus pyogenes. *Vaccine* 32:3810-3815.
106. Kapur V, Maffei JT, Greer RS, Li L-L, Adams GJ, Musser JM. 1994. Vaccination with streptococcal extracellular cysteine protease (interleukin-1 $\beta$  convertase) protects mice against challenge with heterologous group A streptococci. *Microbial pathogenesis* 16:443-450.
107. Shelburne III SA, Olsen RJ, Makthal N, Brown NG, Sahasrabhojane P, Watkins EM, Palzkill T, Musser JM, Kumaraswami M. 2011. An amino-terminal signal peptide of Vfr protein negatively influences RopB-dependent SpeB expression and attenuates virulence in Streptococcus pyogenes. *Molecular microbiology* 82:1481-1495.
108. Musser JM, Stockbauer K, Kapur V, Rudgers GW. 1996. Substitution of cysteine 192 in a highly conserved Streptococcus pyogenes extracellular cysteine protease (interleukin 1beta convertase) alters proteolytic activity and ablates zymogen processing. *Infection and Immunity* 64:1913-1917.
109. Liu T-Y, Elliott SD. 1965. Streptococcal proteinase: the zymogen to enzyme transformation. *Journal of Biological Chemistry* 240:1138-1142.
110. Loughman JA, Caparon M. 2006. Regulation of SpeB in Streptococcus pyogenes by pH and NaCl: a model for in vivo gene expression. *Journal of bacteriology* 188:399-408.

111. Ogburn CA, Harris T, Harris S. 1958. Extracellular antigens in steady-state cultures of the hemolytic streptococcus: production of proteinase at low pH. *Journal of bacteriology* 76:142.
112. Cohen JO. 1969. Effect of culture medium composition and pH on the production of M protein and proteinase by group A streptococci. *Journal of bacteriology* 99:737-744.
113. Lyon WR, Gibson CM, Caparon MG. 1998. A role for trigger factor and an rgg-like regulator in the transcription, secretion and processing of the cysteine proteinase of *Streptococcus pyogenes*. *The EMBO journal* 17:6263-6275.
114. Neely MN, Lyon WR, Runft DL, Caparon M. 2003. Role of RopB in growth phase expression of the SpeB cysteine protease of *Streptococcus pyogenes*. *Journal of bacteriology* 185:5166-5174.
115. Chen Z, Mashburn-Warren L, Merritt J, Federle M, Kreth J. 2017. Interference of a speB 5' untranslated region partial deletion with mRNA degradation in *Streptococcus pyogenes*. *Molecular oral microbiology* 32:390-403.
116. Broglia L, Materne S, Lécrivain A-L, Hahnke K, Le Rhun A, Charpentier E. 2018. RNase Y-mediated regulation of the streptococcal pyrogenic exotoxin B. *RNA biology* 15:1336-1347.
117. Watson RO, Smoot JC, Musser JM. 2001. Identification of Rgg-Regulated Exoproteins of *Streptococcus pyogenes*. *Infection and immunity* 69:822-831.
118. Miller MB, Bassler BL. 2001. Quorum sensing in bacteria. *Annual Reviews in Microbiology* 55:165-199.
119. Waters CM, Bassler BL. 2005. Quorum sensing: cell-to-cell communication in bacteria. *Annu Rev Cell Dev Biol* 21:319-346.
120. Rutherford ST, Bassler BL. 2012. Bacterial quorum sensing: its role in virulence and possibilities for its control. *Cold Spring Harbor perspectives in medicine* 2:a012427.
121. Antunes LCM, Ferreira RB, Buckner MM, Finlay BB. 2010. Quorum sensing in bacterial virulence. *Microbiology* 156:2271-2282.
122. Fuqua WC, Winans SC, Greenberg EP. 1994. Quorum sensing in bacteria: the LuxR-LuxI family of cell density-responsive transcriptional regulators. *Journal of bacteriology* 176:269.
123. Antunes LCM, Ferreira RB. 2009. Intercellular communication in bacteria. *Critical reviews in microbiology* 35:69-80.
124. Thoendel M, Kavanaugh JS, Flack CE, Horswill AR. 2010. Peptide signaling in the staphylococci. *Chemical reviews* 111:117-151.
125. Neiditch MB, Capodagli GC, Prehna G, Federle MJ. 2017. Genetic and structural analyses of RRNPP intercellular peptide signaling of Gram-positive bacteria. *Annual review of genetics* 51:311-333.
126. Rocha-Estrada J, Aceves-Diez AE, Guarneros G, de la Torre M. 2010. The RNPP family of quorum-sensing proteins in Gram-positive bacteria. *Applied microbiology and biotechnology* 87:913-923.
127. Cook LC, Federle MJ. 2014. Peptide pheromone signaling in *Streptococcus* and *Enterococcus*. *FEMS microbiology reviews* 38:473-492.
128. Kleerebezem M, Quadri LE. 2001. Peptide pheromone-dependent regulation of antimicrobial peptide production in Gram-positive bacteria: a case of multicellular behavior. *Peptides* 22:1579-1596.
129. Declerck N, Bouillaut L, Chaix D, Rugani N, Slamti L, Hoh F, Lereclus D, Arold ST. 2007. Structure of PlcR: Insights into virulence regulation and evolution of quorum sensing in Gram-positive bacteria. *Proceedings of the National Academy of Sciences* 104:18490-18495.
130. Sylva GL, Sturdevant DE, Smoot LM, Graham MR, Watson RO, Musser JM. 2002. Rgg influences the expression of multiple regulatory loci to coregulate virulence factor expression in *Streptococcus pyogenes*. *Infection and immunity* 70:762-770.
131. Caserta E, Haemig HA, Manias DA, Tomsic J, Grundy FJ, Henkin TM, Dunny GM. 2012. In vivo and in vitro analyses of regulation of the pheromone-responsive prgQ promoter by the PrgX pheromone receptor protein. *Journal of bacteriology* 194:3386-3394.

132. Zouhir S, Perchat S, Nicaise M, Perez J, Guimaraes B, Lereclus D, Nessler S. 2013. Peptide-binding dependent conformational changes regulate the transcriptional activity of the quorum-sensor NprR. *Nucleic acids research* 41:7920-7933.
133. Slamti L, Perchat S, Huillet E, Lereclus D. 2014. Quorum sensing in *Bacillus thuringiensis* is required for completion of a full infectious cycle in the insect. *Toxins* 6:2239-2255.
134. Mashburn-Warren L, Morrison DA, Federle MJ. 2010. A novel double-tryptophan peptide pheromone controls competence in *Streptococcus* spp. via an Rgg regulator. *Molecular microbiology* 78:589-606.
135. Perchat S, Dubois T, Zouhir S, Gominet M, Poncet S, Lemy C, Aumont-Nicaise M, Deutscher J, Gohar M, Nessler S. 2011. A cell–cell communication system regulates protease production during sporulation in bacteria of the *Bacillus cereus* group. *Molecular microbiology* 82:619-633.
136. Kozłowicz BK, Shi K, Gu ZY, Ohlendorf DH, Earhart CA, Dunny GM. 2006. Molecular basis for control of conjugation by bacterial pheromone and inhibitor peptides. *Molecular microbiology* 62:958-969.
137. Parashar V, Aggarwal C, Federle MJ, Neiditch MB. 2015. Rgg protein structure–function and inhibition by cyclic peptide compounds. *Proceedings of the National Academy of Sciences* 112:5177-5182.
138. Baker MD, Neiditch MB. 2011. Structural basis of response regulator inhibition by a bacterial anti-activator protein. *PLoS biology* 9:e1001226.
139. Diaz AR, Core LJ, Jiang M, Morelli M, Chiang CH, Szurmant H, Perego M. 2012. *Bacillus subtilis* RapA phosphatase domain interaction with its substrate, phosphorylated Spo0F, and its inhibitor, the PhrA peptide. *Journal of bacteriology* 194:1378-1388.
140. Parashar V, Jeffrey PD, Neiditch MB. 2013. Conformational change-induced repeat domain expansion regulates Rap phosphatase quorum-sensing signal receptors. *PLoS biology* 11:e1001512.
141. Parashar V, Mirouze N, Dubnau DA, Neiditch MB. 2011. Structural basis of response regulator dephosphorylation by Rap phosphatases. *PLoS biology* 9:e1000589.
142. del Sol FG, Marina A. 2013. Structural basis of Rap phosphatase inhibition by Phr peptides. *PLoS biology* 11:e1001511.
143. Blatch GL, Lässle M. 1999. The tetratricopeptide repeat: a structural motif mediating protein-protein interactions. *Bioessays* 21:932-939.
144. Cervený L, Strasková A, Danková V, Hartlová A, Cecková M, Staud F, Stulik J. 2013. Tetratricopeptide repeat motifs in the world of bacterial pathogens: role in virulence mechanisms. *Infection and immunity* 81:629-635.
145. D'Andrea LD, Regan L. 2003. TPR proteins: the versatile helix. *Trends in biochemical sciences* 28:655-662.
146. Jimenez JC, Federle MJ. 2014. Quorum sensing in group A *Streptococcus*. *Frontiers in cellular and infection microbiology* 4:127.
147. Morrison DA, Guédon E, Renault P. 2013. Competence for natural genetic transformation in the *Streptococcus bovis* group streptococci *S. infantarius* and *S. macedonicus*. *Journal of bacteriology* 195:2612-2620.
148. Cantas L, Shah SQA, Cavaco LM, Manaia C, Walsh F, Popowska M, Garelick H, Bürgmann H, Sørum H. 2013. A brief multi-disciplinary review on antimicrobial resistance in medicine and its linkage to the global environmental microbiota. *Frontiers in Microbiology* 4:96.
149. Tanwar J, Das S, Fatima Z, Hameed S. 2014. Multidrug resistance: an emerging crisis. *Interdisciplinary perspectives on infectious diseases* 2014.
150. Andersson DI, Hughes D. 2011. Persistence of antibiotic resistance in bacterial populations. *FEMS microbiology reviews* 35:901-911.

151. Dickey SW, Cheung GY, Otto M. 2017. Different drugs for bad bugs: antivirulence strategies in the age of antibiotic resistance. *Nature Reviews Drug Discovery* 16:457.
152. Heras B, Scanlon MJ, Martin JL. 2015. Targeting virulence not viability in the search for future antibacterials. *British journal of clinical pharmacology* 79:208-215.
153. Rasko DA, Sperandio V. 2010. Anti-virulence strategies to combat bacteria-mediated disease. *Nature reviews Drug discovery* 9:117.
154. McIver KS. 2009. Stand-alone response regulators controlling global virulence networks in *Streptococcus pyogenes*, p 103-119, *Bacterial Sensing and Signaling*, vol 16. Karger Publishers.
155. Organization WH. 2005. Group A streptococcal vaccine development: current status and issues of relevance to less developed countries. Geneva: World Health Organization,
156. LaSarre B, Chang JC, Federle MJ. 2013. Redundant group a streptococcus signaling peptides exhibit unique activation potentials. *Journal of bacteriology* 195:4310-4318.
157. Han S, Machhi S, Berge M, Xi G, Linke T, Schoner R. 2017. Novel signal peptides improve the secretion of recombinant *Staphylococcus aureus* Alpha toxinH35L in *Escherichia coli*. *AMB Express* 7:93.
158. Auclair SM, Bhanu MK, Kendall DA. 2012. Signal peptidase I: cleaving the way to mature proteins. *Protein Science* 21:13-25.
159. van Wely KH, Swaving J, Freudl R, Driessen AJ. 2001. Translocation of proteins across the cell envelope of Gram-positive bacteria. *FEMS microbiology reviews* 25:437-454.
160. Pérez-Pascual D, Gaudu P, Fleuchot B, Besset C, Rosinski-Chupin I, Guillot A, Monnet V, Gardan R. 2015. RovS and its associated signaling peptide form a cell-to-cell communication system required for *Streptococcus agalactiae* pathogenesis. *MBio* 6:e02306-14.
161. Chang JC, Federle MJ. 2016. PptAB exports Rgg quorum-sensing peptides in *Streptococcus*. *PLoS One* 11:e0168461.
162. Perez-Pascual D, Monnet V, Gardan R. 2016. Bacterial cell-cell communication in the host via RRNPP peptide-binding regulators. *Frontiers in microbiology* 7:706.
163. Monnet V, Gardan R. 2015. Quorum-sensing regulators in Gram-positive bacteria: 'cherchez le peptide'. *Molecular microbiology* 97:181-184.
164. Podbielski A, Leonard BA. 1998. The group A streptococcal dipeptide permease (Dpp) is involved in the uptake of essential amino acids and affects the expression of cysteine protease. *Molecular microbiology* 28:1323-1334.
165. Monnet V. 2003. Bacterial oligopeptide-binding proteins. *Cellular and Molecular Life Sciences CMLS* 60:2100-2114.
166. Guyer CA, Morgan DG, Osheroff N, Staros J. 1985. Purification and characterization of a periplasmic oligopeptide binding protein from *Escherichia coli*. *Journal of Biological Chemistry* 260:10812-10818.
167. Chang JC, LaSarre B, Jimenez JC, Aggarwal C, Federle MJ. 2011. Two group A streptococcal peptide pheromones act through opposing Rgg regulators to control biofilm development. *PLoS pathogens* 7:e1002190.
168. Detmers FJ, Lanfermeijer FC, Abele R, Jack RW, Tampé R, Konings WN, Poolman B. 2000. Combinatorial peptide libraries reveal the ligand-binding mechanism of the oligopeptide receptor OppA of *Lactococcus lactis*. *Proceedings of the National Academy of Sciences* 97:12487-12492.
169. Garai P, Chandra K, Chakravorty D. 2017. Bacterial peptide transporters: Messengers of nutrition to virulence. *Virulence* 8:297-309.
170. Samen U, Gottschalk B, Eikmanns BJ, Reinscheid DJ. 2004. Relevance of peptide uptake systems to the physiology and virulence of *Streptococcus agalactiae*. *Journal of Bacteriology* 186:1398-1408.

171. Payne JW, Smith MW. 1994. Peptide transport by micro-organisms, p 1-80, *Advances in microbial physiology*, vol 36. Elsevier.
172. Podbielski A, Pohl B, Woischnik M, Körner C, Schmidt KH, Rozdzinski E, Leonard BA. 1996. Molecular characterization of group A streptococcal (GAS) oligopeptide permease (opp) and its effect on cysteine protease production. *Molecular microbiology* 21:1087-1099.
173. Do H, Makthal N, VanderWal A, Saavedra M, Olsen R, Musser J, Kumaraswami M. 2019. Environmental pH and peptide signaling control virulence of *Streptococcus pyogenes* via a quorum-sensing pathway. *Nature communications* 10:2586-2586.
174. Shi K, Brown CK, Gu Z-Y, Kozlowicz BK, Dunny GM, Ohlendorf DH, Earhart CA. 2005. Structure of peptide sex pheromone receptor PrgX and PrgX/pheromone complexes and regulation of conjugation in *Enterococcus faecalis*. *Proceedings of the National Academy of Sciences* 102:18596-18601.
175. Grenha R, Slamti L, Nicaise M, Refes Y, Lereclus D, Nessler S. 2013. Structural basis for the activation mechanism of the PlcR virulence regulator by the quorum-sensing signal peptide PapR. *Proceedings of the National Academy of Sciences* 110:1047-1052.
176. Carapetis JR. 2007. Rheumatic heart disease in developing countries. *New England Journal of Medicine* 357:439-441.
177. Shelburne SA, Sumby P, Sitkiewicz I, Granville C, DeLeo FR, Musser JM. 2005. Central role of a bacterial two-component gene regulatory system of previously unknown function in pathogen persistence in human saliva. *Proceedings of the National Academy of Sciences* 102:16037-16042.
178. Davidopoulou S, Diza E, Menexes G, Kalfas S. 2012. Salivary concentration of the antimicrobial peptide LL-37 in children. *Archives of oral biology* 57:865-869.
179. Yoon H, McDermott JE, Porwollik S, McClelland M, Heffron F. 2009. Coordinated regulation of virulence during systemic infection of *Salmonella enterica* serovar Typhimurium. *PLoS pathogens* 5:e1000306.
180. Somerville GA, Proctor RA. 2009. At the crossroads of bacterial metabolism and virulence factor synthesis in *Staphylococci*. *Microbiol Mol Biol Rev* 73:233-248.
181. Chandler JR, Flynn AR, Bryan EM, Dunny GM. 2005. Specific control of endogenous cCF10 pheromone by a conserved domain of the pCF10-encoded regulatory protein PrgY in *Enterococcus faecalis*. *Journal of bacteriology* 187:4830-4843.
182. Ibrahim M, Nicolas P, Bessieres P, Bolotin A, Monnet V, Gardan R. 2007. A genome-wide survey of short coding sequences in streptococci. *Microbiology* 153:3631-3644.
183. Perego M, Brannigan JA. 2001. Pentapeptide regulation of aspartyl-phosphate phosphatases. *Peptides* 22:1541-1547.

## ACKNOWLEDGEMENTS

I would like to express my sincere gratitude to my advisor in Houston Methodist Research Institute, Prof. Muthiah Kumaraswami for his continuous support throughout my Ph.D study and related research. I greatly appreciate his patience, motivation, guidance and immense knowledge. His guidance helped me in all the time of research and in writing this thesis. Thank you for always being there.

I am immensely grateful to my advisor in Ludwig-Maximilians University of Munich, Prof. Kai Papenfort for giving me the opportunity to join his lab as a Ph.D candidate. This thesis wouldn't have been possible without his constant help and support in all respects. Thank you so much.

My sincere thanks also goes to my fellow lab members (Dr. Hackwon Do, Arica VanderWal, Kimberly Nguyen) for engaging in constant research discussions which greatly helped the progress of this study. I am extremely thankful to Dr. Priyanka Kachroo for her help in performing RNA-sequencing and analyzing the data. I would also like to thank Concepcion Cantu for performing the animal studies when required.

Last but not the least, I would like to thank my parents, brother and extended family for their constant support throughout my life. This work wouldn't have been possible without them.

**NISHANTH MAKTHAL**

Department of Biology I

Ludwig-Maximilians-University of Munich (LMU)

Munich, Germany

[Nishanth.makthal@biologie.uni-muenchen.de](mailto:Nishanth.makthal@biologie.uni-muenchen.de)**Education:**

- 2016 – current      **Ludwig-Maximilians University of Munich, Munich, Germany / Houston Methodist Research Institute, Houston, USA**  
Ph.D. candidate in Microbiology
- 2008 – 2010      **Texas Tech University, Lubbock, USA**  
Master of Science in Biotechnology  
Graduation Date: August 2010  
GPA: 3.40
- 2004 – 2008      **Jawaharlal Nehru Technological University, Hyderabad, India**  
Bachelor of Technology in Biotechnology  
Graduation Date: May 2008  
GPA: 3.60

**Work Experience**

- 2010 – 2016      **Houston Methodist Research Institute** Lab Manager
- 2009 – 2010      **Texas Tech University** Graduate Research Assistant

**Media Appearances/Interviews**

Co-first authored research on “Leaderless secreted peptide signaling molecule alters global gene expression and increases virulence of a human bacterial pathogen” was broadcasted on 8 news channels across United States and published in 14 news outlet all around the world with estimated audience of 44 million in 6 countries.

**Major News Channel Coverage**

- <http://www.fox26houston.com/news/local-news/mans-flesh-eating-bacteria-diagnosis-from-harvey-leads-to-medical-breakthrough>
- <http://abc13.com/health/man-catches-flesh-eating-bacteria-from-harvey-flood/2453528/>

**Major News Outlet Coverage**

- <http://www.newsweek.com/death-hurricane-cure-flesh-eating-bacteria-almost-killed-man-texas-667825>
- <https://phys.org/news/2017-09-potential-pathway-flesh-eating-bacteria.html>

## Editorial Duties & Peer Reviewer

- Editorial board member, *Journal of Microbial Pathogenesis*, 2017-present.
- Peer reviewer for *Journal of Molecular and Genetic Medicine*, *Journal of Visualized Experiments*, *Clinical Groups Journals*.

## Scholarships

2009 – 2010     **Texas Tech University**    Teaching Assistant

Assisted a Master's level class of 32 students on a project titled "Functional Expression, Purification and Characterization of 3alpha Hydroxysteroid Dehydrogenase/Carbonyl Reductase from *Comamonas Testosteroni*.

## Scientific Publications

- 2019     Do H, **Makthal N**, VanderWal A, Saavedra M, Olsen R, Musser J, Kumaraswami M. 2019. Environmental pH and peptide signaling control virulence of *Streptococcus pyogenes* via a quorum-sensing pathway. *Nature communications* 10:2586-2586.
- 2019     Do H, **Makthal N**, Chandrangsu P, Olsen RJ, Helmann JD, Musser JM, Kumaraswami M. 2019. Metal sensing and regulation of adaptive responses to manganese limitation by MtsR is critical for group A streptococcus virulence. *Nucleic acids research*.
- 2018     Horstmann N, Tran CN, Brumlow C, DebRoy S, Yao H, Gonzalez GN, **Makthal N**, Kumaraswami M, Shelburne SA. 2018. Phosphatase activity of the control of virulence sensor kinase CovS is critical for the pathogenesis of group A streptococcus. *PLoS pathogens* 14:e1007354.
- 2018     **Makthal N**, Do H, VanderWal AR, Olsen RJ, Musser JM, Kumaraswami M. Signaling by a Conserved Quorum Sensing Pathway Contributes to Growth *Ex vivo* and Oropharyngeal Colonization of Human Pathogen Group A Streptococcus. *Infect Immun* 85(5), pii: e00169-18.
- 2017     **Makthal N**, Kumaraswami M. Zinc'ing it out: zinc homeostasis mechanisms and their impact on the pathogenesis of human pathogen group A streptococcus (2017 Dec). *Metallomics*, 1:9(12): 1693-1702.
- 2017     Do H, **Makthal N\***, VanderWal AR, Rettel M, Savitski MM, Peschek N, Papenfort K, Olsen RJ, Musser JM, Kumaraswami M. Leaderless secreted peptide signaling molecule alters global gene expression and increases virulence of a human bacterial pathogen (2017 Oct). *Proc Natl Acad Sci*, 114(40): E8498-E8507.

**\*Co First author**

- 2017 **Makthal N**, Nguyen K, Do H, Gavagan M, Chandrangsu P, Helmann JD, Olsen RJ, Kumaraswami M. A Critical Role of Zinc Importer AdcABC in Group A Streptococcus-Host Interactions During Infection and Its Implications for Vaccine Development (2017 Jul). *EBioMedicine*, 21:131-141.
- 2017 VanderWal AR, **Makthal N\***, Pinochet-Barros A, Helmann JD, Olsen RJ, Kumaraswami M. Iron efflux by PmtA is critical for oxidative stress resistance and contributes significantly to group A streptococcus virulence (2017 May). *Infect Immun*, 85(6), e00091-17 **\*Co First author**
- 2016 Ramalinga A, Danger JL, **Makthal N**, Kumaraswami M, Sumbly P. Multimerization of the virulence-enhancing group A Streptococcus transcription factor RivR is required for regulatory activity (2016 Dec). *J Bacteriol*, 199(1). pii: e00452-16.
- 2016 **Makthal N**, Gavagan M, Do H, Olsen RJ, Musser JM, Kumaraswami M. Structural and functional analysis of RopB – a major virulence regulator in *Streptococcus pyogenes* (2016 Mar). *Mol Microbiol*, 99(6):1119-33.
- 2015 Danger JL, **Makthal N**, Kumaraswami M, Sumbly P. The small Regulatory RNA FasX negatively regulates the expression of two fibronectin-binding proteins in the group A Streptococcus (2015 Dec). *J Bacteriol*, 197(23):3720-30.
- 2015 Sanson M, **Makthal N\***, Gavagan M, Cantu C, Olsen RJ, Musser JM, Kumaraswami M. Phosphorylation events in the Multiple Gene Regulator of Group A Streptococcus (Mga) Significantly Influences Global Gene Expression and Virulence (2015 Jun). *Infect Immun*, 83(6):2382-95. **\*Co First author**
- 2015 Sanson M, O'Neill BE, Kachroo P, Anderson JR, Flores AR, Valson C, Cantu CC, **Makthal N**, Karmonik C, Fittipaldi N, Kumaraswami M, Musser JM, Olsen RJ. A naturally occurring single amino Acid replacement in multiple gene regulator of group a streptococcus significantly increases virulence (2015 Feb). *Am J Pathol*, 185(2):462-7.
- 2015 Sanson M, **Makthal N\***, Flores AR, Olsen RJ, Musser JM, Kumaraswami M. Adhesin competence repressor (AdcR) from *Streptococcus pyogenes* controls adaptive responses to zinc limitation and contributes to virulence (2015 Jan). *Nucleic Acids Res*, 43(1):418-32. **\*Co First author**
- 2013 **Makthal N**, Rastegari S, Sanson M, Ma Z, Olsen RJ, Helmann JD, Musser JM, Kumaraswami M. Crystal structure of peroxide stress regulator (PerR) from *Streptococcus pyogenes* provides functional insights into the mechanism of oxidative stress sensing (2013 Jun). *J Biol Chem*, 288(25):18311-24.
- 2011 Shelburne SA 3rd, Olsen RJ, **Makthal N**, Brown NG, Sahasrabhojane P, Watkins EM, Palzkill T, Musser JM, Kumaraswami M. An amino-terminal signal peptide of Vfr protein negatively influences RopB-dependent SpeB expression and attenuates virulence in *Streptococcus pyogenes* (2011 Dec). *Mol Microbiol*, 82(6):1481-95.